France-Lanord, C., Spiess, V., Klaus, A., Schwenk, T., and the Expedition 354 Scientists
Proceedings of the International Ocean Discovery Program Volume 354
publications.iodp.org

doi:10.14379/iodp.proc.354.101.2016

Expedition 354 summary[1]

C. France-Lanord, V. Spiess, A. Klaus, T. Schwenk, R.R. Adhikari, S.K. Adhikari, J.-J. Bahk, A.T. Baxter, J.W. Cruz, S.K. Das, P. Dekens, W. Duleba, L.R. Fox, A. Galy, V. Galy, J. Ge, J.D. Gleason, B.R. Gyawali, P. Huyghe, G. Jia, H. Lantzsch, M.C. Manoj, Y. Martos Martin, L. Meynadier, Y.M.R. Najman, A. Nakajima, C. Ponton, B.T. Reilly, K.G. Rogers, J.F. Savian, P.A. Selkin, M.E. Weber, T. Williams, and K. Yoshida[2]

Keywords: International Ocean Discovery Program, IODP, Expedition 354, *JOIDES Resolution*, Site U1449, Site U1450, Site U1451, Site U1452, Site U1453, Site U1454, Site U1455, Bengal Fan

Contents

Abstract

International Ocean Discovery Program Expedition 354 to 8°N in the Bay of Bengal drilled a seven-site, 320 km long transect across the Bengal Fan. Three deep-penetration and an additional four shallow holes give a spatial overview of the primarily turbiditic depositional system that comprises the Bengal deep-sea fan. Sediments originate from Himalayan rivers, documenting terrestrial changes of Himalayan erosion and weathering, and are transported through a delta and shelf canyon, supplying turbidity currents loaded with a full spectrum of grain sizes. Mostly following transport channels, sediments deposit on and between levees while depocenters laterally shift over hundreds of kilometers on millennial timescales. During Expedition 354, these deposits were documented in space and time, and the recovered sediments have Himalayan mineralogical and geochemical signatures relevant for reconstructing time series of erosion, weathering, and changes in source regions, as well as impacts on the global carbon cycle. Miocene shifts in terrestrial vegetation, sediment budget, and style of sediment transport were tracked. Expedition 354 has extended the record of early fan deposition by 10 My into the late Oligocene.

Introduction

Of regions where tectonics and climate interact, southern Asia seems to illustrate their possible influences on each other more dramatically than any other region. The high elevation of the Tibetan Plateau and the rapid rise from the lowlands of northern India across the Himalaya profoundly affect both the average temperature structure of the atmosphere responsible for the seasonal winds and the distribution of precipitation that characterize the south Asian monsoon (Molnar et al., 2010; Boos and Kuang, 2011). Concurrently, monsoonal precipitation along the Himalaya generates one of the most important erosion fluxes of the planet. This surface mass transfer acts on the thermal structure and stress field of the mountain range and partly controls its morphology (Avouac and Burov, 1996). Finally, the erosion processes contribute to the global atmospheric CO_2 drawdown responsible for Cenozoic global cooling (Figure **F1**) through organic carbon burial and silicate weathering. However, if the Tibetan Plateau and the Himalaya have influenced climate during Cenozoic time, the evidence suggesting such an influence is wholly inadequate to understand quantitatively how these geographical features have developed through time. This inadequacy is mostly due to the fact that direct records of the erosion of the mountain range are rare or limited in duration, so there is no consensus on the mass accumulation rate generated by the Tibet-Himalayan erosion to date (Métivier et al., 1999; Clift, 2006). Because of the lack of adequate sedimentary archives, the early stages of Himalayan evolution since the continental collision ~55 My ago to the Miocene are essentially unknown.

Expedition 354 was proposed to obtain data that can not only test hypothetical links between climate and tectonics but also provide new data not easily acquired but relevant for understanding a number of Earth processes. This expedition focuses on the erosional record of the Himalaya and on the development of the Asian monsoon over Cenozoic time. Because geology lacks the tools for determining paleoelevations except in unusual and ideal circumstances, the sedimentary record of material eroded from a mountain belt holds the least ambiguous record of its paleotopography. Approximately 80% of the material eroded from the Himalaya was deposited in the Bay of Bengal, which therefore hosts the most complete record.

Reconstructing accumulation rates from fan deposits is challenging because (1) the 2500 km length of the fan leads to variable thickness and onlap time from north to south and (2) the nature of fan deposition means that accumulation at a given location is highly

[1] France-Lanord, C., Spiess, V., Klaus, A., Schwenk, T., Adhikari, R.R., Adhikari, S.K., Bahk, J.-J., Baxter, A.T., Cruz, J.W., Das, S.K., Dekens, P., Duleba, W., Fox, L.R., Galy, A., Galy, V., Ge, J., Gleason, J.D., Gyawali, B.R., Huyghe, P., Jia, G., Lantzsch, H., Manoj, M.C., Martos Martin, Y., Meynadier, L., Najman, Y.M.R., Nakajima, A., Ponton, C., Reilly, B.T., Rogers, K.G., Savian, J.F., Selkin, P.A., Weber, M.E., Williams, T., and Yoshida, K., 2016. Expedition 354 summary. *In* France-Lanord, C., Spiess, V., Klaus, A., Schwenk, T., and the Expedition 354 Scientists, *Bengal Fan*. Proceedings of the International Ocean Discovery Program, 354: College Station, TX (International Ocean Discovery Program). http://dx.doi.org/10.14379/iodp.proc.354.101.2016
[2] **Expedition 354 Scientists' addresses.**
MS 354-101: Published 7 September 2016

Figure F1. Cenozoic changes: global cooling and glaciations (Zachos, 2001), Oligocene atmospheric pCO_2 drawdown (Beerling and Royer, 2011) possibly related to a change in the balance between erosion and volcanic input of CO_2, Oligocene rise of seawater $^{87}Sr/^{86}Sr$ (Koepnick et al., 1985) likely reflecting the erosion of radiogenic formations analog of the modern Himalaya, and Eocene slowdown of the Indian plate motion following the collision and Tibet uplift (Copley et al., 2010). Right: extent of existing sedimentary records in the Bengal Fan and Himalayan foreland.

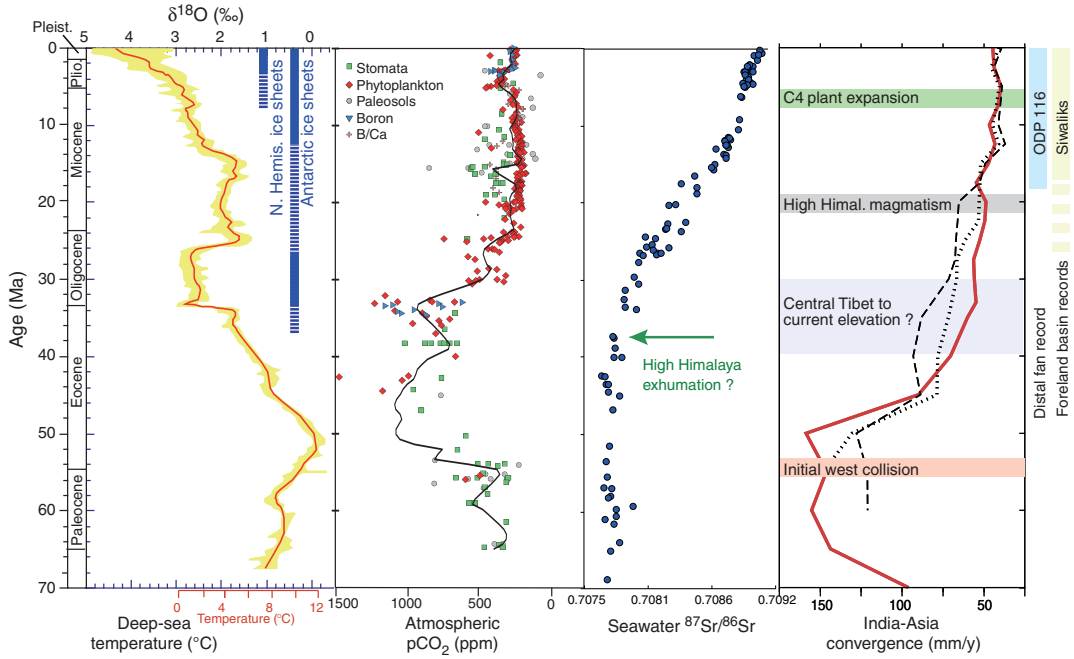

discontinuous and hence cannot capture a regional trend of accumulation. For these reasons, this expedition is based on an east–west transect approach with a large number of holes. As the transect crosses the fan at 8°N latitude (middle fan), Paleogene deposits, if they exist, are in reach of reasonable drilling depths. The transect is anchored on the western flank of the Ninetyeast Ridge with a deep hole located to recover the oldest fan deposits. From there, the transect extends west across the central axis of the fan and ends at Deep Sea Drilling Project (DSDP) Site 218 above the 85°E Ridge. To resolve characteristics of fan construction during the Quaternary, a spacing of ≈50 km between sites was chosen based on the typical width of channel-levee systems.

During Expedition 354, seven sites were drilled on an east–west transect at 8°N (Figures **F2**, **F3**, **F4**, **F5**, **F6**; Table **T1**), including

- One deep site to ~1200 meters below seafloor (mbsf) (Site U1451) to recover a complete sequence of fan deposits and in particular to reach prefan deposits;
- Two sites to ~900 mbsf (Sites U1450 and U1455) complementing Site U1451 to provide a transect of three sites across ~300 km to recover Pliocene and upper Miocene sediment to study Neogene fan evolution and the impact of the monsoonal system on sediment supply and flux; and
- Four dedicated shallow sites to 200–300 mbsf (Sites U1449, U1452, U1453, and U1454) to recover a complete terrigenous record of the Himalayan flux over the last 1–2 My, complemented by the shallow portion of the three deep-penetration sites.

During Expedition 354, the original transect of six sites was complemented by a seventh, alternate site (U1454) west of Site 218 that extended the transect to ~300 km.

Figure F2. Map of the Himalayan erosion system showing the position of existing DSDP and ODP sites documenting the Bengal and Indus Fans or the monsoon history. Box = location of Expedition 354 transect at 8°N. Star = position of SO93-117-120KL levee record at 16°N (Hübscher et al., 1997). Bengal Fan sediment isopachs (blue lines; in kilometers) are simplified from Curray et al. (2003) and represent the total sedimentary and metasedimentary rocks above the oceanic basalt as interpreted from seismic reflection and refraction data.

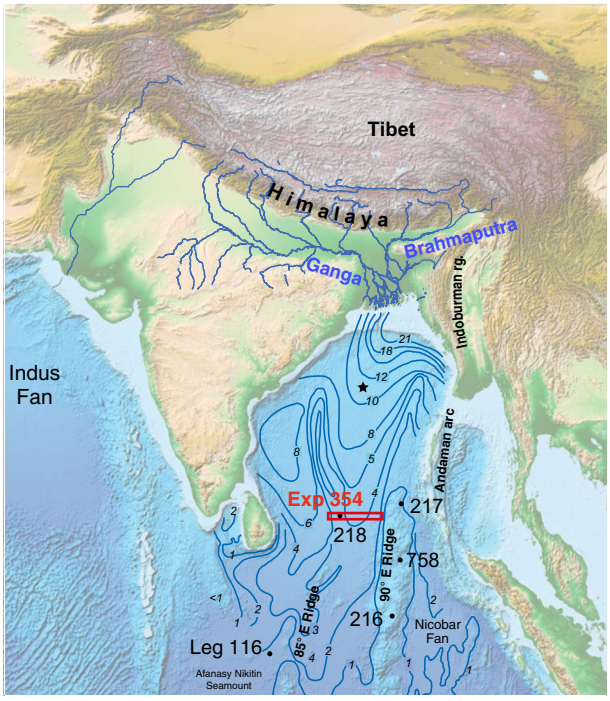

Figure F3. A. Seismic Profile GeoB097-020/027 showing the positions of Expedition 354 drill sites in relation to regional fan architecture. The tops of the Pliocene and Miocene, as well as the 10 Ma horizon, are traced through the profile based on results from DSDP Site 218 (Moore et al., 1974). The distinct unconformity in the east penetrated only by the deepest part of Site U1451 is inferred to represent the Eocene onset of fan deposition. CMP = common midpoint. B. Interpreted line drawing of Profile GeoB97-020/027 showing the later stage channel-levee systems, regional unconformities, and faults. Modified from Schwenk and Spiess (2009). VE = vertical exaggeration. Horizontal scale = CMP, CMP distance = 20 m. Naming of channels follows Curray et al. (2003).

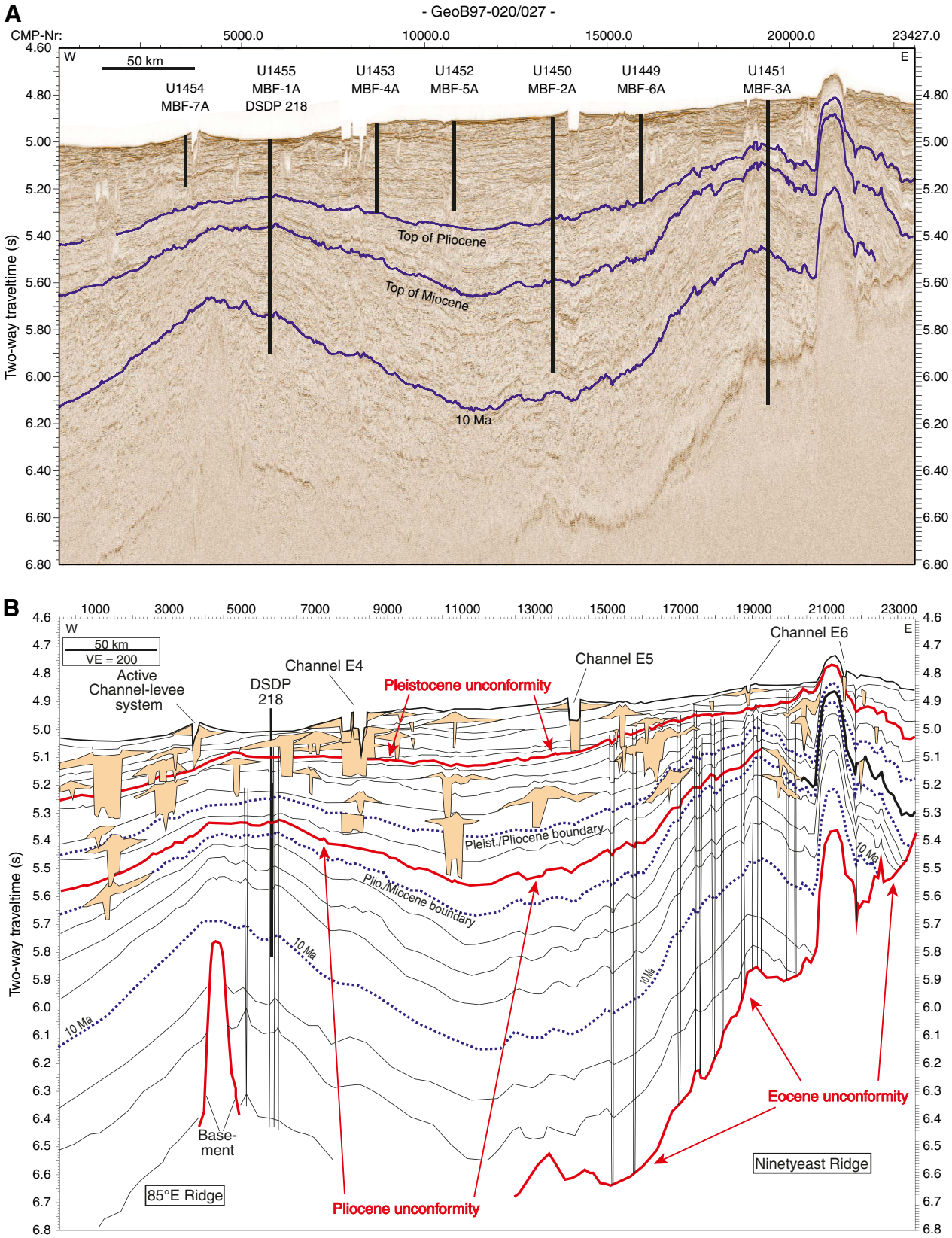

Figure F4. Location of Expedition 354 drill sites.

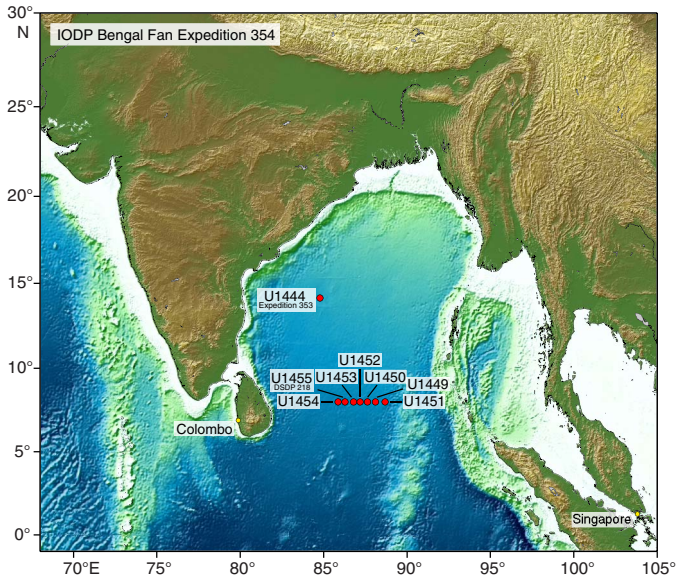

Figure F5. Compilation for the upper 250 m of the seven-site drilling transect at 8°N from west to east, comprising subbottom depth axis, core numbers and recovery, and major and minor lithologies for the deepest hole at each site. Geographic longitude is given for each hole.

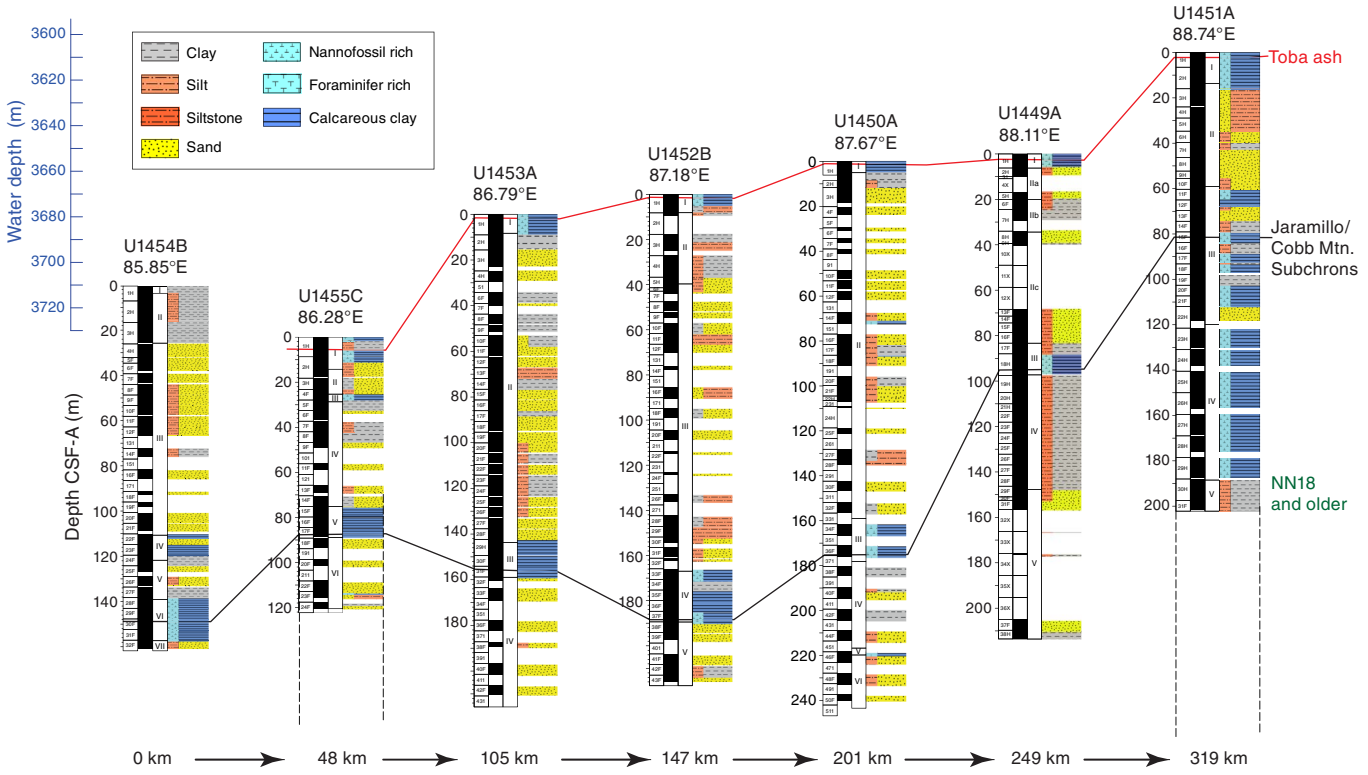

Expedition 354 builds on knowledge acquired during earlier drilling and seismic exploration of the Bengal Fan (DSDP Leg 22; Ocean Drilling Program [ODP] Leg 116; and R/V *Sonne* Cruises SO93 [Legs 1–3] and SO125, SO126, and SO188 [Legs 1 and 2]) and on current studies of the tectonic, geologic, geomorphological, and sedimentological processes acting on the Himalaya, the floodplain and delta of the Ganga-Brahmaputra, and the Bengal Fan. This expedition is one part of an integrated effort for International Ocean Discovery Program (IODP) drilling syntectonic basins around the Himalaya to improve our knowledge of monsoon evolution and its interaction with Himalayan growth and erosion. This includes in particular IODP Expeditions 353 (Indian Monsoon) and 355 (Arabian Sea Monsoon) on the Indus Fan.

Figure F6. Compilation of the three deep holes of the drilling transect at 8°N from west to east, comprising subbottom depth axis, recovery, and major and minor lithologies for each site.

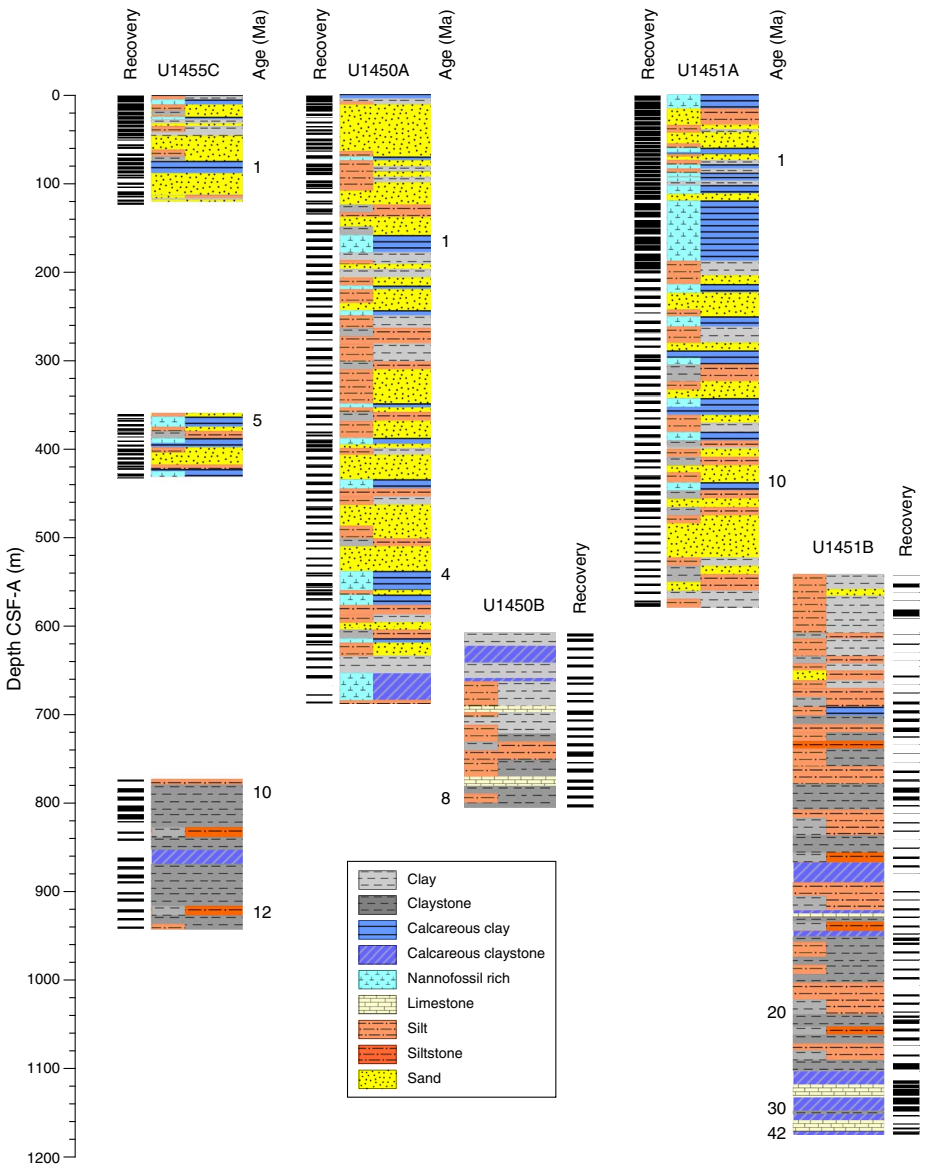

Table T1. Expedition 354 operations summary. See Figure **F4** for location of drill sites. **Download table in .csv format.**

Hole	Proposed site	Location	Water depth (mbsl)	Total penetration (m)	Interval cored (m)	Interval drilled without coring (m)	Core recovery (m)	Core recovery (%)	Time on hole (d)	Cores (*N*)
354-										
U1449A	MBF-6A	8°0.4194′N, 88°6.5994′E	3652.7	213.5	212.5	1.0	129.38	61	2.9	37
U1449B		8°0.4206′N, 88°6.6091′E	3651.9	7.9	7.9	0.0	7.91	100	0.5	1
			Site U1449 totals:	221.4	220.4	1.0	137.29	62	3.4	38
U1450A	MBF-2A	8°0.4201′N, 87°40.2478′E	3655.3	687.4	444.7	242.7	282.73	64	6.4	86
U1450B		8°0.4192′N, 87°40.2586′E	3655.4	811.9	203.9	608.0	46.67	23	4.0	21
			Site U1450 totals:	1499.3	648.6	850.7	329.40	51	10.4	107
U1451A	MBF-3A	8°0.4195′N, 88°44.5012′E	3607.3	582.1	394.9	187.2	337.80	86	4.8	72
U1451B		8°0.4203′N, 88°44.4745′E	3607.2	1181.3	627.6	553.7	180.86	29	13.1	70
			Site U1451 totals:	1763.4	1022.5	740.9	518.66	51	17.9	142
U1452A	MBF-5A	8°0.4196′N, 87°10.9001′E	3670.5	8.0	8.0	—	8.03	100	0.6	1
U1452B		8°0.4191′N, 87°10.9128′E	3670.3	217.7	174.5	43.2	138.21	79	1.8	34
U1452C		8°0.4088′N, 87°10.9116′E	3671.5	41.3	41.3	—	33.30	81	0.8	6
			Site U1452 totals:	267.0	223.8	43.2	179.54	80	3.1	41
U1453A	MBF-4A	8°0.4193′N, 86°47.8973′E	3679.5	215.7	186.7	29.0	164.78	88	3.6	37
			Site U1453 totals:	215.7	186.7	29.0	164.78	88	3.6	37
U1454A	MBF-7A	8°0.4067′N, 85°50.9882′E	3709.9	7.5	7.5	—	7.54	101	0.4	1
U1454B		8°0.4083′N, 85°51.0025′E	3710.3	161.8	147.4	14.4	129.51	88	1.6	29
U1454C		8°0.3968′N, 85°51.0033′E	3710.3	37.2	37.2	—	30.16	81	0.4	6
U1454D		8°0.3975′N, 85°50.9927′E	3710.7	37.1	37.1	—	24.46	66	3.4	5
			Site U1454 totals:	243.6	229.2	14.4	191.67	84	5.7	41
U1455A	MBF-1A	8°0.4189′N, 86°16.9983′E	3732.5	0.9	0.9	—	0.90	100	0.4	1
U1455B		8°0.4198′N, 86°17.0096′E	3733.0	6.9	6.9	—	6.88	100	0.1	1
U1455C		8°0.4081′N, 86°17.0090′E	3732.5	949.0	350.7	598.3	198.00	56	7.1	54
			Site U1455 totals:	956.8	358.5	598.3	205.80	57	7.6	56
			Expedition 354 totals:	5167.2	2889.7	2277.5	1727.12	60	51.6	462
353-										
U1444A	MBF-10	14°0.0057′N, 84°49.7405′E	3127.7	330.6	330.6	0.0	226.05	68	3.0	37
U1444B		13°59.9940′N, 84°49.7412′E	3131.8	128.6	81.1	47.5	74.16	91	1.0	9
			Expedition 353 totals:	459.2	411.7	47.5	300.21	73	3.9	46

Background

Geological setting

The Bengal Fan covers the entire floor of the Bay of Bengal (Figure **F2**), from the continental margins of India and Bangladesh to the sediment-filled Sunda Trench off Myanmar and the Andaman Islands and along the west side of the Ninetyeast Ridge. It spills out south of the Bay of Bengal at its distal end to ~7°S. Another lobe of the fan, the Nicobar Fan, lies east of the Ninetyeast Ridge, but it apparently was cut off from its primary source of turbidites, the head of the Bay of Bengal, during the Pleistocene by convergence between the northern end of the Ninetyeast Ridge and the Sunda Trench. The northeastern edges of the fans are subducted, and some of the Tertiary turbidites cropping out in the Indo-Burman Ranges of Myanmar, the Andaman and Nicobar Islands, and the outer arc ridge off Sumatra are interpreted as old Bengal and Nicobar Fan sediments.

Following the initial bathymetric discovery of the fan extension by Heezen and Tharp (1966), the Bengal and Nicobar Fans were delineated and named by Curray and Moore (1974), who also noted two horizons in reflection and refraction seismic data that pass into unconformities over the exposed and buried hills of folded sediments in the southern part of the fan and over the Ninetyeast Ridge. They concluded that these two horizons are regional and used them to divide the sedimentary section into three units in the Bay of Bengal. The ages of these unconformities were tentatively determined to be uppermost Miocene and upper Paleocene to middle Eocene during Leg 22 (Moore et al., 1974; Shipboard Scientific Party, 1974) at Sites 218 and 217, respectively (Figure **F2**). Curray and Moore (1974) interpreted the older unconformity as having been initiated by the India-Asia collision, with the pre-Eocene sedimentary unit consisting of pelagic sediment and terrigenous material derived from India before the collision. Hence, the upper two sedimentary units define the Bengal Fan sensu stricto. Curray and Moore (1974) associated the upper Miocene unconformity with intraplate deformation, probably correlated with a plate edge event. These tentative age assignments were further confirmed and refined by later drilling during ODP Legs 116 and 121 (Cochran, Stow, et al., 1990; Peirce, Weissel, et al., 1989), although the interpretation and significance of the older unconformity and the time of initiation of Bengal Fan deposition and progradation remain very controversial.

The older unconformity was drilled and sampled only on the Ninetyeast Ridge. Correlation of this unconformity off the ridge into the fan section is possible along some but not all seismic lines (e.g., Gopala Rao et al., 1994, 1997; Krishna et al., 1998; Schwenk and Spiess, 2009). Leg 22 sites sampled the older unconformity. DSDP Site 215 showed a hiatus from early Eocene to late Miocene (Figure **F7**). DSDP Site 211, located at the eastern distal edge of the Nicobar Fan, showed a hiatus from some time after the Maastrichtian until the Pliocene. The overlying younger sections are interpreted as distal fan.

Eocene initiation of Bengal Fan deposition is also suggested by the geology of Bangladesh, the Indo-Burman Ranges of India and Myanmar, and the Andaman-Nicobar Ridge. Hydrocarbon explora-

Figure F7. Estimated age span of Bengal Fan sedimentation vs. distance from the present apex or source of the fan. Shaded area at each site = known age span of fan sedimentation. The duration of the apparent hiatus was short near the source and long in the lower and distal fan. This plot is oversimplified because the distance from the fan apex changed through time with convergence of the Indian and Eurasian plates and with progradation of the delta in Bangladesh. IB ranges = Indo-Burman ranges, A-N Ridge = Andaman-Nicobar Ridge. DSDP and ODP numbers are sites.

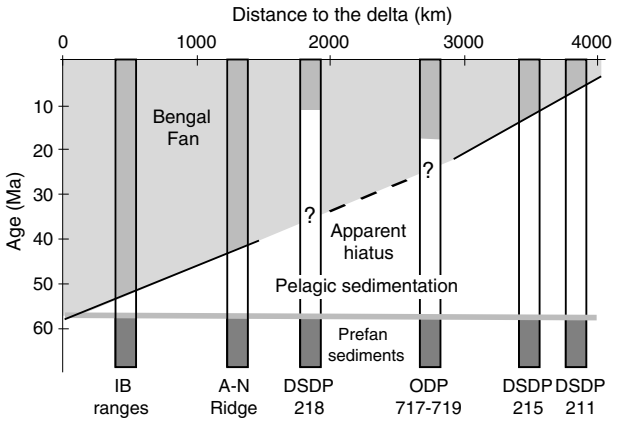

tion onshore and offshore from southeastern Bangladesh (e.g., Kingston, 1986) shows total sediment thicknesses calculated from gravity to be >20 km, apparently with the Eocene and Oligocene Disang Series of deepwater shales and turbidites overlying oceanic crust. These are in turn overlain by Neogene prograding deposits of the Bengal Delta and the Ganga-Brahmaputra (Jamuna) river system, the Meghna River, and their ancestral rivers. Some of these rocks are mildly metamorphosed and uplifted into the accretionary prism in the Indo-Burman Ranges, with some sparsely fossiliferous flysch units correlated with the Disang Series (e.g., Brunnschweiller, 1966; Bender, 1983; Najman et al., 2008). Similar turbidites, the Andaman Flysch or Port Blair Formation, are found in the Andaman and Nicobar Islands, again usually assigned to Eocene and Oligocene ages (e.g., Karunakaran et al., 1975; Acharyya et al., 1991) and interpreted to represent parts of the early Bengal Fan, some of which are incorporated into the Sunda arc accretionary complex.

The initiation of deposition and progradation of the Bengal Fan followed the collision of India with Asia and the formation of a large proto-Bay of Bengal. Continued convergence of the Indian and Australian plates with the Southeast Asian plate reduced the size of the bay and focused the source of turbidites into the present Bengal Basin, Bangladesh shelf, and the Swatch-of-No-Ground (SoNG) shelf canyon (Curray et al., 2003).

Fans grow by progradation, and the first sediments are deposited at the mouth of a canyon and at the base of the slope, typically the continental slope. With time, fans prograde farther from the original base of the slope. Our limited information suggests that the Bengal Fan has prograded, as shown in Figure **F7**. The oldest rocks interpreted as Bengal Fan in the Indo-Burman Ranges are early Eocene; the oldest such turbidites in the Andaman and Nicobar Islands are middle Eocene. Sites 215 and 211 revealed upper Miocene and Pliocene turbidites, respectively. Neither Site 218 nor the Leg 116 sites reached the base of the fan. The interpretation that the Eocene unconformity marks the base of the fan suggests that it may represent a hiatus of variable duration (Figure **F7**).

Sediment delivery into the Bengal Fan originates from the SoNG (Kottke et al., 2003; Michels et al., 1998; Palamenghi, 2011), which represents the only feature of this kind today. Sediments from the Ganges, Brahmaputra, and Meghna Rivers are transported to the mouth and then westward by currents parallel to the delta front (Kudrass et al., 1998). Approximately one-third of the Himalayan material is stored in the floodplain, and a significant portion is constructing a prograding shelf sequence (Goodbred et al., 1999). The remaining portion, approximately one-third, enters the SoNG, for example, by coast-parallel currents, partially initiated by storm events (Kudrass et al., 1998), to be finally delivered to the Bengal Fan.

Mechanisms of this transport, which must be associated with the initiation of turbidity currents, are largely unknown. However, sediment physical data for 47 cores along the 3000 km long transport path from the delta platform to the lower fan distinguish different turbiditic environments (Weber et al., 2003). One of the main characteristics of the Bengal Fan is the presence of channel-levee systems of remarkable size (e.g., Hübscher et al. 1989; compilation by Curray et al., 2003). They are believed to form from mostly unchannelized turbidity currents. If they are able to erode the seafloor to the degree that an incision forms, subsequent turbidity currents are confined. As a consequence, erosion is enhanced, the cross section of the turbidity current is further constrained, and turbulent energy can be maintained over very long distances. If sufficient fine-grained material is incorporated in the suspension cloud, spillover deposits can form a wedge-shaped geometry because the sedimentation decreases with lateral distance from the channel axis (levee), constructing a channel-levee system.

For the Bengal Fan, these turbidity current characteristics were described in detail along the active channel by Hübscher et al. (1997), Weber et al. (1997, 2003), and Schwenk et al. (2003, 2009). Work by Hübscher et al. (1997) and Schwenk and Spiess (2009) confirms an overall similarity of channel-levee complexes and their geometries, scales, and distribution downfan between 8°N and 16°N. Weber et al. (1997) show that these levees can build up over short time spans of several thousand years. Schwenk et al. (2003) further demonstrate that the evolution of these deep-sea channels led to a pronounced, meandering formation of cut-off loops and their subsequent fill. In this sense, the latitudinal drilling transect will well recover the characteristics of Bengal Fan architecture, whereas the sediment delivery system through channels will likely reveal a pronounced spatial and temporal variability over relatively short time periods.

Interlevee sediments are assumed to represent a lobe of progradational coarse-grained silty to sandy facies with the channel termination upslope, as it may occur, for example, after a channel avulsion. Subsequently, levee units form after the establishment of a channel, which typically erodes into previously deposited units. At the early stage, wedge-shaped units of high reflectivity may form from coarser grain size because of limited channel depth. The wedge-shaped units of lower reflectivity are supposed to be caused by overspill and flowstripping from turbidity currents that pass through the channel, likely originating at the SoNG on the Bangladesh shelf. Levee sediments are supposed to be mostly composed of silty to clayey material with a tendency to fine upward with increasing levee height. Hemipelagic units form when sediment supply is shut down or distal, thus creating a layer of almost constant thickness throughout large areas of the fan.

So far, distal (Leg 116) and middle fan sediments were demonstrated to reflect Himalayan geological sources (Stow et al., 1990; France-Lanord et al., 1993) and were used to track the evolution of the erosion rate of the Himalayan range (Copeland and Harrison, 1990) and the paleovegetation of the basin (France-Lanord and

Derry, 1994; Galy et al., 2010) and to scale the impact of Himalayan erosion on the long-term carbon cycle through silicate weathering and organic carbon burial (France-Lanord and Derry, 1997).

Seismic studies/site survey data

The original IODP proposal for this expedition (552) was based on a single 500 km long multichannel seismic line at 8°N (GeoB97-020/027), which was acquired during R/V *Sonne* Cruise SO125 in 1997 (Spiess et al., 1998) to gain a better understanding of the buildup of the fan with respect to channel-levee geometries and stacking patterns (Figure **F3**). For stratigraphic calibration, this seismic profile crossed DSDP Site 218, where sediments were cored and dated to the middle Miocene at 773 mbsf.

To further support IODP Proposal 552, a dedicated presite survey during R/V *Sonne* Cruise SO188-1 was carried out in June–July 2006. This cruise collected multichannel seismic, swath bathymetric, and Parasound subbottom profiler data on crossing lines through all previously proposed Sites MBF-2A through MBF-6A (Sites U1449–U1453). These additional data provided further understanding of the spatial variation of sediment structures, particularly the underlying complex structures of buried channels (Figures **F3**, **F8**). Shallow-penetration sediment cores were taken at selected sites to complement the data already available from Site 218 (Site U1455).

The long seismic reflection Profile GeoB97-020/027 (Figure **F3**) was interpreted with respect to the presence of channels, channel-levee systems, and seismic stratigraphy (Schwenk and Spiess, 2009). Several major reflectors and unconformities were traced across the drilling transect, revealing increased average sedimentation rates as a function of distance from the basement ridges at 85°E and 90°E. Age constraints provided by correlation to Site 218 (Figure **F9**) suggest that the shallow-penetration sites (U1449, U1452, U1453, and U1454) extend to near the Pleistocene/Pliocene boundary and the mid-depth penetration sites (U1450 and U1455) extend to at least 8 Ma. Our deepest penetration and easternmost site (U1451) was selected to provide prefan sediments by drilling through the regional Reflector P (Eocene unconformity).

For Expedition 354, these data were reprocessed to improve lateral resolution from 20 to 10 m and vertical resolution to a higher bandwidth through conservative filtering and advanced noise suppression. Data examples shown in this report originate from these new data sets, which are superior to the original data set used by Schwenk and Spiess (2003).

Swath bathymetric data were acquired during Cruise SO125 using a Hydrosweep DS System and during Cruise SO188-1 using a Simrad EM120 echo-sounder system. The total multibeam coverage width is 19 km, increasing in those areas where crossing lines were shot. Although bathymetry reveals a clear picture of the recent or Quaternary channel systems in the area, this information only applies to the upper few tens of meters of the section, which is otherwise a mix of stacked older channels and interlevee sequences. Digital Parasound subbottom profiler data (4 kHz) were also routinely collected during both cruises.

Figure F8. Map showing proposed Expedition 354 drill sites of on top of multibeam bathymetry. Available seismic lines from R/V *Sonne* Cruises SO125 (black) and SO188 (red) are indicated. Profiles crossing the sites are highlighted. See Site summaries and appendix figures in France-Lanord et al. (2014) for seismic data at each proposed site.

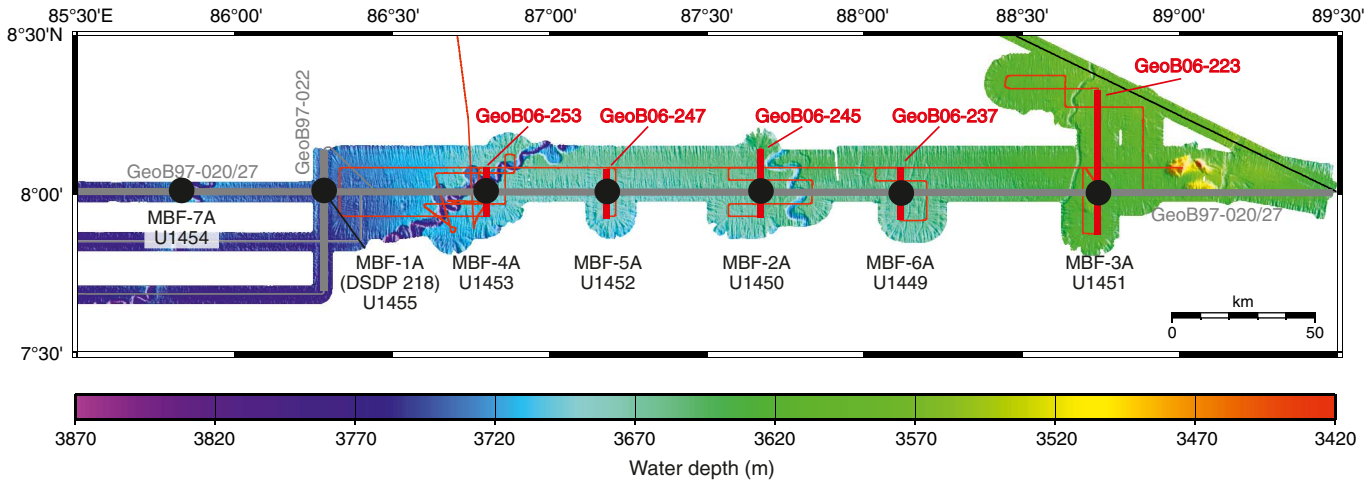

Figure F9. Core recovery, lithostratigraphic column (von der Borch, Sclater, et al., 1974), and carbon isotopic composition of total organic matter showing the transition from C3 to C4 photosynthetic plants around 380 mbsf (Galy et al. 2010), DSDP Site 218.

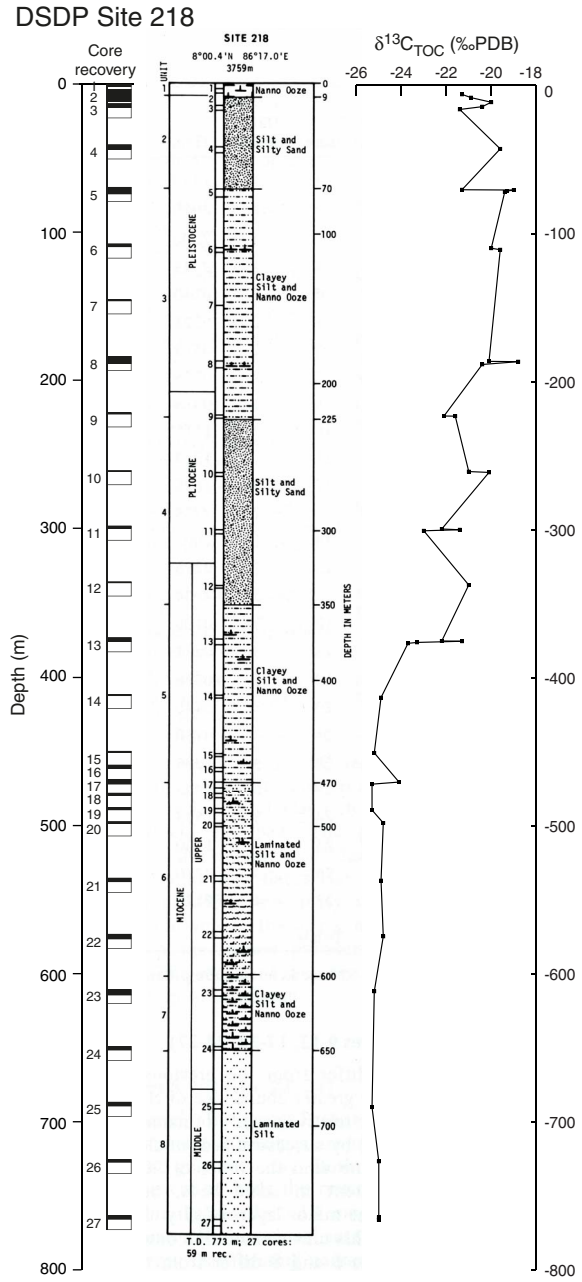

Scientific objectives

Expedition 354 was designed to reconstruct the erosional history of the Himalaya and its bearing on the development of the Himalaya and Tibet as topographic features and to document the relationship between erosion and climate throughout long-term and short-term fluctuations of the Indian monsoon as recorded in the Bay of Bengal.

1. *Calibration of Neogene to present changes*

Although the Miocene to recent sedimentary records in the Bengal Fan suggest that since 18 Ma Himalayan erosion was comparable to the modern regime in many ways, tectonic and climatic changes have occurred that are both likely to have influenced sedimentation in the Bay of Bengal. This includes upper Miocene changes in accumulation rate, continental vegetation, and weathering intensity that are documented both in the continental basin and the Bengal Fan (e.g., Quade and Cerling, 1995; France-Lanord et al., 1993; Burbank et al., 1993; France-Lanord and Derry, 1994; Martinod and Molnar, 1995; Clift et al., 2008; Galy et al., 2010). The development of intense channel-levee deposition in the Bengal Fan starts appearing in the upper Miocene or Pliocene and is also the mark of major change in sediment delivery to the Bay of Bengal (Schwenk and Spiess, 2009). During the late Pliocene, global cooling led to the growth of ice sheets in the Northern Hemisphere, which appears to be related to a global increase in detrital sedimentation rate and grain size (Zhang et al., 2001). Although the reality of this change has been questioned (Willenbring and von Blanckenburg, 2010) the evolution to higher climate instability should prevent an equilibrium state of fluvial and glacial basins and trigger their erosion. Such changes were observed in the distal Bengal Fan around ~0.8–1 Ma when the 100 ky cycle became strong. This expedition documents this critical period in Earth's most intense erosion system, as tectonic and climate changes have left signatures in accumulation rates, grain sizes, physical properties, clay mineralogy, isotopic ratios, organic carbon burial, and so on, that will be tracked with postexpedition studies.

First, to what extent are variations in accumulation rates, clay mineralogy, and grain sizes from ODP Sites 717–719 (Figures **F2**, **F7**) representative of other parts of the fan? Because those holes only recovered sediments from the most distal parts of the Bengal Fan within a growing syncline, sedimentation might have been affected both by the large distance from the source and by the barrier imposed by the surrounding anticlines. The decreases in accumulation rate and grain size at ~7 Ma and the synchronous increased percentage of smectite (Bouquillon et al., 1990) suggest that if the monsoon strengthened at that time, it apparently did so without creating a more energetic erosive system, as might be expected from the strong seasonal precipitation of the monsoon. Obviously, if we find the same pattern of low accumulation rates, small grain sizes, and a large percentage of smectite at 7–8 Ma in the holes cored at 8°N during Expedition 354, we must consider the possibility that if the monsoon strengthened at that time, it did so by decreasing, not increasing, erosion rates. If we find a sediment history different from that at Sites 717–719, it is possible that the sedimentary record at the distal edge of the fan does not record faithfully the changes in input at the source of the fan.

The present-day monsoon, if named originally for the seasonally steady winds over the Arabian Sea, also evokes the image of heavy rain over the Indian subcontinent. We have no evidence to date, or perhaps conflicting evidence, showing that precipitation increased over the Ganga and Brahmaputra drainage basins and the Bay of Bengal at 7–8 Ma (Derry and France-Lanord, 1997; Dettman et al., 2001) despite enhanced Indian monsoon seasonality over this period (Zhisheng et al., 2001). Assessing paleomonsoon intensity is challenging and can be tracked with two approaches. First, the efficiency of sediment transport from the Himalaya to the Bay of Bengal is somewhat controlled by the seasonality and intensity of rainfall that trigger high river discharge (Lupker et al., 2011). This transport in turn exerts control on sediment fluxes to the Bay of Bengal that can be traced by accumulation rates. Second, $\delta^{18}O$ in planktonic foraminifers deposited in the Bay of Bengal in the late Quaternary is related to precipitation amounts (Duplessy, 1982). If

these microfossils can be recovered, they will provide another tool to assess the strength of the monsoon.

The main reason for drilling more than one site at 8°N is to minimize the effects of (1) varying sedimentation rates associated with pronounced increases in the vicinity of the active channel over time and (2) the migration of the active channel, hence avoiding biases that one site (or a set of adjacent sites) might give. Although the main focus of these sites is on the changes near 7–8 Ma, obviously we will obtain a Himalayan erosion record over a longer period that will allow analysis of the Himalayan response to monsoon fluctuation over the early Miocene, as proposed by Ramstein et al. (1997) and Fluteau et al. (1999), or the Oligocene (Licht et al., 2014).

In addition, we plan to study other temporal and spatial variations in the sediment over the last 7 My. Site 218 and sites cored during Leg 116 show changes that possibly reveal other variations in the erosion regime. Data from Kroon et al. (1991) show a dip in the abundance of *Globigerina bulloides* at ~5 Ma, which might indicate a lull in the monsoon, the temporary dominance of another upwelling-sensitive foraminifer (Kroon et al., 1991), or some other inadequacy of *G. bulloides* to measure monsoon strength. We also seek quantitative measures of the interaction between climate change and sedimentation associated with global cooling and the onset of Northern Hemisphere glaciation at ~2.7–3.3 Ma and with the change from precession- and obliquity-dominated climate variations to the strong 100 ky cycle at 0.8–1.2 Ma. The latter change appears to be marked by changes in deposition rates, grain sizes, and clay mineralogy at Sites 717–719 (France-Lanord et al., 1993). Again, one objective is to decide how representative the results from Sites 717–719 are. The same proxies for monsoon strength and erosion will be available for study of this period. The results from Sites 717–719 reveal no evidence of a change in erosion rate at 2.7–3.3 Ma, in contrast with what might be expected if glacial erosion were important and increased at that time. Moreover, if the only important change in sedimentation rate, and hence presumably in erosion rate, occurred at 0.8–1.2 Ma, such a change would provide a clue to what kind of change was important. We anticipate being able to resolve temporal variations on the timescale of orbital variations, but obviously we must expect significant variations in sedimentation rates. Hence, the seven-site transect approach was designed to resolve as completely as possible the time record for a given time slice.

The 7 Ma transition is also marked by an expansion of C4 photosynthetic plants in the Himalayan basin (Quade et al., 1989). Although C4 plant expansion may result from a global decrease in atmospheric pCO_2 (Cerling, 1997), studies suggest that PCO_2 was already low at that period (Pagani et al., 1999; Beerling and Royer, 2011). In the latter hypothesis, C4 plant expansion would instead require an adaptation to more arid conditions in the floodplain. Sediments sampled during Leg 116 show close links among variations in clay mineralogy (smectite/illite ratio), total organic carbon (TOC), and $\delta^{13}C$ (C3 versus C4 plants) (Figure **F10**) (France-Lanord and Derry, 1994; Freeman and Colarusso, 2001). These relationships suggest changes in sediment provenance, with a mountain end-member delivering material unaltered with low organic carbon content of C3 type and a floodplain end-member delivering altered material with high organic carbon content of C4 type. If confirmed by new drilling at the scale of the entire fan, such relations would favor the hypothesis of a regional climate change to dryer conditions. Combining these with more sophisticated molecular and isotopic biomarkers (e.g., Galy et al., 2011; Contreras-Rosales et al., 2014) will reveal more accurately the link between monsoon intensity and plant distribution as a function of sediment origin.

2. Forcing of the carbon cycle and climate

Drilling the Bengal Fan should allow investigation of the effect of Himalayan erosion on the global carbon cycle, which has been debated (e.g., Raymo and Ruddiman, 1992; France-Lanord and Derry, 1997; Galy et al., 2007; Goddéris and Donnadieu, 2009). Ero-

Figure F10. Accumulation rate (Gartner, 1990), clay mineralogy (Bouquillon et al., 1990), Nd isotopic data (Derry and France-Lanord, 1996; France-Lanord et al., 1993; Galy et al., 1996), and TOC isotopic composition (France-Lanord and Derry, 1994), ODP Holes 717C and 718C. Ages recalculated using timescale of Cande and Kent (1995). Low sedimentation rates, smectite-kaolinite clays, and organic carbon derived from C4 plants characterize the interval from 7.4 to 0.9 Ma. Nd isotopic composition does not change during the entire time recovered, suggesting the eroded source of material is not significantly changing. Biostratigraphic constraints on sediment accumulation are uncertain for the early Miocene. The apparent increase in sedimentation rate near 12 Ma could be an artifact of poor biostratigraphic control prior to that time.

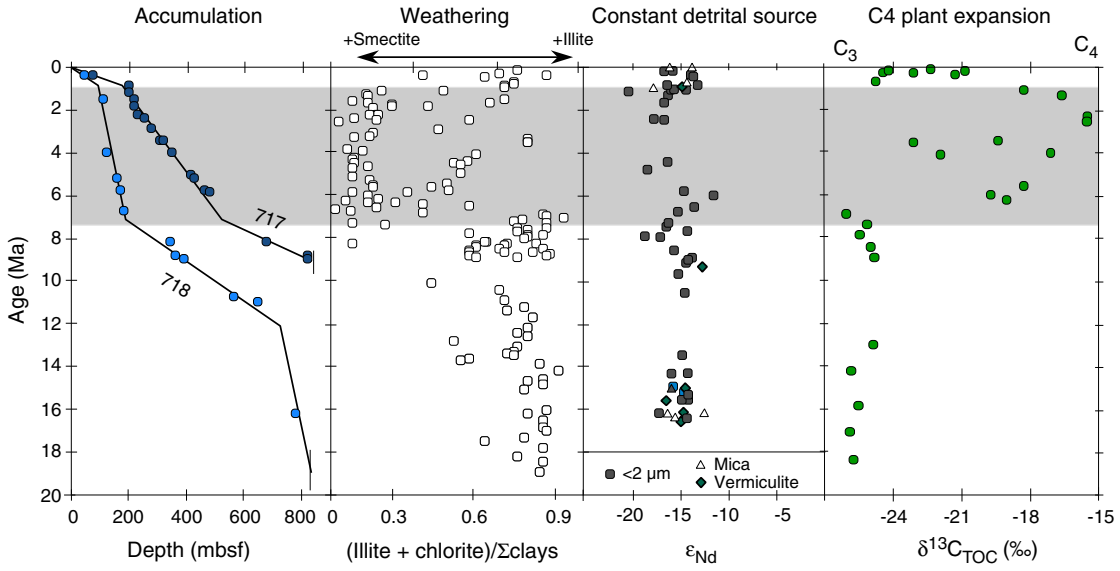

sion tends to consume atmospheric carbon by two mechanisms. First, weathering of silicates produces fluvial alkalinity flux that can later precipitate as carbonate in seawater. Second, plant debris and organic carbon are transported with the particulate flux and can be buried in deep-sea sediment. Ultimately, both mechanisms will take up carbon from the atmosphere and store it over long periods in the sedimentary reservoir. Observation of modern fluxes of erosion and of Bengal sediments suggests that the Himalayan erosion mostly consumes atmospheric CO_2 through burial of organic carbon preferentially to silicate weathering. Nevertheless, it remains impossible to assess the magnitude of these processes at a global scale because past fluvial fluxes are unknown. Sediment volume and geochemistry can provide direct and interpretable records of these fluxes if their accumulation rates in the Bengal Fan can be determined with sufficient accuracy. Our transect of drill sites at 8°N was designed to document the regional scale of such fluxes during the Neogene that can be extrapolated throughout the entire fan. The deepest penetration Site U1451 was designed to allow exploration of weathering and carbon burial prior to the Neogene.

3. Sampling of the oldest sediment of the fan

Scenarios of the timing and geometry of the collision between India and the rest of Eurasia suggest that collision in the western Himalaya occurred between 50 and 55 Ma, and perhaps later (~45 Ma) in the eastern Himalaya, near Everest for example (Rowley, 1996, 1998). However, there are contrasting models for the slowdown of Indian plate motion and the geometry of the collision (e.g., Dupont-Nivet et al., 2010; Van Hinsbergen et al., 2011; Aitchison et al., 2007; Zhang et al., 2012). When the Himalaya emerged as a mountain range, however, remains less certain. Extending the record of sedimentation back in time should allow determination not only of when erosion began but also of when erosion penetrated deep enough into the crust to expose rapidly cooled minerals. In particular, we should be able to determine cooling ages of minerals whose closure temperatures are different, and from the isotopic signature, we should be able to identify what rock of the Himalaya has eroded. Differences between cooling ages and stratigraphic ages will then allow estimates not only of when erosion began but also of when erosion exhumed rock from different depths (Copeland and Harrison, 1990; Corrigan and Crowley, 1992; Galy et al., 1996).

Determining when emergence of the Himalaya took place might not provide any surprises. Nevertheless, all of the rock cropping out in the Himalaya was carried by the Indian subcontinent and scraped off it following collision with Eurasia. Thus, given India's convergence rate of ~50 km/My toward Eurasia since 45 Ma, if collision occurred at 45 Ma but erosion began only at 35 Ma, we might infer that as much as 500 km of intact lithosphere was subducted beneath southern Eurasia before a significant mountain range formed. Conversely, if deposition of rock with a Himalayan isotopic fingerprint began shortly after 45 Ma, we must infer that some off-scraping of Indian crust occurred early in the history of the collision to build the initial Himalaya. Finally, we can imagine a flux of sediment early in the history of the collision, but of Tibetan, not Himalayan, origin. This would suggest some not necessarily easily quantified subduction of India beneath southern Tibet before thrust faulting within India created the Himalaya.

The well-known increase in the $^{87}Sr/^{86}Sr$ ratio of seawater beginning at ~40 Ma (DePaolo and Ingram, 1985; Hodell et al., 1989) is commonly attributed to increased erosion and weathering in the Himalaya (Edmond, 1992; Galy et al., 1999; Krishnaswami et al., 1992). A strong Himalayan signature, not only beginning at ~38 Ma but also contributing a pulse near 18 Ma (Richter et al., 1992), should, therefore, be corroborated in the sedimentary record of Himalayan erosion. This would be supported if detrital silicates with high $^{87}Sr/^{86}Sr$ ratios increased both at ~40 Ma and near 18 Ma. By extending the sedimentary record in the Bay of Bengal through the Oligocene, we can examine the hypothesized correlation of the increased marine Sr isotopic ratio at 18 Ma with weathering of Himalayan rock rich in radiogenic strontium. If we can sample the early history of Himalayan erosion, we can test the assumption that the increasing Sr isotopic ratio beginning at ~38 Ma also results from weathering of Himalayan rock. The sensitivity of the seawater Sr isotopic budget to the Himalayan flux is so high (Galy et al., 1999) that the seawater evolution through time provides a unique system where erosion rate may be estimated using a proxy other than accumulation rates.

The Bengal Fan is one of the thickest sediment sections in the world, and it is far too thick to sample the very old section. The oldest part of the fan sampled to date was at Site 718 more than 2500 km from the present apex of the fan, where early Miocene sediment (~17 Ma) was recovered. Because of its southern position and great water depth, this site is not adequate to penetrate the "oldest" sediment derived from the Himalaya because the fan may not have prograded so far south (e.g., Curray, 1994). Our deepest proposed site (U1451; proposed Site MBF-3A) is located on the west flank of the Ninetyeast Ridge, ~1300 km from the thickest section of the fan, where the section is thinner and where a possible Paleocene–Eocene unconformity ("P" horizon) could be reached at a reasonable depth (Curray et al., 1982).

4. Fan architecture and spatial depocenter variability

Since the Pliocene, sedimentation in the Bengal Fan has been dominated by deposition in channel-levee systems (Schwenk and Spiess, 2009). During this period, it appears the fan was built by an accumulation of lenses corresponding to distinct channel-levee episodes intercalated by more slowly accumulating intervals of fine-grained sediment (Figure **F3**). Channels carry a flux of sediment for a brief period, apparently only for approximately thousands of years, and then fill with sediment as portions are abandoned and a new channel is cut into the levee system or outside it. Thus, accumulation at any point is likely very irregular. In the upper fan, accumulation varies from rates >30 m/ky for periods as long as 3000 y (Hübscher et al., 1997; Michels et al., 1998; Spiess et al., 1998; Weber et al., 1997) to very low accumulation rates in intervening periods. Nd-Sr isotopic signatures and bulk mineralogical and geochemical properties demonstrate that sediment accumulated in levees is dominated by Himalayan material, whereas very low accumulation hemipelagic deposits have distinct isotopic signatures in the upper fan, showing that other sources are mixed with Himalayan flux (Pierson-Wickmann et al., 2001). Determining the distribution and typical lifetime of depocenters is vital for interpreting the older sedimentary record of the fan and assigning different types of sedimentary facies and successions found in deep drill holes to structural units. To address this objective, the seven sites distributed over a 300 km transect were designed to obtain sufficient spatial resolution on the basis of a typical width of a channel-levee system on the order of ~50 km. The shallower, ~300 m penetration sites will record the stacking of more than two systems.

Expedition 354 was designed to significantly improve and refine the poor existing age constraints (currently based only on spot-cored Site 218; Figure **F9**) of the stratigraphic and structural elements identified in the seismic data. This improvement is especially

critical for constraining the transition from early sheet-like turbidite deposition to the onset of channel-levee systems that occurred in the latest Miocene (Schwenk and Spiess, 2009). Because most surface channels reach this part of the fan, it is believed that this marks the start of the development of channel-levee systems on the Bengal Fan generally (Figure **F3**). Two reasons might be responsible for the onset of the channel-levee systems: (1) the initial creation of a canyon as point source or (2) changes in grain size of the delivered sediments transported by turbidity currents to the fan. The three drill sites targeting recovery of late Miocene sediments (Sites U1455, U1450, and U1451) will prove whether there were changes in grain size (as interpreted from Leg 116 results) and whether the onset of the channel-levee systems represents the first margin setting with a canyon and probably associated delta. Additionally, because several levees will be penetrated, new insights about the lifetime of distinct channel-levee systems will be gathered, which is so far only known for the active channel in the upper fan (Weber et al., 1997).

Additional objectives

Although Expedition 354 has been designed principally to document (1) Himalayan evolution and interactions with Indian monsoon evolutions and (2) turbiditic fan construction, drilling the Bengal Fan will allow additional important objectives to be addressed. This includes fan hydrology, Bengal Basin deformation, and deep biosphere issues.

1. *Fan hydrology and hydrochemistry*

The Bengal Fan is a major sedimentary reservoir filled by continental material including clays and organic matter that are likely to evolve during diagenesis. Pore water chemistry and O-H isotopic compositions documented on Leg 116 cores revealed a high variability of compositions that imply that low-salinity fluid is released through dehydration reactions probably deeper than in the cored sections and that fluid advection occurs under thermoconvective conditions at least in that portion of the fan (Boulègue and Barriac, 1990; Ormond et al., 1995). There are also indications for diverse diagenetic reactions that release significant amounts of Ca and Sr into the pore water reservoir. Pore water analyses and physical properties, along with downhole measurements, will constrain the magnitude of compaction, dehydration reactions, and possible fluid transfer. This will lead to refined estimates of geochemical fluxes from the fan to the ocean.

2. *Bengal Basin deformation*

Throughout the Neogene, the Bengal Basin underwent significant multiphase deformation that resulted in folding of the plate between the Ninetyeast Ridge and the 85°E Ridge (Krishna et al., 2001). In addition to the Miocene and Eocene unconformities (Curray et al., 2003), site survey data revealed two additional regional unconformities. Using the Site 218 age control, these were dated as Pleistocene and Pliocene, respectively (Schwenk and Spiess, 2009). These unconformities are interpreted to be equivalent to unconformities found in the central Indian Ocean, which are related to deformation events of the ocean lithosphere there (Cochran, 1990; Stow et al., 1990; Krishna et al., 2001). Additionally, several faults were identified in the seismic data, especially above the western flank of the Ninetyeast Ridge. These faults terminate within Pleistocene sediments, which also suggests tectonic events at least until the Pleistocene. As Site 218 dating is poorly constrained, we expect Expedition 354 results to allow more precise dating of unconformities and fault terminations, which in turn will improve the understanding of deformation events in the Bengal Basin.

3. *Deep biosphere*

Deep biosphere objectives were not specifically planned as a primary objective of this expedition, but specific sampling was conducted to document bacterial activity near the surface of the fan and at depth. These samples will allow us to explore the impact of terrigenous flux on bacterial development. The Bengal Fan represents one of the largest fluxes of terrestrial matter to the ocean with relatively fast accumulation. The apparent high preservation of terrigenous organic matter is a peculiar aspect of Bengal Fan sedimentation (Galy et al., 2007). Microbial activity is intimately intertwined with diagenesis and organic carbon degradation. Because preservation and burial of organic matter is one crucial parameter of the impact of Himalayan erosion on the carbon cycle, there is high interest in studying these processes.

Operations plan/drilling strategy

The operations plan and drilling strategy developed for Expedition 354 is fully described in the *Scientific Prospectus* (France-Lanord et al., 2014). Because Expedition 354 started in Singapore and ended in Colombo (Sri Lanka), an east–west sequence of sites was the most efficient. However, to better initiate overall shipboard laboratory operations and to best address the specific concern about the best approach to core in a sand-rich environment, we decided not to start with the easternmost site (U1451; proposed Site MBF-3A), which is the most challenging, deepest penetration site. Instead, we decided to start drilling at a short 300 m penetration location (Site U1449; proposed Site MBF-6A) with the advanced piston corer (APC) system, followed by a 900 m penetration location (Site U1450; proposed Site MBF-2A), to determine the depth of APC penetration and quality of XCB coring. The initial operations and time estimates for Expedition 354 planned for 56 days of operations on a very tight schedule. Nevertheless, large uncertainties were expected because of potentially poor recovery in sands and uncertain penetration rates that could affect good core recovery, feasibility of wireline logging, and overall hole conditions in rapidly deposited and loose sands. For these reasons and based on scientific interest, Site U1454 (proposed Site MBF-7A) was added during the expedition as an alternate site to extend the transect west of Site U1455 (proposed Site MBF-1A; DSDP Site 218) to core the most recent levee sequence.

The initial coring plan and time estimate included using only APC/extended core barrel (XCB) at all sites, except for Site U1451 (proposed Site MBF-3A), where rotary core barrel (RCB) coring would be needed for deep penetration. Time was allocated for only a single hole at each site to the total target depth. If coring conditions (recovery, core quality, and penetration rate) required, the half-length APC (HLAPC) would be used to obtain deeper high-quality cores, but the additional wireline time was not included in the pre-expedition time estimates. We also planned for orientation for all full-length APC cores using nonmagnetic hardware as much as possible and a basic program of formation temperature measurements. A second hole was planned at our deepest penetration site (Site U1451; proposed Site MBF-3A) consisting of RCB coring through the Eocene unconformity estimated to be at ~1500 m. The option to stabilize this second hole with a preassembled reentry cone with 400 m casing was considered the best approach to achieve the deep coring and logging objectives, but the time to install it was not included in the pre-expedition time estimates.

Wireline logging was planned for our three deepest penetration sites (Sites U1451, U1450, and U1455; proposed Sites MBF-3A,

MBF-2A, and MBF-1A, respectively). These were intended to consist of two logging runs (triple combination [triple combo] and Formation MicroScanner [FMS]-sonic tool strings) and a check shot survey (Versatile Seismic Imager [VSI]) if hole conditions allowed.

Sampling and data sharing strategy

The shipboard sampling strategy was defined with each laboratory group to obtain the necessary shipboard observations and analyses. Special care was taken to obtain data from the differing lithologies. Because the exact nature of recovered sediment and quality of recovery was somewhat difficult to predict, we decided that the Scientific Party had to take a conservative approach to define personal sampling and that the majority of sampling for personal research had to be deferred until after the expedition. However, we defined some sampling objectives to conduct groups of exploratory analyses to test and refine sampling strategies to prepare for postexpedition sampling. This included large volumes of samples of sand to test heavy mineral separation and critical grain size, samples for preliminary $\delta^{13}C$ of TOC analyses to determine the position of the C3–C4 transition in the deep sites, samples to determine the feasibility of high-resolution analyses and relative dating with foraminifer $\delta^{18}O$ of a levee sequence, samples to test terrestrial and oceanographic biomarkers, and samples to test the feasibility of optically stimulated luminescence (OSL) dating in Late Pleistocene cores. Some suites of samples were taken for grain size analyses in turbidites, nannofossil biostratigraphy, and high-resolution analyses of specific hemipelagic horizons (including U-channels for paleomagnetism studies).

Site summaries

Site U1449

Site U1449 (proposed Site MBF-6A) is part of our seven-site transect designed to document turbiditic transport processes and the architecture of deposition in the Middle Bengal Fan at 8°N since the Pleistocene. Sediments will also be used to trace sources of eroded material in the Himalaya and reconstruct erosion rates as a function of climate change. Site U1449 is located at 08°0.419′N, 088°6.599′E in a water depth of 3653 m. The main Hole U1449A penetrated to 213.5 m drilling depth below seafloor (DSF) and was cored by a combination of the APC, HLAPC, and XCB systems. Hole U1449B consists of a single APC core from the mudline taken for microbiological studies.

Principal results

Different structural elements of the sedimentary fan were cored, including a more than 40 m thick levee succession, interlevee sand sheets, and hemipelagic sequences. General lithologic boundaries correlate well with downcore variability in all physical properties and were attributed to major seismic facies types and reflectivity characteristics. In situ and average core seismic velocities are in close agreement, which confirms that the major lithologies were properly sampled and sections not recovered by XCB drilling likely contained unconsolidated sand.

Cored sediments allowed us to characterize the sedimentological, physical, and geochemical properties of the material delivered mostly through turbidity currents and likely originating from the Himalayan range. Integration of lithology, physical properties, seismic facies, and geochronological data shows that sedimentation varies over several orders of magnitude between centimeters per thousand years for hemipelagic units that represent a local absence of turbiditic sedimentation and much higher rates (>>10 cm/ky) for interlevee units and levees that built up rapidly.

High accumulation rates of turbiditic deposition in the lower 120 m of Hole U1449A since ~2 Ma were followed by a low-accumulation hemipelagic episode around ~0.8–1.3 Ma. Intercalated levee and interlevee deposits then formed until ~300 ky ago, after which hemipelagic sedimentation dominated again.

Operations

Hole U1449A was drilled to total depth of 213.5 m DSF. The APC system penetrated 57.1 m of formation and recovered 52.37 m (92%). The HLAPC penetrated 71.9 m of formation and recovered 74.98 m (104%). The XCB system penetrated 83.5 m of formation and recovered only 2.03 m (2%). Because of low recovery with the XCB system and because most objectives were achieved, drilling was terminated before reaching the initially planned depth of 300 mbsf to save time. Hole U1449B consists of a single APC core from the mudline taken for microbiological investigations and recovered 7.91 m of sediments.

This first Expedition 354 drilling experience in the fan sediments allowed us to refine the drilling strategy for subsequent drill sites. As expected, recovery of sands intercalated between muddy units was challenging, but the HLAPC system proved to be particularly efficient for sampling both turbiditic sequences and loose sand intervals.

Lithostratigraphy

The predominant lithology is siliciclastic and composed of normally graded intervals of mica-rich quartz-dominant fine sand, silt, and clay of varying thicknesses (i.e., turbidites). The observed mineralogical assemblage is characteristic of sediments found in Himalayan rivers. Turbidite sequences are generally separated by hemipelagic intervals (mottled calcareous clays) and occasional glassy volcanic ash layers. Lithologic differences between siliciclastic units and variations in grain size and bed thickness reflect cycles of proximal turbidity current channel activity, including activation, flow-stripping, avulsion, and abandonment. Bioturbated calcareous clays likely represent times of channel-levee inactivity at Site U1449 and hence reduced deposition of terrigenous material.

Biostratigraphy

Calcareous nannofossils and planktonic foraminifers provide biostratigraphic constraints at Site U1449. Overall, the abundance and preservation of these microfossils is dependent on the type of lithology recovered. Coarser sandy intervals contain few to barren calcareous nannofossils and barren to <0.1% foraminifers, but abundance and preservation improve considerably in the pelagic and hemipelagic intervals. These intervals are discontinuous at this site because of the regular influx of turbidites and levee sedimentation. Biostratigraphic controls are based on 53 nannofossil and 34 planktonic foraminifer samples, which provide a total of six biomarker horizons and a lower Pleistocene age at the bottom of Hole U1449A.

Paleomagnetism

We studied 30 of the 38 cores collected from Hole U1449A, avoiding deformed or sandy intervals. Most cores were unoriented, so polarity reversals were identified using declination data within each core, both from discrete samples and archive section halves. The upper 91 m in Hole U1449A reveals normal polarity corresponding to the Brunhes Chron (<0.781 Ma). A pelagic deposit between 88 and 97 m core depth below seafloor (CSF-A) contains

several magnetic polarity transitions, including the Brunhes/Matuyama boundary and the boundaries of the Jaramillo and Cobb Mountain Subchrons. Interpretation of the magnetic polarity beneath the hemipelagic unit is difficult, but at least two cores (20H and 22H) may have reverse magnetization. Correlation between multiple holes from our transect, particularly in pelagic and hemipelagic intervals, is expected to clarify the interpretation of the magnetostratigraphy of Hole U1449A.

Physical properties

Acquired data allow three lithologic groups to be distinguished. Sand-dominated lithologies reveal high acoustic velocity (~1700 m/s), high wet bulk density (~2.1 g/cm^3), generally high magnetic susceptibility (~50 × 10^{-5} to 200 × 10^{-5} SI), and intermediate levels of natural gamma radiation (NGR) (~70 counts/s). Silty clay lithologies show intermediate values of acoustic velocity (~1550 m/s), wet bulk density (~2.0 g/cm^3), and magnetic susceptibility (30 × 10^{-5} to 100 × 10^{-5} SI) and the highest NGR levels (~90 counts/s). Hemipelagic lithologies are easily distinguished by their low acoustic velocity (~1500 m/s), low wet bulk density (~1.6 g/cm^3), very low magnetic susceptibility (0–20 × 10^{-5} SI), low NGR (~25 counts/s), and the lightest color. Detailed comparisons between lithology and physical properties on selected intervals confirm the predictive capabilities of physical property data for high-resolution reconstruction of depositional processes. Also, the data show a particularly high variability in coarser grained intervals, which were probably disturbed by coring; thus, deviation from in situ properties cannot be excluded.

Geochemistry

Shipboard sampling allowed analysis of 39 interstitial water samples, including a detailed sampling of the upper 9 m in single-core Hole U1449B. Inorganic and organic geochemical analyses were acquired on 12 samples for major and trace elements and 37 samples for organic and inorganic carbon. Data from turbidite sediments exhibit geochemical compositions similar to those observed for sediments from Himalayan rivers and from the upper fan levees and shelf. A total of 31 samples were taken for postexpedition microbiological research.

Site U1450

Site U1450 (proposed Site MBF-2A) occupies a central position at 8°0.42′N and 87°40.25′E in the east–west transect across the Bengal Fan at 8°N. It is located at equal distance from Site U1451 on the flank of the Ninetyeast Ridge and Site U1455 on the flank of the 85°E Ridge. The overall thickness of the fan reaches ~4 km at this location (Curray et al., 2003). Neogene sediment thickness decreases toward the two ridges, which is likely the result of ongoing deformation on both ridges during the Neogene (Schwenk and Spiess, 2009). At this central position of the transect, the upper Miocene and Pliocene–Pleistocene sections of the fan appear to be most expanded and are inferred to contain a higher resolution record, as well as accumulating, on average, coarser grained material. The shallow section at this site is one of the seven ~200 m deep sections along the 8°N transect that constrain the Middle Bengal Fan architecture in space, time, and sediment delivery rate during the Pleistocene. The deeper section at this site will document the delivery mechanisms of the fan and the climatically and tectonically influenced sediment supply from the Himalaya during the Neogene. Changes in the source regions in response to tectonic and climatic evolution of the Himalaya are expected to be reflected in the sediment's mineralogical and geochemical compositions, the geochronological data, and in accumulation rates across the transect.

Principal results

HLAPC coring combined with 4.8 m advances by drilling without coring was essential to achieve sufficient recovery in difficult lithologies with reasonable drilling times to reach 812 mbsf. This approach proved to be particularly efficient in recovering loose sand that otherwise would have been washed out during RCB or XCB coring. Because of remarkably low lithification of the sediment formation, this HLAPC approach permitted piston coring to 550 mbsf, and seven HLAPC cores were taken in even deeper intervals to a maximum depth of 688 mbsf.

As at other transect sites, the sedimentary succession is dominated by turbidites of siliciclastic composition with detrital carbonate contents between 5% and 10%. These turbidites have high accumulation rates (~5–10 cm/ky) from the upper Miocene to lower Pliocene. From the Pliocene to Pleistocene, turbidite accumulation peaks around 20–25 cm/ky. These turbidites have close mineralogical and geochemical affinities with sand and silt sampled in the Ganges, Brahmaputra, and lower Meghna Rivers. They carry all the mineral characteristics and major element composition characteristics of river sediments derived from high-grade metamorphic rocks of the Himalayan range. Sand comprises ~40% of the section cored at Site U1450; this composition is similar to the grain size spectrum expected from river-derived detrital material, so bias due to turbiditic transport may be minor. Downhole logging was not possible at this site because of poor hole conditions, so it remains difficult to estimate the exact proportion of sand, silt, and clay. Overall, the mineralogical and chemical composition of the turbidites appears almost uniform, but detrital carbonate content tends to be gradually higher in sediment older than the Pliocene, reaching concentrations twice as high as in modern rivers and Pleistocene turbidites. This evolution suggests a change in eroded lithologies (i.e., a higher proportion of Tethyan formations exposed to erosion during the Miocene) and/or a change in weathering conditions.

Another distinctive, more carbonate-rich lithology is represented by about 10 relatively thin hemipelagic intervals composed of calcareous clays. These intervals correspond to periods of slow accumulation at the site when pelagic deposition is significant enough to be identified but is still diluted in variable proportions by a clay component. This clay is assumed to be related to the plumes generated by surrounding turbidity currents that originate from canyons and the slope offshore Bangladesh. However, this affinity remains to be determined by geochemical and clay mineralogical approaches. These low-accumulation intervals will provide geochronological control through a combination of paleomagnetic and biostratigraphic ground-truth data and orbital tuning, which will be essential for constraining detailed accumulation rates. Testing their continuity across the transect will be a key element for the integrated study of fan construction dynamics and long-term detrital sedimentary input utilizing seismic correlation across the transect.

Site U1450 represents a reference section for shore-based studies of the erosion of the Himalaya during the Neogene. The detrital sediments cored here present little evidence of a change over the last 8 My, suggesting rather steady conditions of erosion in the Himalayan basin. Such a change would require a major mountain range undergoing fast erosion and a monsoonal climate that allows rapid transport to inhibit weathering of the sediment in the floodplain. Unlike in the distal fan cored during Leg 116 (Cochran, Stow, et al., 1989), Site U1450 sediments show no clear change in accumu-

lation rate, grain size, and clay mineralogy. This stability suggests that the smectite-rich fine turbidites recorded in the distal fan from 7 to 1 Ma (Bouquillon et al., 1990) may relate more to a change in the channel and turbidity current routing to the distal fan than to a change in Himalayan erosion. Site U1450 also covers the interval of expansion of C4 photosynthetic flora (i.e., savanna at the expense of forest) recorded in both the continental basin and distal and middle fan (Galy et al., 2010). Sediments recovered at Site U1450 will allow detailed studies of this ecological transition and its possible connection with climate changes or erosion conditions.

Operations

Site U1450 consists of two holes. Hole U1450A was cored to 687.4 m DSF using primarily the HLAPC system alternating with short (4.8 m) advances without coring. The APC and XCB systems were used in the shallow and deepest portions of the hole, respectively. Because of very low recovery at depth with the XCB system, we pulled out and planned for deeper penetration coring and logging in a second hole later in the expedition. Overall, 282.7 m of core was recovered for the 444.7 m cored in Hole U1450A. Hole U1450B was drilled without coring to 608.0 m DSF and then RCB cored continuously to 811.9 m DSF. Coring in Holes U1450A and U1450B overlaps from 608.0 to 677.8 m DSF. This deeper section cored 203.9 m and recovered 46.7 m of sediment (23%). Downhole logging was attempted with the triple combo tool string. On the way down, the bottom of the tool string encountered an obstruction at 133.7 m DSF and was stuck, likely in a collapsing sand layer. After the tool string was released, a short section of logging data was acquired, and deep logging of the site was abandoned.

Lithostratigraphy

Recovered sediments from Site U1450 are divided into 24 lithostratigraphic units based on lithologic and paleontological characteristics obtained through macroscopic and smear slide analyses and on physical property measurements.

The overall dominant lithology for Site U1450 (84% of total recovered material) is siliciclastic and comprises fining-upward sequences of fine sand, silt, and clay (i.e., turbidites), as well as homogenized sands and mixed silt-clay layers. These turbidites carry major and trace mineral characteristics of Himalayan rivers and of high-grade metamorphic rocks of the Himalaya. Clay assemblages are dominated by illite, which is indicative of the same rivers. Siliciclastic units alternate with at least 10 units of calcareous clay (16% of total recovered material). The thickest continuous calcareous clay intervals are in lithostratigraphic Unit III and consist of 5.14 m in Core 354-U1450A-34F and 4.8 m in Core 36F. Sediments give way downhole in Hole U1450B to increasingly more lithified material (e.g., limestone and claystone) from 627.50 m CSF-A to the base of recovered material. Additionally, Site U1450 contains three volcanic ash layers.

Lithologic differences between units and variations in grain size and bed thickness reflect cycles of turbidity current activity and channel abandonment. Sand intervals may represent interlevee sheet flows, whereas finer grained fractions are more likely preserved in levee deposits. Bioturbated calcareous clays represent times of local channel inactivity with reduced and finer siliciclastic deposition that reflects a relative increase in the contribution of biogenic origin from the pelagic zone. Many intervals of calcareous clay show repeated sequences of color-graded beds, which can be attributed to increased entrainment of siliciclastic material, changes in water column productivity, or changes in the oxidation/reduction horizons of pore water. In Hole U1450B, intervals dominated by calcareous and/or clayey material become increasingly lithified with depth, and many are intercalated with very thin to thin silt or siltstone layers. Plant fragments occur throughout the cored section, more commonly in silt and siltstone intervals, although a few sand-dominated units also contain macroscopic organic material. At the top of Hole U1450A, an 18 cm thick ash layer presumably corresponds to the ~75 ka Toba volcanic eruption that produced widespread tephra deposits across the Bay of Bengal (e.g., Gasparotto et al., 2000).

Biostratigraphy

Calcareous nannofossil and planktonic foraminiferal biostratigraphic analyses conducted on Site U1450 samples identified 18 biomarker events. These events were used to construct 4 foraminiferal and 11 nannofossil biozones, providing excellent age control extending back to the late Miocene. The recovery of a late Miocene succession achieves one of the key objectives of this expedition and includes sediments that may contain the C4 photosynthetic flora expansion (Galy et al., 2010).

The succession of biostratigraphic zones at this site appears continuous, as no significant nannofossil biostratigraphic hiatuses were observed, indicating that the fan has been accumulating sediments, albeit at highly variable accumulation rates, since the late Miocene.

Paleomagnetism

A preliminary paleomagnetic study was conducted on 36 of the 86 cores collected from Hole U1450A, comprising 108 archive section-half and 52 discrete sample measurements. Sandy and/or deformed intervals were not measured. Polarity zones corresponding to the Jaramillo and Cobb Mountain Subchrons were identified in a calcareous clay unit in Core 36F (173.30–174.60 and 175.70–175.90 m CSF-A, respectively). An additional pair of reversals was observed in Core 52F (248.38 and 248.51 m CSF-A), but the polarity chron to which they belong has not yet been identified. The thickness of the Jaramillo and Cobb Mountain polarity zones in Hole U1450A suggests an accumulation rate for the calcareous clay interval similar to that in Hole U1449A (~1.5 cm/ky).

Physical properties

Physical property data acquired on Site U1450 cores includes density, magnetic susceptibility, *P*-wave velocity, NGR, and thermal conductivity. The data are mostly of good quality, but the results from disturbed and partially filled sections are less reliable, as described below.

Physical properties at Site U1450 primarily reflect lithologic variations, with downcore compaction having a relatively minor effect. Using the principal lithologic name from the core description, which assigned six types of lithologies, we calculated the total thickness and average physical property value for each lithology. From the 319 m total core recovery assigned to lithology (39.6%), sand accounts for 131 m (41%), silt for 46 m (14%), clay for 72 m (22%), calcareous clay for 45 m (14%), claystone for 13 m (4%), calcareous claystone for 6 m (2%), and limestone for 7 m, with additional thin ash layers. In general, sands and silts have the highest density and *P*-wave velocity, sands have the highest magnetic susceptibility, clays have the highest NGR, and calcareous clay has the lowest values in all measurements. Some sand-rich intervals were difficult to recover and were often fluidized, which sometimes resulted in incompletely filled core liners; these cores had the effect of giving

unexpectedly low gamma ray density, magnetic susceptibility, and NGR values. Cores that had inflow of core material ("suck in") also likely have lower than expected values in these physical properties Because of volume reduction.

Geochemistry

Detailed pore water measurements distinguish four hydrologic units based on sulfate, phosphate, silica, magnesium, potassium, calcium, and alkalinity contents. Carbonate contents of bulk sediments vary widely from 1.2 to 63.2 wt% $CaCO_3$, reflecting contrasting depositional environments and significant contributions from detrital carbonates. The carbonate contents of turbiditic sediments, however, exhibit a significant change at ~620 m CSF-A, where they roughly double from an average of 3.8 wt% above to 7.3 wt% below. This transition occurs around the Miocene/Pliocene boundary and most likely reflects a change in detrital carbonate supply. A similar change was also observed at Site U1451 and can be deduced from DSDP Site 218 total inorganic carbon (TIC) data (von der Borch, Sclater, et al., 1974). Overall, TOC contents are low, with an average value of 0.4 wt%. Within turbidites, TOC broadly covaries with Al/Si ratios—a proxy for sediment grain size and mineral composition—reflecting preferential association of organic matter with clays previously documented in both the modern Ganga-Brahmaputra river system and in active channel-levee sediments in the Bay of Bengal deposited over the past 18 ky (e.g., Galy et al., 2007). The TOC budget is likely also affected by the frequent presence of woody debris concentrated in the lower part of many turbiditic sequences. In turbiditic sediments, major element composition (e.g., Fe/Si and Al/Si) closely matches the chemical composition observed in sediments from the modern Ganga-Brahmaputra river system for both the trend and the range of variation (e.g., Galy and France-Lanord, 2001). At the low end of Al/Si ratios, the lack of significant difference suggests that extreme sorting documented in coarse bed sediments from these rivers is also generated by turbidity current at Site U1450. Conversely, the clay-rich end-member recovered at Site U1450 is only slightly more aluminous (and likely finer) than monsoonal surface-suspended sediments from the lower Meghna River.

Microbiological subsampling of sediments and pore water at Site U1450 included establishing a microbial cell counting method, with further processing of the samples to be performed following the expedition.

Downhole measurements

Five downhole measurements were taken in Hole U1450A with the advanced piston corer temperature tool (APCT-3), ranging from 4.6°C at 86.3 m DSF to 13.5°C at 318.1 m DSF. These measurements return a geothermal gradient of 38°C/km, which appears to be in the expected range.

Stratigraphic summary

Lithologic and physical property results confirm the expectation that Site U1450 would contain a high proportion of sand in the recovered cores; it may be even higher in the formation. As at Site U1449, the match between these data sets and seismic facies and reflectors will allow us to assign broad lithologic categories to the seismic units and thus extrapolate throughout the seismic data set and between Expedition 354 drill sites. These data also allow identification of major depositional processes, which can be integrated to reconstruct the stacking pattern and evolution of fan deposition.

Because Site U1450 reaches back to 8 Ma at 812 m DSF, a precise seismic stratigraphy will be established postexpedition, based on major hemipelagic units and associated distinct seismic reflectors. These units and reflectors will be used to estimate accumulation for various subfan units in time slices on the order of several hundred thousand to millions of years, one of the main expedition objectives. Site U1450 is located in a key position between the two other deep penetration sites (U1451 and U1455).

Recovering material of sufficient quality was a challenge during Expedition 354 and particularly at Site U1450 because of the high proportion of sand. It was unexpected that the consolidation state of sand apparently does not change much with depth. Although loose sand was recovered with the APC and HLAPC systems to refusal depth (560 and 630 m DSF in Holes U1450A and U1450B, respectively), the XCB and RCB systems provided little or no recovery of sand. The sand proportion is likely underrepresented in cores from the deeper section of the site. Based on discrete sample measurements of density and porosity, a downhole trend of porosity loss is observed, but from lithologic observations we infer that consolidation state is different for different grain sizes. Clay shows a gradual transition to claystone with depth, with increasing *P*-wave velocities and densities downhole. However, sand was not recovered in any more consolidated state within the entire 800 m cored section.

Based on biostratigraphic and paleomagnetic data, the upper Miocene to lower Pliocene portion of the site is characterized by a relatively uniform accumulation, averaging about 5–10 cm/ky. From the early Pliocene to the Pleistocene, fan accumulation has intensified (~20–25 cm/ky), accompanied by a transition from more silt-dominated to sand-dominated lithologies. As at Sites U1449 and U1451, turbidite deposition ceased at this site at ~300 ka, as observed at 11°N in the axial fan (Weber et al., 2003).

Site U1451

Site U1451 (proposed Site MBF-3A) is the easternmost site of our Bengal Fan transect at 8°N and was the only one aimed at coring the oldest part of the fan. The site is located above the western flank of the Ninetyeast Ridge at 8°0.42′N, 88°44.50′E in 3607.3 m water depth. Seismic data show that the overall fan section is condensed at Site U1451 compared to the axial part of the fan because of ongoing deformation along the Ninetyeast Ridge since the Miocene (Schwenk and Spiess, 2009). The drilling objective was to recover the complete fan section down to a seismic unconformity, which is believed to indicate the onset of fan deposition at this location. Site U1451 also contributes to the Miocene–Pliocene transect of three ~900 m deep holes documenting Himalayan erosion and paleoenvironment. Finally, the upper section of the site is part of the seven-site transect drilled to investigate late Pliocene to recent depocenter migration and overall fan sedimentation.

Two holes were drilled at Site U1451, Hole U1451A to 582.1 m DSF and Hole U1451B to 1181 m DSF. Hole U1451A was advanced with the APC, HLAPC, and XCB systems. From 200 to 582.1 m DSF, 4.8 m intervals were drilled without coring between HLAPC cores to achieve overall coring depths. In Hole U1451B, a reentry cone with 400 m casing was drilled into the seafloor. Below 400 m DSF, Hole U1451B was cored with the XCB system from 542.0 to 640.8 m DSF and then with the RCB system to 1181 m DSF. Wireline logging failed because of unstable hole conditions. Core recovery was 86% in Hole U1451A and 29% in Hole U1451B.

Principal results

Coring at Site U1451 returned a complete sedimentary record of Bengal Fan construction back to the Paleogene. It constrains the

timing of the fan turbiditic onlap at this location around the Oligocene/Miocene boundary (~23–24 Ma) and provides the longest continuous record of Himalayan erosion throughout the Neogene. The upper section, part of the seven-site transect at 8°N, documents a change since the Miocene to a higher proportion of hemipelagic clay–rich deposition, consistent with a position less exposed to fan turbiditic deposition because of Ninetyeast Ridge uplift.

The recovered turbiditic record extends back to the late Oligocene or early Miocene, which is marked by a transition from late Paleogene pelagic limestones to early Neogene claystones and siltstones, intercalated into pelagic intervals. Although this old turbiditic record carries all characteristics of Himalayan erosion across the full grain-size spectrum, including sands, the growth rate of the fan deposits remained overall relatively low, on the order of a few centimeters per thousand years. A distinct change is observed in the middle Miocene, when fan growth intensified by almost an order of magnitude (>10 cm/ky). In the Pliocene, coarser material is absent, and the time interval between the early Pliocene and early Pleistocene is characterized by accumulation of calcareous clay–rich hemipelagic units. During the Pleistocene, higher fine-grained detrital input is observed but only over the last ~0.4 My. Fan deposits dominate the lithology again. As at other Expedition 354 sites except for Site U1454, hemipelagic sediments dominate the surficial deposition.

The Site U1451 record, combined with that of Site U1450, reflects steady conditions of Himalayan erosion and Himalayan geological and structural evolution as documented by the recovered sediment's relatively uniform chemical composition and clay mineral assemblages. This record will be further constrained and refined postexpedition to reveal information about sources, erosion rates, and evolution of weathering.

At first glance, the Neogene record appears remarkably stable through time. One notable exception is the detrital carbonate contents of the turbidites, which are markedly higher during the Miocene than during the Pliocene–Pleistocene. This exception reflects either a long-term change in the geological sources or a difference in the weathering regime. The petrology of the sand reveals that high-grade metamorphic rock fragments and minerals that are characteristic of modern river sediments have been present since the middle Miocene and were less abundant during the early Miocene and late Oligocene. Such trends are consistent with increasing exhumation of high metamorphic grade rocks through time, but confirmation by postexpedition studies is required. Turbiditic sediments deposited at Site U1451 since the late Oligocene or early Miocene reflect detrital archives similar in many aspects to those of recent fan deposits or modern river sediments. Nonetheless, fan clastic deposition is not only restricted to turbidites; deposition of detrital clays is prevalent in hemipelagic intervals during the Neogene and likely represents deposition associated with distant turbidity currents. Similar processes may also have been involved in the formation of the early Miocene and Oligocene claystones recovered, which have accumulation rates similar to Pleistocene hemipelagic units.

From seismic data, the early history of fan deposition at Site U1451 is associated with a change in depositional style above a seismic unconformity. This unconformity was likely cored at the bottom of the hole, recovering Eocene and Paleocene limestones and containing a 16–18 My hiatus. The structurally disturbed unit immediately overlying the unconformity is an Oligocene/Eocene limestone and claystone unit injected by sand and silt (injectites). On top, parallel strata are onlapping, which clearly indicates turbiditic sedimentation. Tilting of these Miocene strata with respect to the modern stratification indicates tectonic deformation associated with the Ninetyeast Ridge at Site U1451. However, this tectonic deformation has only a minor effect on fan deposition.

The well-represented hemipelagic deposition at Site U1451 during the last 6 My provides an excellent opportunity to develop a stratigraphic framework for the entire transect based on high-resolution biostratigraphy, oxygen isotopes, and cyclostratigraphy. This chronology can be tied into the seismic stratigraphy and will constrain ages throughout the Pliocene–Pleistocene part of the transect, as hemipelagic units prove to be reliable and easily traceable horizons.

The Miocene section reveals pronounced parallel stratification in seismic data, which seems to be related to the different consolidation behavior of sands, silts, clays, and hemipelagic units. Carbonate-bearing and clay-rich units show a much more pronounced lithification, whereas sand remains unconsolidated. This might explain why sand is not well represented in rotary cores. The stratification of the Miocene section, which is similar across the 8°N drill site transect, may in turn indicate a different mode of deposition with less channelized transport and more widespread distribution of turbiditic deposits. Whether this change in deposition is linked to an overall change in sediment transport or grain size has to await further detailed analysis that carefully considers the potential sampling bias.

Operations

Hole U1451A extends from the seafloor to 582.1 m DSF and was advanced using the APC, HLAPC, and XCB systems. Below 200 m DSF, 4.8 m intervals were drilled without coring alternating with most HLAPC cores to achieve required penetration depths within the operation time available. Formation temperature measurements were made with the APCT-3 to 406.4 m DSF, the deepest piston core formation temperature measurement ever obtained. Hole U1451A cored 394.9 m and recovered 337.80 m of core (86%).

In Hole U1451B, a reentry cone with 400 m of casing was drilled into the seafloor. This assembly was intended to stabilize the hole for deep coring and logging operations. XCB coring in the upper 600 m was stopped because of failures of XCB cutting shoes. Hole U1451B was reentered a second time, and RCB coring penetrated to 1181 m DSF. RCB coring penetrated 627.6 m and recovered 180.86 m (29%). Wireline logging failed because of unstable hole conditions, probably due to collapse of the sand formation around 500 m DSF.

Lithostratigraphy

Recovered sediments from Site U1451 were divided into 23 lithostratigraphic units based on lithologic and microfossil characteristics obtained through macroscopic and smear slide analyses, as well as physical property measurements. The overall lithology of the expedition's deepest hole is comparable to that described at other sites, with the exception of the early Miocene–Eocene section, which is lithified and was not penetrated at the other sites. The dominant lithology at Site U1451 is mica- and quartz-rich sand, silt, and clay turbidites, carrying high-grade metamorphic minerals in some intervals. Units of turbidites are separated by bioturbated nannofossil-rich calcareous clays and occasionally calcareous ooze. Five volcanic ash layers with fresh glass shards were identified in nonturbiditic intervals above 154 m CSF-A, including the youngest Toba tuff ash layer, which is present at 2.6 m CSF-A in Hole U1451A.

Hemipelagic calcareous clay intervals of variable carbonate content, observed between 50 and 190 m CSF-A, are common throughout the Pleistocene and Pliocene. These intervals are intercalated with intermittent sand and mud turbidites representing intervals of rapid deposition during the Late Pleistocene. During the Miocene, calcareous clay deposition is reduced and the record is dominated by turbiditic sediments. The latter contains numerous sand-rich layers to 520 m CSF-A (about 9 Ma). Downhole, the proportion of sand decreases. This observation is likely biased by the change in coring technique from the HLAPC system in Hole U1451A to the RCB system in Hole U1451B, as the RCB system was believed to be unable to recover loose sand. Turbidite units from 190 m CSF-A downhole mark an extended period of proximal channel or turbidite activity at this site initiated at 1086 m CSF-A (Core 354-U1451B-62R) around the Oligocene/Miocene boundary. Below this interval, calcareous and clastic sediments become increasingly lithified. Green to brown claystones are interbedded with light green and yellow calcareous claystones and limestones. Within the calcareous claystone sequences, breccias of calcareous claystone clasts in a siltstone and sandstone matrix are postdepositional injectites. The lowermost ~100 m of Hole U1451B contains foraminiferal limestones, mottled calcareous claystones, and claystones reflecting the prefan paleoceanographic environment and much reduced influence of fan sedimentation. The transition from turbidites to limestone around 1100 m CSF-A marks the last occurrence of any significant fan deposition at this site. The present lithostratigraphic section therefore captures the complete sedimentary record of fan deposition to the onlap of the fan onto late Oligocene limestones. This sedimentary record extends existing oceanic archives of the Himalayan erosion (Cochran, 1990) to the Oligocene/Miocene boundary.

Biostratigraphy

Calcareous nannofossils and foraminiferal biostratigraphic analyses at Site U1451 resulted in the identification of 39 biomarkers and the construction of 31 biozones, providing a comprehensive and detailed age model for the long-term development of the Middle Bengal Fan from the Paleogene to recent. Furthermore, the transition from pelagic-dominated sedimentation to probably Himalayan-derived turbiditic sediments is constrained near the Oligocene/Miocene boundary.

The uppermost 120 m of Hole U1451A (lithostratigraphic Units I–III) is a sequence of turbiditic sands and muds with minor intercalated hemipelagic layers. Six biomarkers were identified within this sequence, providing good age control for Pleistocene fan development at this site. A thick (66 m) pelagic sequence was recovered in Cores 23F–29F (lithostratigraphic Unit IV) and contains eight biomarkers. This sequence represents more than 3 My of pelagic sedimentation, with little turbiditic influence. Below lithostratigraphic Unit IV, 450 m of turbidite-dominated sedimentation, present from Core 30F to the base of the hole, was deposited in approximately 3.5 My, based on four biomarkers observed in this sequence. The accumulation rates of ~1 and >10 cm/ky in the pelagic sequence and the turbidite-dominated sequence, respectively, suggest that the majority of turbiditic activity at this position occurred in the Miocene and Pleistocene and is more restricted in the Pliocene. The first occurrence (FO) of *Catinaster coalitus* was observed at the base of Hole U1451A (midpoint = 575.60 m CSF-A) and the top of Hole U1451B (590.06 m CSF-A) and provides tight age control for the overlap succession of the two holes.

The Oligocene/Miocene boundary was recovered and lies between Samples 354-U1451B-54R-CC and 63R-CC. This boundary is identified by the last occurrence (LO) of *Reticulofenestra bisectus* and *Zygrhablithus bijugatus* (nannofossil Zone NP25). A major change from turbidite-dominated to pelagic-dominated sedimentation occurs between Cores 62R and 63R (nannofossil Zone NP24).

Because of intense recrystallization and preservation issues, the depositional age of the limestones is difficult to constrain. Samples 71R-CC and 72R-CC contain *Morozovella aragonensis*, which is a marker species for foraminifer Zone E9 (43.6–52.3 Ma). The radiolarian species *Thyrsocyrtis rhizodon* was observed in Sample 69R-CC, confirming an Eocene age for these sediments.

There appears to be a significant hiatus of 16–18 My between Samples 71R-CC and 72R-CC. Sample 72R-1, 0–1 cm, contains *Discoaster multiradiatus* and *Fasciculithus* spp., which are biomarkers for nannofossil Zone NP10. Sample 73R-CC represents a gap zone marked by the absence of *D. multiradiatus* and places the base of Site U1451 in the Paleocene (Thanetian). Confirming the presence and extent of this hiatus will be the subject of postexpedition research.

Paleomagnetism

Paleomagnetism of 269 archive section halves and 93 discrete samples from Site U1451 allowed us to identify 12 polarity reversals in Hole U1451A, mostly in calcareous clay deposits. We place the boundary between the Brunhes and Matuyama Chrons at 72.24 m CSF-A in Hole U1451A. A calcareous ooze deposit in Hole U1451A contains polarity zones corresponding to the Jaramillo and Cobb Mountain Subchrons (80.35–81.78 and 83.10–83.44 m CSF-A, respectively), allowing us to correlate the interval with similar lithostratigraphic units at Sites U1449 and U1450. Several reversals between 140 and 163 m CSF-A in Hole U1451A are interpreted as the Gauss and Gilbert Chrons and their subchrons. Reversals at 108.30 and 218.70 m CSF-A in Hole U1451A have not yet been linked to the geomagnetic polarity timescale. Multiple declination changes were observed in Hole U1451B, most related to rotation during the coring process. None has yet been identified unambiguously as a polarity reversal.

Physical properties

Physical property data were acquired at Site U1451 for all Hole U1451A and Hole U1451B cores, including density, magnetic susceptibility, *P*-wave velocity, NGR, and thermal conductivity. Data from APC cores are mostly of good quality. However, the whole-round logger data from cores obtained through RCB drilling—the majority of Hole U1451B—underestimate density, magnetic susceptibility, and NGR because the cores typically do not completely fill the liner cross section.

Hole U1451A recovered core material from 0 to 579 m CSF-A, and Hole U1451B recovered core material from 542 to 1175 m CSF-A. Physical properties at Site U1451 primarily reflect lithologic variations but also show downcore compaction and lithification documented by decreasing porosities and increasing densities and *P*-wave velocities, specifically in the lowermost Cores 354-U1451B-65R through 73R. Based on the principal lithologic name from the core description, average physical properties were determined for 10 lithologies. The total core recovery assigned to lithology at Site U1451 was 518.66 m (51%). The most common principal lithology is calcareous ooze (~120 m), followed by clay (~96 m), sand (~84 m), and silt (~74 m). Claystone (~65 m), limestone (~41 m), and siltstone (~21 m) make up the lower part of Hole U1451B. Volcanic ash

occurs only in limited intervals (totaling 0.57 m), and siliceous ooze is absent. Physical property measurements follow the following general trends: limestones have the highest average density and *P*-wave velocity; sands have the highest magnetic susceptibility; volcanic ashes, clays, and claystones have the highest NGR; and calcareous oozes generally have the lowest values in all measurements. Some of the sand-rich intervals were difficult to recover and were often fluidized and filled the core liners only partially, resulting in anomalously low whole-round measurements (gamma ray attenuation [GRA] density, magnetic susceptibility, and NGR values). The same is true for most of the lithified intervals drilled with the RCB system, where GRA values significantly underestimate moisture and density (MAD) values.

Geochemistry

Detailed pore water measurements distinguish five hydrologic units based on sulfate, phosphate, silica, magnesium, potassium, calcium, and alkalinity contents. The deepest unit bears distinct characteristics due to the strong influence of the limestones underlying the fan deposits. It is characterized by a strong rise in calcium content, although alkalinity remains low and constant, buffered by pressure-dissolution and recrystallization of the carbonate-rich lithology and an upward diffusion/advection of interstitial water.

Throughout Site U1451, the carbonate contents of bulk sediments vary widely from 0.2 to 96.6 wt% $CaCO_3$, reflecting contrasted depositional environments, including significant contributions from detrital carbonates. Turbiditic sediments have low carbonate content in the upper section (Pleistocene), with values roughly doubling around 130–180 m CSF-A. This transition occurs around the Miocene/Pliocene boundary and is followed by gradually increasing carbonate content to 700 m CSF-A. These trends in carbonate content of the turbiditic sediments most likely reflect changes in detrital carbonate supply, which correlates with observations at Site U1450. Turbiditic sediments are absent below 1090 m CSF-A, and limestone—at times almost pure ($CaCO_3$ > 97 wt%)—becomes the dominant lithology. Hemipelagic clays are present throughout the entire record and are characterized by highly variable carbonate content, often indistinguishable from that of turbiditic sediments. Major and trace element concentrations (e.g., CaO and Sr) measured via hand-held X-ray fluorescence (XRF) suggest that turbiditic and hemipelagic sediments consist of distinct binary mixings between carbonate and silicate end-members. The contrasted composition of the silicate fraction of hemipelagic clays is further supported by their frequent K-depletion and Fe-enrichment compared to turbiditic clays. In turbiditic sediments, the major element composition (e.g., Fe/Si and Al/Si) closely matches the chemical composition of sediments from the modern Ganga-Brahmaputra river system.

Overall, TOC content is low, with an average value of 0.3 wt%. Within turbidites, TOC broadly covaries with Al/Si ratios—a proxy for sediment grain size and mineral composition—reflecting preferential association of organic matter with clays previously documented in both the modern Ganga-Brahmaputra river system and in active channel-levee sediments in the Bay of Bengal deposited over the past 18 ky (e.g., Galy et al., 2007). Miocene and Pliocene clay-rich turbiditic sediments are often characterized by significant organic carbon depletion compared with sediments from the modern Ganga-Brahmaputra river system and the active channel-levee system at 17°N. However, the organic carbon budget is likely to be also affected by the frequent presence of woody debris concentrated in the lower part of turbiditic sequences.

Microbiological subsampling of sediments and pore water at Site U1451 included establishing a microbial cell counting method, with further processing of the samples to be performed following the expedition.

Site U1452

Site U1452 (proposed Site MBF-5A) is in the center of our seven-site transect. It is located in a relatively flat environment with a smooth morphology. Topographic expressions of channels are absent in the vicinity of the site. The seismic profile at this site reveals a prominent, >20 km wide, and up to 40 m thick levee; the top is only at ~5 m below the seafloor.

At this site, we focused on coring the upper levee to provide a detailed record of this type of depositional system. Two holes were cored through this levee to allow high-resolution sedimentological, geophysical, geochemical, and micropaleontological investigations. A single mudline core from Hole U1452A was devoted to detailed study of the hemipelagic deposition during the last glacial cycle and to the Toba ash. Hole U1452B was cored to 217.7 m DSF for the study of the Upper Pleistocene section. Finally, Hole U1452C was cored to 41.3 m DSF to provide a more complete record of the levee and to allow more extensive sampling.

Principal results

Coring at Site U1452 contributed to the Pleistocene transect of seven sites, which was one of the primary Expedition 354 objectives. The levee sequence recovered will allow detailed integrated sedimentological and geochemical investigations. On such rapidly accumulated sediments, $\delta^{18}O$ measurements on planktonic foraminifers are expected to provide the high-resolution biostratigraphy and paleoclimate conditions (i.e., glacial to interglacial) necessary to constrain potential evolution of erosion and transport processes. This record is also essential for the understanding of channel and levee formation. Site U1452 cored a fine-grained levee, such as the one cored deeper in Site U1449, but also penetrated the coarser basal unit. Physical properties seem to indicate progradation and the transition from sand deposition, through erosion, to levee construction.

The successful interpretation of seismic facies types with respect to grain size allowed coring strategies to target specific horizons. Hemipelagic layers, after being identified in several previous sites, were used to establish a preliminary Pleistocene seismic stratigraphy. Also, coring that targeted these layers was successful and provided an improved chronology even when HLAPC coring alternated with short 4.8 m advances without coring.

A hemipelagic unit deposited from ~0.8 to ~1.2 Ma between 166 and 190 m DSF marks a period when turbiditic deposition was diverted to other parts of the fan and only clays were supplied to this area; this history was also observed at other sites to the east (Sites U1449–U1451). Fan sedimentation intensified between 800 and 300 ka, as represented by sheeted sands and the levee. These sheeted sands and the levee grew by 100 m in 500 ky, equivalent to an average sedimentation rate of 20 cm/ky. The end of this intense period of fan sedimentation at 300 ka is constrained by the basal age of the surficial hemipelagic unit.

Operations

In Hole U1452A, a single APC mudline core (1H) recovered 8 m of sediments, including the mudline.

In Hole U1452B, we completed oriented APC coring to 41.4 m DSF and continued coring with the HLAPC system. From 71.1 to

142.4 m DSF, we alternated 4.7 m long HLAPC cores with 4.8 m intervals drilled without coring. In this interval, seven HLAPC cores (14F–26F) penetrated 32.9 m and recovered 21.41 m of core (65%). The eight 4.8 m advances without coring penetrated 38.4 m, with nearly continuous HLAPC coring to 217.7 m DSF. Nine 4.8 m advances without coring were intercalated with cores in units predicted to be sandy. Overall recovery was 79% for Hole U1452B.

Hole U1452C was continuously cored from the seafloor to 41.3 m DSF to obtain a more complete record of the uppermost levee sequence to the sand layer at the base of the levee. All APC cores were oriented, and core recovery in this hole was 81%.

Lithostratigraphy

Drilling at Site U1452 targeted a Pleistocene-aged levee identified in the pre-expedition seismic data. The lithology and structures of recovered sediments indicate the initiation and cessation of an entire levee sequence (8–40 m DSF) was captured, as well as underlying prelevee sand sheets (40–167 m DSF) and calcareous clays (>167 m DSF). The prelevee sand sheets mark the initiation of turbiditic deposition at this location prior to the building of the levee. These turbiditic sand sheets are dominated by mica- and quartz-rich sand characteristic of sediments found in Himalayan rivers. The sand was likely deposited as interlevee sheet flows originating from a nearby channel. The hemipelagic calcareous clay unit extends to 190 m DSF and overlies older interlevee sand-rich turbidites.

Sediments at this site document the channel system shifting across the fan. Initially, proximal channel sand deposition was reduced and succeeded by increased deposition of hemipelagic nannofossil-rich calcareous clays. Overlying this calcareous interval, a very thick (~160 m) section of levee deposits (i.e., sand and mud turbidites) reflects activation of a nearby channel and the associated levee building that forms the top of the section. The levee is overlain by a relatively thin unit of bioturbated calcareous clay, representing the end of proximal channel activity and in turn a decrease in detrital input. This surficial calcareous clay unit at the top of the levee contains a glassy volcanic ash layer likely from the Toba eruption that occurred at ~75 ka.

Biostratigraphy

Biostratigraphic control at Site U1452 is limited, but four tie points were observed that help constrain levee development during the Pleistocene. Although the foraminiferal biomarker *Globorotalia tosaensis* (0.61 Ma) was found in Holes U1452B and U1452C (at 8.97 and 23.29 m CSF-A, respectively), its FO is at a shallower depth than the nannofossil biomarkers *Emiliania huxleyi* (0.29 Ma) and *Pseudoemiliania lacunosa* (0.44 Ma), indicating that this foraminifer was either reworked or has a longer range in the Indian Ocean. Cores 345-U1452B-33F through 37F are dominated by hemipelagic calcareous clay, are abundant in nannofossils, and contain abundant to barren foraminifers. Interestingly, fragmentation of planktonic foraminifers was higher in the hemipelagic sediments than in the turbiditic sediments. The nannofossil biomarkers agree well with the magnetic polarity reversals found at Site U1452.

Paleomagnetism

As observed in the upper parts of Sites U1449–U1451, Site U1452 sediments record the Brunhes/Matuyama boundary (184.10 m CSF-A) and both boundaries of the Jaramillo and Cobb Mountain Subchrons (186.00–187.20 and 188.33–188.61 m CSF-A, respectively). Relative to the seafloor, these are the deepest instances of these polarity transitions identified on our transect to date. Also similar to Sites U1449–U1451, the Jaramillo and Cobb Mountain Subchrons occur at Site U1452 within an interval of hemipelagic sedimentation. The Brunhes/Matuyama boundary is associated with an ash layer, believed to be from Toba. Microtektites, likely from the Australasian Microtektite Event dated at 790 ka, were found deeper than the Brunhes/Matuyama boundary, further supporting the identification of this polarity transition.

Physical properties

Physical property data were acquired on all cores from Holes U1452A and U1452B, including density, magnetic susceptibility, *P*-wave velocity, NGR, and thermal conductivity. Physical property data are mostly of good quality and reflect lithologic variations. Using the principal lithologic name from the core description to assign five lithologies (sand = ~46 m, silt = ~27 m, clay = ~33 m, calcareous clay = ~26 m, and volcanic ash), we calculated their minimum, maximum, and average physical properties. Average wet bulk densities are rather uniform for terrigenous sediment (sand, silt, and clay), ranging from 1.89 to 2.03 g/cm^3, calcareous clay has lower average densities (1.72 g/cm^3), and volcanic ash has substantially lower wet bulk densities (1.54 g/cm^3). Average *P*-wave velocities are highest in sand (1697 m/s) and lowest in clay and in calcareous clay (~1525 m/s). Average magnetic susceptibilities are also highest in sand (107 × 10^{-5} SI), followed by silt (80 × 10^{-5} SI) and clay (58 × 10^{-5} SI). The lowest values occur in calcareous clay (22 × 10^{-5} SI). Average NGR is high throughout the terrigenous components sand, silt, and clay (around 65 counts/s) and lower in calcareous clay (45 counts/s). Average thermal conductivity is highest in silt (1.63 W/[m·K]) and lowest in calcareous clay (1.18 W/[m·K]).

Geochemistry

Detailed pore water measurements distinguish two hydrologic units based on sulfate, phosphate, silica, magnesium, potassium, calcium, and alkalinity content. Carbonate contents of turbiditic sediments vary from 0.6 to 7.4 wt% $CaCO_3$. Similar carbonate contents were measured in Pliocene and Pleistocene turbiditic sediments recovered at Sites U1449–U1451. A 4.6 m thick hemipelagic interval at 184 m CSF-A was analyzed at high resolution with XRF scanning. It reveals that carbonate content varies between 18 and 60 wt% with an average of ~40 wt%. Sr/Ca ratio and carbonate content variations suggest a single binary mixing between marine biogenic carbonate and a silicate end-member.

Site U1453

Site U1453 (proposed Site MBF-4A) is in the center of our seven-site transect of shallow-penetration holes. It is located at 8°0.42′N, 86°47.90′E in a water depth of 3690.5 m. Combined with the other transect sites, Site U1453 will document depocenter migration and quantify overall sediment delivery to 8°N since the Pleistocene.

Site U1453 is located ~1 km south and ~5 km east of a prominent surficial channel. The channel exhibits pronounced meandering point bars and internal terraces. Sediment transported by this channel has therefore significantly influenced deposition at this site during the channel's lifetime. A prominent buried point bar is located <1 km west of the site. The overall seismic reflectivity at the drill site is relatively high, indicating coarse material throughout most of the drilled section, except for the lower portion of the drill hole. Distinct and variable local spillover deposits were expected at the site in response to the channel and meander evolution. Toward

the base of the hole, lower seismic reflectivity and distinct layering is inferred to reflect hemipelagic or distal levee deposition.

In addition to coring, downhole logging was introduced as an important objective of Site U1453 after attempts to log at Sites U1450 and U1451 were unsuccessful. Logging data are essential for determining the inventory of lithofacies and structures in the fan given the limitations in completely recovering unconsolidated coarse material and the importance of measuring in situ physical properties and imaging fine-scale sedimentary structures. Therefore, we decided to log Hole U1453A despite its shallow ~215 m penetration to increase chances that we could acquire this critical in situ log data. This was particularly important for characterizing the in situ properties of thick sandy intervals that HLAPC cores returned as loose and liquefied sand.

Principal results

Site U1453 contributes to the overall seven-site transect drilled during Expedition 354. When integrated with the seismic profile and refined chronostratigraphic data from the remaining part of the transect, this site will document fan construction processes and the depocenter migration time frame. Specifically, Site U1453 provides an almost completely recovered succession of silt- and/or sand-dominated sheeted units related to the formation and evolution of a large meandering channel system lacking a distinct levee unit. Intercalation of these sheets with thinner levee units either from the large channel or from nearby smaller channels may help us understand why the channel has been apparently maintained in this position for a relatively long time period. This type of configuration is part of the different processes that influence interlevee deposition. A few thin hemipelagic layers are also observed between sandy turbiditic units, which may indicate that sheeted sedimentation was restricted to short time periods only and was not always followed by an erosional and levee formation phase. The interval cored between 144 and 159 m CSF-A represents an expanded hemipelagic unit dated between 0.8 and 1.2 Ma. Fan sedimentation intensified between 800 and 300 ka, the basal age of the overlying hemipelagic unit at the surface. Accordingly, fan deposits grew by 100 m in 500 ky, equivalent to an average sedimentation rate of 20 cm/ky.

The successful acquisition of the expedition's only downhole log data will allow detailed comparison of how well the fine-scale (centimeter to decimeter) structure in the formation has been preserved in cores. Particularly, the proportion of sand in the formation versus the amount recovered by coring will help calibrate sedimentary records from other sites.

Analyzing some graded variations within the sandy units using magnetic susceptibility data from both cores and downhole data shows that despite the HLAPC coring process and curatorial procedures (vertical settling of sands) the average physical properties still match with in situ data and can hence be used to characterize the formation. This match confirms that cored structureless sand truly reflects, on average, the sand unit at depth even though several meter thick sand cores were recovered with the HLAPC system, which apparently did not fully penetrate the formation.

Operations

In Hole U1453A, APC and HLAPC coring penetrated the seafloor to 172.9 m CSF-A, except for one 5 m interval advanced without coring. Most of the coring was done with the HLAPC system. However, the APC system was used for the uppermost four cores and one deeper core around 145 m CSF-A when we attempted to recover a hemipelagic layer in a single core. From 172.9 to 215.7 m CSF-A, the hole was deepened with HLAPC cores alternating with five 4.8 m advances without coring. Hole U1453A penetrated 186.7 m, of which 164.8 m was cored with 88% recovery.

After coring was completed, we collected downhole logging data with two tool strings (triple combo and FMS-sonic). Logging was very successful with good hole conditions and reached the full depth of the hole.

Lithostratigraphy

The overall lithology of Site U1453 is similar to that of other Expedition 354 sites in that it is dominated by mica- and quartz-rich sand, silt, and clay turbidites separated by bioturbated nannofossil-rich calcareous oozes and occasional glassy volcanic ash layers. Turbidite sequences at Site U1453 represent cycles of channel-levee activity and abandonment that constructed the fan. The base of the section contains thick sand units, which are most likely sheet deposits from nearby channels. Above these sands, a moderately thick (~15 m) section of calcareous clay indicates a time when channel activity and coarse detrital supply to this area of the fan was reduced. The middle of the section contains a 127 m thick interval of fine sand interbedded with mud turbidites and occasional calcareous clay beds, suggesting onset and waxing and waning of proximal channel activity and levee building. The stratigraphic section is topped with 10 m of calcareous clay, indicating reduced turbiditic input.

Biostratigraphy

Calcareous nannofossil and planktonic foraminiferal biostratigraphic analyses were conducted at Site U1453 on 37 samples and resulted in the identification of 4 biomarker events. The sedimentary succession at Site U1453 extends to the early Pleistocene. As with other sites, planktonic foraminiferal assemblages are characteristic of tropical–subtropical environments. Foraminiferal preservation ranges from poor to good in samples where they occur, and fragmentation of planktonic foraminifers ranges from light to severe. As at Site U1452, the LO of the foraminiferal biomarker *Globorotalia tosaensis* (0.61 Ma) was found at a shallower depth than the nannofossil biomarkers *Emiliania huxleyi* (0.29 Ma) and *Pseudoemiliania lacunosa* (0.44 Ma), indicating that this foraminifer was either reworked or has a longer duration in the Indian Ocean. Foraminiferal biostratigraphy was limited at this site because of the large section of sands recovered from Cores 354-U1453A-10F through 28F, in which samples are either barren of foraminifers or have a very rare occurrence (<0.1%). The LO of the nannofossil *Helicosphaera sellii* (1.26 Ma) is found at approximately 116 m CSF-A. However, the Brunhes/Matuyama boundary (0.781) is found at 152 m CSF-A, indicating that either *H. sellii* was reworked or has a longer duration in the Indian Ocean. This discrepancy was observed at several Expedition 354 sites and will be further studied in postexpedition work.

Paleomagnetism

The Brunhes/Matuyama boundary and both boundaries of the Jaramillo and Cobb Mountain Subchrons were identified at Site U1453 in hemipelagic calcareous clay units between ~142 and 160 m CSF-A. A ~180° change in declination associated with a thin ash layer is interpreted as the Brunhes/Matuyama boundary (152.59 m CSF-A). Changes in declination also clearly delineate the Jaramillo and Cobb Mountain Subchrons (155.76–156.71 and 157.99–158.23 m CSF-A, respectively) in calcareous clay deposits at Site U1453.

Physical properties

Physical property data were acquired on all Hole U1453A cores, including density, magnetic susceptibility, *P*-wave velocity, NGR, and thermal conductivity. Physical property data at Site U1453 are mostly of good quality and reflect lithologic variations. Using the principal lithologic name from the core description to assign five lithologies (sand = ~73 m, silt = ~11 m, clay = ~45 m, calcareous clay = ~23 m, and volcanic ash), we calculated their minimum, maximum, and average physical properties. Wet bulk densities are rather uniform for terrigenous sediment (sand, silt, and clay), ranging from 1.89 to 1.96 g/cm^3. Calcareous clay has the lowest densities (1.62 g/cm^3), followed by volcanic ash (1.68 g/cm^3). *P*-wave velocities are highest in sand (1666 m/s on average) and lowest in silt and clay (~1530 m/s). Magnetic susceptibilities are also highest in sand (109 × 10^{-5} SI), followed by silt (90 × 10^{-5} SI) and clay (56 × 10^{-5} SI). The lowest values occur in calcareous clay (20 × 10^{-5} SI). NGR is high throughout the terrigenous components sand, silt, and clay (around 70 counts/s) and low in calcareous clay (43 counts/s). Thermal conductivity is highest in sand (1.82 W/[m·K]) and lowest in calcareous clay (1.17 W/[m·K]).

Downhole logging

The triple combo (magnetic susceptibility, NGR, and resistivity) and FMS-sonic velocity tool strings were run in Hole U1453A. The hole was filled with 12 lb/gal heavy viscous mud to inhibit borehole wall collapse. In contrast to our previous logging attempts, logging was successful with a single run of the triple combo tool string and two runs of the FMS-sonic tool string to the bottom of the hole at 220 m wireline log depth below seafloor (WSF). The hole diameter varied between 9 and 14 inches with only a few washout zones.

Downhole measurements of magnetic susceptibility and NGR match the equivalent core measurements well and permit preliminary interpretation of lithology based on the log data in the intervals where core was not recovered. The FMS resistivity images in particular provide a good record of the depth and thickness of the sand beds in the hole. Sand-rich cores were sometimes fluidized when recovered, but the log data could confirm that the sands in the 9.5 m core came from the same 9.5 interval in the hole and that compositional trends over several cores were similar in core and log data. Additionally, downhole *P*-wave velocities are higher than those measured in the laboratory, reflecting in situ conditions in the borehole.

Geochemistry

The close proximity of a channel incising deeper than 100 m CSF-A, associated with the variable dip angle of the formations, provided the opportunity to investigate a subseafloor hydrology that is potentially more affected by lateral flow than other drill sites. Based on sulfate and alkalinity data, a well-defined boundary between two hydrologic units is observed around 30 m CSF-A. However, this formation is very similar to what was observed at Sites U1449 and U1452, implying that the proximity of the channel does not affect the hydrology at this site.

Pleistocene turbidites are characterized by carbonate content of 0.8 to 5.9 wt%, and hemipelagic calcareous clays have an average carbonate content of 25.9 wt%. For turbidites, these characteristics are similar to what is observed in modern Ganga-Brahmaputra river sediments and the uppermost 150 m at Sites U1449–U1452 and DSDP Site 218. TOC content in turbidites averages 0.7 wt% and covaries with bulk-sediment Al/Si ratios, reflecting the preferential association of organic matter with clays that is documented in both the modern Ganga-Brahmaputra river system and in active channel-levee sediments in the Bay of Bengal deposited over the past 18 ky. Bulk geochemical composition closely matches that observed at Sites U1449–U1452 and in modern sediments in the Ganga-Brahmaputra river system. Samples offset from the main trends are from hemipelagic units and suggest the occurrence of Fe-rich clays and/or a low K/Al subpopulation, possibly reflecting a different terrigenous input or an effect of particle sorting.

Site U1454

Site U1454 (proposed Site MBF-7A) is the westernmost of the transect of seven shallow-penetration sites drilled in the Bengal Fan at 8°N during Expedition 354. The site was introduced during the expedition as an alternate site to capture the most recent and Late Pleistocene fan deposition at high resolution. Expedition 354 sites in the eastern and central part of the transect revealed that fan deposition above and below the Toba ash layer (~75 ka) was remarkably low, indicating migration of turbidite channel activity to the west of the 85°East Ridge for probably the last 300 ky.

Site U1454 is located ~50 km west of Site U1455 (DSDP Site 218) at 08°0.39′N, 85°51.00′E, in a water depth of 3721.4 m. It is situated on the western levee of a channel-levee system believed to be the modern active channel of the fan (Hübscher et al., 1997). The levee surface rises ~50 m above the thalweg of the meandering channel that is well imaged with multibeam bathymetry. Site U1454 is intended to provide a sequence through a channel-levee system that can be dated by ^{14}C and δ^{18}O and thereby be related to global climatic and sea-level cycles and other proxies for sediment flux and weathering. The general objective of the Pleistocene transect at 8°N is to document depocenter migration and overall accumulation rates since the Pliocene, and Site U1454 completes this approach by focusing on the Late Pleistocene and Holocene fan deposition. Obtaining a high-resolution levee record that could extend into the Holocene will allow comparison of this middle fan deposition to an upper fan levee likely constructed across the same channel levee at 16°N since 18 ka (Hübscher et al., 1997; Weber et al., 1997). Obtaining information on how the fan system developed during the last glacial cycle will provide insight into the relation of fan growth, sea-level change, and erosion changes driven by well-constrained climate evolution. The levee at 16°N records changing weathering and vegetation conditions since the Last Glacial Maximum (Galy et al., 2008; Lupker et al., 2013) that can be correlated to Site U1454.

Principal results

Site U1454 provides a key expanded section to the overall understanding of depositional processes in the Pleistocene Bengal Fan. This site was added during the expedition because of the inferred Holocene age of the channel with sediments suitable for dating with oxygen isotopes and radiocarbon or foraminiferal tests and on terrestrial organic material, in addition to high-resolution nannofossil biostratigraphic work. Accordingly, we will be able to determine the time spans over which the levee units have formed. Also, the surficial calcareous clay unit will constrain the timing of turbidite input at this location. Furthermore, we expect a high-resolution record that will allow us to link channel activity with sea level and glacial–interglacial climatic cycles.

Beneath the levee unit, coring recovered a sand-rich section comparable to Site U1452 that likely represents the progradational facies of early channel formation and erosion. Several other smaller channel systems in the vicinity contributed to sediment accumulation at Site U1454, and it will be interesting to investigate their tem-

poral relationships with the active channel. Mud turbidites, silt, and sand beds are intercalated between hemipelagic units, indicating episodic channel activity.

An organic-rich turbidite was recovered at ~34 m CSF-A in the sand-rich section. It comprises an 18 cm thick layer of organic debris deposited at the base of a sand layer. The base of the organic layer contains a centimeter-sized wood branch. Unlike the Miocene and Pliocene, organic debris is not frequently found in Pleistocene turbidites, and this one represents an unusual transport from the delta to the fan. Identification of wood species may constrain the source of this deposit and the vegetation zone from which is derived.

Site U1454 also completes the recovery of the Middle Pleistocene hemipelagic interval to the westernmost position and allows detailed study of the transition to intensified fan activity over a lateral distance of 300 km. This will shed light on the distances over which the active channel can deliver fine particles and contribute to the dilution of pelagic accumulation.

Operations

Four holes were cored at Site U1454. Hole U1454A is a single mudline core to 7.5 m DSF for microbiology and geochemical studies. Hole U1454B was cored with the APC and HLAPC systems to 161.8 m DSF and recovered 129.51 m of sediment (88%). This hole also included three 4.8 m advances without coring. The four upper cores utilized the APC system with an orientation tool and nonmagnetic hardware. Holes U1454C and U1454D were shallow penetrations (37.2 and 37.1 m DSF, respectively) and recovered 30.16 and 24.46 m of sediment (81% and 66%, respectively). The latter were cored to fully record the uppermost levee, provide sufficient samples for high-resolution studies, and avoid gaps. Cores from Holes U1454C and U1454D were not split during the expedition; they will be split following the expedition at the IODP core repository.

Lithostratigraphy

Coring at Site U1454 recovered a full levee sequence most probably associated with the modern active channel of the Bengal Fan. The sequence is well represented by the 25 m sequence of mud turbidites in Unit II. Intervals of calcareous clay occur in the top 20 cm of Hole U1454B and are rare to about 110 m CSF-A. Deeper calcareous and clastic units alternate to 139.14 m CSF-A, where an 18 m thick interval of mottled calcareous clay with occasional color banding appears. Plant fragments occur in several silt intervals, including large (~2 cm) wood fragments. In the lower hemipelagic interval, one 8 cm thick volcanic ash layer is present at 145.5 m CSF-A. It is much thinner than the shallowest ash layers recovered at other Expedition 354 sites (~20 cm) and is likely related to the Toba eruption before the Brunhes/Matuyama boundary (790 ka).

Overall, siliciclastic units (silt, clay, and sand) at Site U1454 are compositionally classified as mica rich (muscovite and biotite) and quartz rich. Sand occurs mostly in fine to medium grain size ranges, with rare occurrences of coarse-grained particles. Feldspars and heavy minerals (e.g., amphibole, garnet, clinozoisite, zoisite, tourmaline, zircon, rutile, epidote, sillimanite, chloritoid, pyroxene, staurolite, and opaque minerals) are common in silt- and sand-rich layers and occasionally contain euhedral carbonate minerals and carbonate aggregate grains. Lithic fragments (e.g., biotite-gneiss, amphibole-mica schist, sillimanite-biotite-gneiss, and phyllite fragments) appear in sand. These minerals are consistent with a general provenance from Himalayan river sands (e.g., Garzanti et al., 2004).

Biostratigraphy

The levee system targeted for drilling at Site U1454 was expected to be of Pleistocene age. Biostratigraphic age control within the Pleistocene is limited to three nannofossil zones and two foraminiferal biomarkers (at 0.61 and 1.88 Ma). Calcareous nannofossil assemblages were observed in 44 samples from Site U1454, and the sediments contain a recent to early Pleistocene sequence. Foraminiferal assemblages were observed in 19 samples, and 19 samples were barren of foraminifers because of the recovery of turbidite sands in core catcher samples. Postexpedition work on nannofossils may further constrain sediment ages, as there are additional biostratigraphic markers that could potentially be used to refine the Pleistocene age model.

Paleomagnetism

We identified the Brunhes/Matuyama boundary and the Jaramillo and Cobb Mountain Subchrons in hemipelagic calcareous clay at 145–151 m CSF-A at Site U1454; they can be correlated with similar intervals in other holes within the Expedition 354 transect based on both magnetostratigraphy and seismic stratigraphy. The Brunhes/Matuyama boundary occurs at 145.83 m CSF-A, roughly similar to the depth of the same transition at Site U1453; as at Site U1453, the transition is associated with an ash layer. The upper boundary of the Jaramillo Subchron is likely in an interval that was not recovered between Cores 354-U1454B-29F and 30F. Core 30F contains the lower boundary of the Jaramillo Subchron (148.63 m CSF-A) and both boundaries of the Cobb Mountain Subchron (149.86–150.20 m CSF-A).

Physical properties

Physical property data were acquired on all Hole U1453A cores, including density, magnetic susceptibility, *P*-wave velocity, NGR, and thermal conductivity. Physical property data from Site U1453 are mostly of good quality and reflect lithologic variations. Average physical properties were determined for five principal lithologies based on visual core description: the most common principal lithology is sand (~73 m), followed by clay (~45 m), calcareous clay (~23 m), and silt (~11 m), with volcanic ash occurring in traces. Wet bulk densities are rather uniform for terrigenous sediment (sand, silt, and clay), ranging from 1.89 to 1.96 g/cm^3. Calcareous clay has the lowest density (1.62 g/cm^3), followed by volcanic ash (1.68 g/cm^3). *P*-wave velocities are highest in sand (average = 1666 m/s) and lowest in silt and clay (~1530 m/s). Magnetic susceptibilities are also highest in sand (109 × 10^{-5} SI), followed by silt (90 × 10^{-5} SI) and clay (56 × 10^{-5} SI). The lowest values occur in calcareous clay (20 × 10^{-5} SI). NGR is high throughout the terrigenous components sand, silt, and clay (around 70 counts/s) and low in calcareous clay (43 counts/s). Thermal conductivity is highest in sand (1.82 W/[m·K]) and lowest in calcareous clay (1.17 W/[m·K]).

Geochemistry

At Site 1454, interstitial water measurements were conducted only on sediments from the top 7 m. As at other sites studied during this expedition, the hydrochemistry in this upper section is dominated by biogenic processes that release dissolved phosphate, ammonium, and CO_2 (leading to a rise in alkalinity) and consume sulfate.

Turbidites recovered at Site U1454 have $CaCO_3$ contents between 2 and 5 wt%, except for four samples from the upper 16 m of the levee that have $CaCO_3$ contents between 6 and 7.4 wt%. These four values are significantly higher than all carbonate content mea-

sured in turbidites from the seven Pleistocene sections cored during Expedition 354 (0.5–6 wt%). They are, however, identical to the carbonate content recorded in sediments deposited during the last deglaciation at the 17°N active channel-levee (Lupker et al., 2013). This could indicate a match between the 17°N and 8°N levee records; however, the pattern of K-depletion observed during the Holocene at 17°N was not observed at Site U1454.

Site U1455

Site U1455 (proposed Site MBF-1A) is the last site drilled during Expedition 354 in the Bengal Fan. It is a reoccupation of DSDP Site 218 (Figure **F11**) (von der Borch, Sclater, et al., 1974), which was the first attempt to drill the Bengal Fan and was only spot cored with the RCB system to 773 mbsf. The site is above the eastern flank of the 85°E Ridge at 8°0.42′N, 86°16.97′E at 3743 m water depth. Site U1455 is one of three deep-penetration sites along the Expedition 354 transect dedicated to reveal Neogene fan evolution and Himalayan erosion. This site will also document Pleistocene fan architecture when integrated into the complete seven-site transect. Coring to 900 mbsf was planned to determine Miocene to Pliocene accumulation rates and changes related to Himalayan erosion and environment. The deeper part of the site will extend the existing Site 218 record back into the middle Miocene. Because of time constraints at the end of the expedition, we focused coring on three objectives: the Pleistocene (0–122 mbsf), the late Miocene terrestrial vegetation transition from C3 to C4 plants (360–431 mbsf), and the middle Miocene (773–949 mbsf) to extend the existing core record of Site 218.

Because Site U1455 is above the 85°E Ridge, which has undergone deformation since the Miocene (Schwenk and Spiess, 2009), accumulation rates at this site are lower than at Site U1450 in the axial part of the fan transect and similar to those at Site U1451. The overall thickness of the fan is less than 4 km in this location according to Curray et al. (2003). These lower accumulation rates offer the possibility to capture a longer stratigraphic range within an achievable depth of penetration. Site U1455 was intended to help establish a representative accumulation history from the middle Miocene to recent, which is essential to complete the 8°N transect of the Bengal Fan.

Principal results

Site U1455, located above 85°E Ridge, is a key location for the transect approach, particularly for investigating Miocene fan deposition. A comparison between the easternmost Site U1451 and this site should elucidate whether depocenter migration occurred in a similar manner as in the Pliocene and Pleistocene. Because of the absence of major channel-levee systems, addressing these objectives can only be achieved by integrating core and seismic data. This integration will require good chronostratigraphic control to allow comparison of the same time periods, which has to await postexpedition work.

Site U1455 cored critical intervals that will address different objectives. In the upper section of Core 354-U1455C-1H, the Toba ash layer is found at 5.6 m DSF instead of being consistently around 2 m deep as at other eastern Expedition 354 sites. The vicinity of the most recently active channel (Site U1454, ~50 km west) is the likely

Figure F11. Actual and planned Expedition 354 operations.

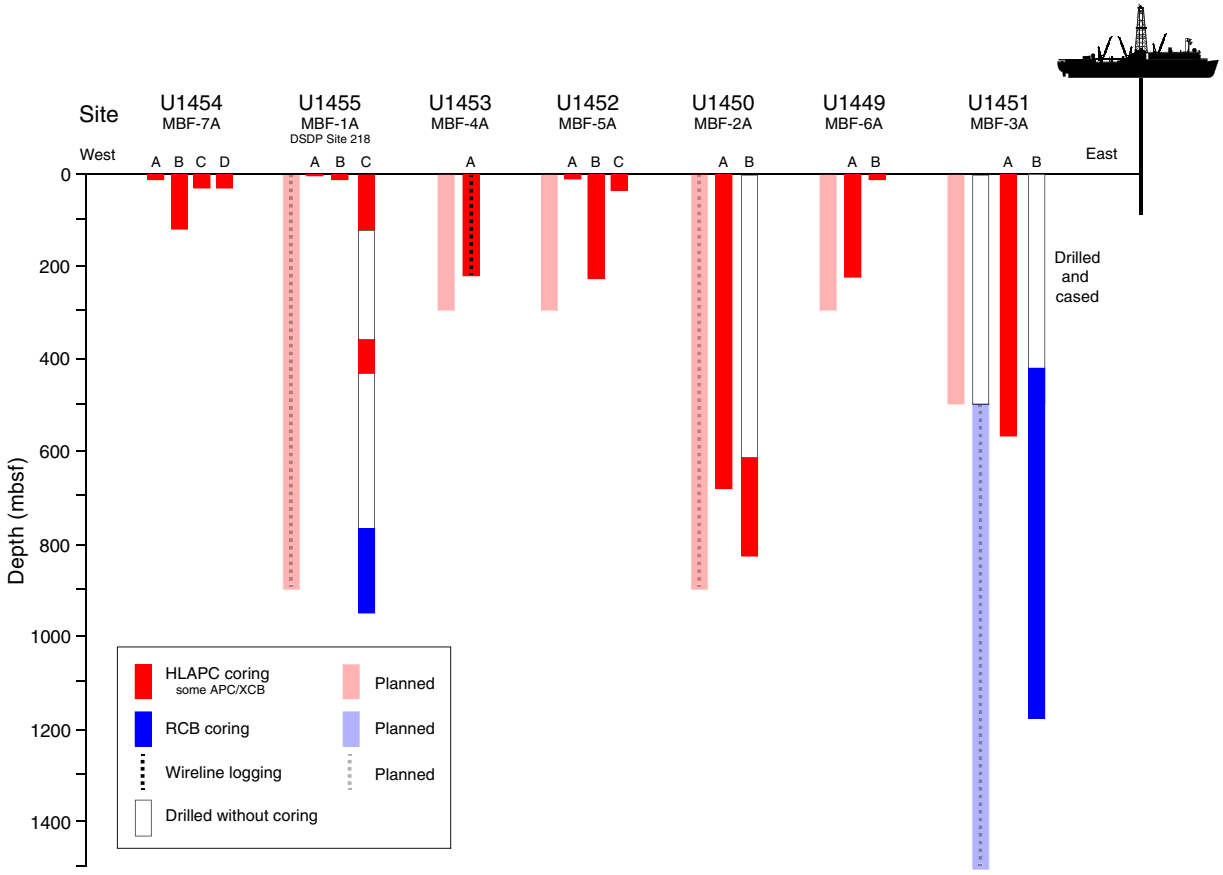

explanation for this increased recent sedimentation, and discrete detrital deposition was observed above the Toba ash layer at this site. This site will further highlight deposition of clay and silt in the context of a distant active channel.

Second, the deeper late Miocene interval cored between 360 and 431 m DSF returned a relatively continuous record across the terrestrial vegetation change from the C3 to C4 photosynthetic types of plant, known to occur around 380 mbsf at Site 218. A number of short hemipelagic intervals are present in this section that should provide good chronological constraint for this transition. They may also document ecological variability on shorter timescales.

Coarser grained deposition has been found deeper than 770 mbsf, even though recovery of sand was limited by RCB drilling. Intervals with penetration rates as high as 0.5–1 min/m without recovery in this deep section of the hole revealed the presence of thick unconsolidated layers of sand. Coarser grained material suitable to study Himalayan erosion was found, although it was not recovered at Site U1451 for the same period. In this particular depth interval, further detailed sedimentary analyses may shed light on the causes for the depositional facies being different from Pliocene and Pleistocene times and may help to determine whether the absence of levees originated from a change in sediment supply or transport pathways or from other factors.

Operations

We cored three holes at Site U1455. Holes U1455A and U1455B each consist of a single mudline core; the cores penetrated to 0.9 and 6.9 m DSF, respectively. Hole U1455C consists of coring in three intervals: 0–122.3 m DSF (APC and HLAPC systems), 359.8–431.4 m DSF (HLAPC system), and 773.0–949.0 m DSF (RCB system).

The uppermost interval of Hole U1455C consists of APC and HLAPC coring and four 4.8 m advances without coring (19.2 m). Cores 1H–24F penetrated 103.1 m in this interval and recovered 89.82 m of sediment (87%). We drilled 237.5 m without coring from 122.3 to 359.8 m DSF and then resumed continuous HLAPC coring. Cores 26F–41F penetrated from 359.8 to 431.4 m DSF (71.6 m) and recovered 48.82 m of sediment (68%). After dropping a free-fall funnel (FFF) and retrieving the drill string to switch to the RCB system, we reentered Hole U1455C and drilled ahead without coring from 431.4 to 773.0 m DSF. We RCB cored from that depth to 949.0 m DSF. Cores 43R–60R penetrated 176.0 m and recovered 59.36 m of sediment (34%). Coring ended on 28 March 2015 at 1435 h when the operational time for the expedition expired.

Lithostratigraphy

As at other Expedition 354 sites, lithologic differences between units and variations in grain size and bed thickness reflect cycles of proximal turbidity current channel activity and abandonment. Sand intervals may represent interlevee "sheet flows" (e.g., Curray et al., 2003), whereas finer grained fractions are more likely preserved in leveed sections. Calcareous clay units reflect cessation of proximal channel activity, but the intervals also resemble episodes of minor increase in siliciclastic deposition.

Coring in Hole U1455C was divided into three segments. The uppermost segment (from the seabed to 120.51 m CSF-A) is principally composed of micaceous quartz-rich siliciclastic sediments, many containing typical characteristics of turbidites (sharp base, normal grading, and laminations). In this segment, the lower sand units are overlain by 13.5 m of calcareous clay covered by a 45.86 m thick section of sand and mud turbidites. There are two glassy volcanic ash layers at 5.68–5.75 and 82.80–82.89 m CSF-A. The second recovered segment of Hole U1455C (359.80–431.39 m CSF-A) is also predominantly micaceous and quartz-rich sand, silt, and clay, although fewer turbiditic characteristics are present. Calcareous clay units alternate with siliciclastic sediments. The lowermost segment (773.0 m CSF-A to the base of the hole at 942.35 m CSF-A) contains claystone and siltstone intervals with preserved turbiditic characteristics, as well as a ~4 m thick unit of calcareous claystone. Organic fragments are prevalent in this segment.

Overall, siliciclastic units (silt, clay, and sand) at Site U1455 are compositionally classified as micaceous (muscovite and biotite) and quartz rich. Sand occurs mostly in fine to medium grain size ranges, with rare coarse-grained particles. Feldspars and heavy minerals (e.g., amphibole, garnet, clinozoisite, zoisite, tourmaline, zircon, rutile, sphene, epidote, sillimanite, chloritoid, pyroxene, staurolite, and opaque minerals) are common in silt and sand layers and occasionally contain euhedral carbonate minerals and carbonate aggregate grains. Lithic fragments (e.g., biotite-gneiss, amphibole-mica schist, sillimanite-biotite-gneiss, and phyllite fragments) appear in sand. From previous sites (see **Principal results** for Site U1450, above), we know that siliciclastic sediments in the fan contain between ~3% and 10% of detrital carbonate as well. Calcareous clays contain calcareous nannofossils, clay minerals, foraminifers, diatoms, and radiolarians.

Biostratigraphy

Calcareous nannofossil and planktonic foraminiferal biostratigraphic analyses were conducted at Site U1455 on 113 samples and resulted in the identification of 14 biomarker events. These events were used to construct 3 foraminiferal and 10 nannofossil biozones, providing good age control extending back to the middle Miocene. The age model reconstruction is limited to the drilled intervals from 0 to 120 m CSF-A and from 360 to 430 m CSF-A and by the very low abundance and barren intervals from 773 m CSF-A to the bottom of Hole U1455C. Foraminiferal species diversity decreased with depth, which could be due to preservation changes in the sediments or could reflect a change in environmental conditions of the overlying water column.

Paleomagnetism

We identified the Brunhes/Matuyama boundary and the Jaramillo Subchron in a calcareous clay interval at Site U1455 that was correlated with similar intervals in other holes within the Expedition 354 transect based on both magnetostratigraphy and seismic stratigraphy. The Brunhes/Matuyama boundary occurs at 82.83 m CSF-A in Core 354-U1455C-6F. As at all other sites where the Brunhes/Matuyama boundary is identified, the transition is associated with an ash layer. Core 17F contains the Jaramillo Subchron (86.40–87.92 m CSF-A). Unlike all other sites, the Cobb Mountain Subchron was not recorded at Site U1455 and is likely located between Cores 17F and 18F.

Physical properties

Physical property data were acquired on all Hole U1455C cores, including density, magnetic susceptibility, *P*-wave velocity, NGR, and thermal conductivity. Physical property data at Site U1455 are mostly of good quality. Using the principal lithologic name from the core description, we assigned eight lithologies and calculated their average physical properties. Accordingly, the most common principal lithology is sand (~56 m), followed by clay (~40 m), claystone

(~38 m), silt (~22 m), clay (~21 m), calcareous claystone (~10 m), siltstone (~6 m), and volcanic ash occurring in minor proportions. Average wet bulk densities vary from 1.84 to 2.06 g/cm^3 for terrigenous sediment (sand, silt, and clay). Lithified sediments (claystone, calcareous claystone, and siltstone) have higher average wet bulk densities (2.12–2.20 g/cm^3). Average *P*-wave velocities are also higher for lithified intervals (1795–1931 m/s), whereas they are lowest in clay and calcareous clay (~1540 m/s). Average magnetic susceptibilities are highest in sand (112 × 10^{-5} SI), followed by silt (166 × 10^{-5} SI) and clay (55 × 10^{-5} SI). The lowest values occur in calcareous clay and volcanic ash (~20 × 10^{-5} SI). NGR is elevated throughout the terrigenous and lithified sediment (64–71 counts/s) and low in calcareous clay (37 counts/s). Thermal conductivity is highest in claystone (2.23 W/[m·K]) and lowest in calcareous clay and calcareous claystone (~1.2 W/[m·K]).

Geochemistry

Interstitial water chemistry was only conducted in the upper section of Site U1455 and suggests active biotic processes releasing dissolved phosphate and ammonium and influencing pore water alkalinity and sulfate concentrations. Phosphate and ammonium contents covary, and the rise in alkalinity in the upper section of the core is associated with a drop in calcium and magnesium contents.

Bulk-sediment major and trace element concentrations correspond closely to sediment lithology and are consistent with observations made at other Expedition 354 sites and within the Ganga-Brahmaputra river system. The increase in carbonate content in turbiditic sediments deeper than 360 m CSF-A is consistent with a similar increase at Sites U1450 and U1451 and Site 218 and indicates a regional change in the delivery of detrital carbonate to the fan. TOC contents in Pleistocene turbiditic sediments covary with Al/Si, a proxy for grain size and mineral composition, reflecting preferential association of organic matter with clay. This behavior is consistent with similar observations in the Ganga-Brahmaputra river system, in modern (18 ka) fan deposits, and at all sites along the 8°N transect across the Bengal Fan. The organic carbon content of pelagic and hemipelagic sediments broadly decreases with depth, consistent with organic carbon concentrations observed at Site 218.

Preliminary assessment

Expedition 354 was planned to core the sedimentary record of erosion of the Himalayan mountain range for paleoerosion studies, to determine associated accumulation rates at the scale of one cross-section across the sedimentary fan in the Bay of Bengal, and to ultimately constrain fluxes of erosion. To meet these objectives, a transect approach perpendicular to the axis of the fan at 8°N was adopted. One challenge was to cover the Neogene and late Paleogene at several sites where these objectives could be achieved within a reasonable depth of penetration. Another challenge was to be able to recover cores from sandy formations, which are very difficult to sample with most coring techniques. Recovering sand samples, however, was essential for paleoerosion studies, many of which are based on single grain measurements. Sand recovery was also required to reconstruct fan depositional processes. As core recovery in sand was expected to be incomplete, downhole logging was a key element in the expedition planning. With these constraints, our original objective was to core and log the three deep sites and to core three additional shallower sites to increase the level of resolution of the Pleistocene transect to the spatial scale of 50 km.

Figure **F11** compares our original drilling plans with the operations conducted during the expedition. Figures **F3** and **F4** show the locations of the drill sites. Further information on coring is presented in Table **T1**.

Following our first coring experience at Site U1449, it appeared that the APC system would be limited to the uppermost 3–5 cores in these formations because it is typically stopped in sand well before full penetration and that the HLAPC would be the best compromise to recover firm yet unconsolidated material. The HLAPC was efficient in providing excellent recovery of the sedimentary record in unconsolidated silts and sand but resulted in much longer coring times. In order to meet time constraints for the full expedition, HLAPC coring was often alternated with 4.8 m advances without coring, particularly in deeper sections of the holes. Deep drilling in the fan revealed that lithification did not increase much with depth and was highly variable depending on lithology. Sand layers remained essentially unconsolidated even at 900 mbsf. This significantly limited our ability to obtain downhole logging data, as sand collapse prevented logging in all deep holes. Logging was finally achieved only in a single 220 m deep hole at Site U1453. This logging operation was very successful and is critical for documenting the different lithologic facies and guiding the interpretation of core and seismic data throughout the drilling transect. Because of the lack of late Quaternary (<300 ka) turbiditic deposition at all originally planned Expedition 354 transect sites, Site U1454 was added, extending the transect west to core through a levee unit supplied by the presently active channel.

Given these adaptations to the initial strategy, during Expedition 354 we drilled at all of the originally planned sites plus one additional site and succeeded in establishing (1) a seven-site transect to cover Pleistocene deposition and fan architecture, (2) a transect of three deep sites (U1450, U1451, and U1455) to record Miocene and Pliocene accumulation, and (3) a single deeper site to 1180 mbsf (Site U1451) to core the oldest fan deposits possible. Shallow logging at one site (U1453) provided valuable characterization of sand deposition. Although logging was a very important objective to reconstruct the full succession of lithologies, borehole conditions did not allow extensive measurements. However, the excellent match between the cored sediments and seismic data indicates that correlation across the transect sites can definitely be achieved and will reliably document fan sedimentation processes and help to reconstruct overall fan growth rates. The expedition was able to successfully address most of the research objectives originally planned. Core and log data, along with their preliminary results, provide excellent material and a strong scientific foundation for postexpedition research. In the following sections, we briefly review how Expedition 354 science objectives were addressed.

1. *Fan architecture and depocenter variability*

Expedition 354 pursued for the first time the approach to systematically drill a large number of sites along a transect across a sedimentary fan. This approach intended to account for the lateral shifting of depocenters on relatively short timescales and incomplete documentation of fan activity at any single site. Altogether, seven sites were drilled, all with an almost full recovery of the upper 150 to 220 m of the sedimentary section. This lower limit in continuous coring penetration was constrained by the capabilities of the APC technology for coring sequences with minor or major amounts of silt and sand. APC coring (9.7 m) was only possible within the upper 20 to 50 m. Deeper core barrels did not penetrate sufficiently because of frictional forces, resulting in low recovery and significant drilling disturbance. Only the HLAPC (4.7 m) was able to sufficiently penetrate the formation, and it provided cores with limited disturbance and up to 100% recovery. However, coring time in-

creased significantly with the HLAPC, and the original depth targets (300 mbsf) had to be adjusted to ~200 mbsf. Accordingly, Pliocene fan sediments were recovered at Site U1450 with coring gaps. Sediments of comparable age were completely cored at Site U1451, but with minor fan turbiditic representation. The primary objective was adjusted to focus on the Pleistocene.

The primary stratigraphic framework for constraining Pleistocene sedimentation across the seven-site transect was provided by two units with comparably higher average carbonate contents of 21 wt% (varying between 2 and 80 wt%; mostly calcareous clays). These sediments provide adequate biostratigraphic and magnetostratigraphic age constraints. The most recent of these units dates back to ~0.2–0.3 Ma. It is present across the eastern part of the transect with a thickness of ~5 m (Sites U1449–U1453) to >10 m at Site U1455. At Site U1454, the active channel-levee system of the modern Bengal Fan delivers most of the sediments, and the hemipelagic proportion is significantly diluted. The absence of any indication of turbiditic activity at distances >100 km from the active channel clearly indicates that the Bengal Fan channels supply fine-grained material for the buildup of levees perpendicular to the channel axis but only to a limited distance away from the channel. Detection of fan activity would have in this case only been possible at best closer than 100 km to the channel axis—a strong support of our transect approach to document Pleistocene fan activity and ensure continuous recovery of material delivered to the fan. As a confirmation, pelagic calcareous deposition is significantly diluted at Site U1455, which is located closer (~30 km southeast) to the active channel.

The second stratigraphically important calcareous clay unit dates back to the Middle Pleistocene and is well constrained to ~1.2 to ~0.8 Ma by magnetostratigraphy. Some combination of the Brunhes/Matuyama boundary and the Jaramillo and Cobb Mountain Subchrons was repeatedly recovered within this unit at all seven sites. This is of particular interest, as it marks a long interval of absence of fan deposition in this segment of the Bengal Fan, which likely shifted farther to the west than today. This allows investigation of a very well constrained time slice. Overlying this unit, the most intense fan deposition of all cored time periods is recorded, with overall growth rates on the order of 20 cm/ky. Across the transect, mid-Pleistocene growth rates are relatively uniform, which in turn indicates an episode of stability in a highly dynamic system. Given the large number of larger and smaller channels imaged in seismic data, the lifetime of a single channel-levee system is likely short. Accordingly, the intercalation of units from different channels has to be reconstructed to first generate a channel stacking succession from each site, which is then integrated into the fan perspective.

It is astonishing that despite the rapid shifts of depocenters, the overall fan growth rate is relatively uniform (the same order of magnitude at all sites). This uniformity ensures that the fan maintains a relatively smooth surface, through eventual leveling of depressions between channel-levee systems. As a consequence, although seismic data indicated tectonic activity that has faulted the fan sediments and has influenced topography, the rapid fan deposition maintained the average surface of the fan. In uplifting areas, average growth rates are overall smaller. On shorter timescales, however, such as the Late Pleistocene time slice (0.8–0.3 Ma), levee-induced topography is not fully leveled and is still visible in the bathymetry (Figure **F3**).

Expedition 354 sites were strategically placed so that different elements of the fan architecture could be studied by coring the upper 100–200 m. Dedicated coring operations recovered several larger levee units at Site U1449 and duplicate cores from levee units at Sites U1452 and U1454, the latter representing the active Holocene channel. Although the finer material is known to be well recovered with the APC coring technique, silty and sandy units were surprisingly well cored with the HLAPC system. Large volumes of unconsolidated sand and massive silt beds were retrieved. These sediments will allow study of the progradational phase of early channel formation; these are found at the base of all levees (Sites U1449, U1452, and U1454). However, sheeted sand and silt deposits were also observed in areas where seismic data show no associated channel-levee structure. These indicate "interlevee sedimentation," which may spread over wider distances than the levees and may result from readjustments within terminal lobes or short-lived episodes of avulsion followed by the reoccupation of an older channel. Interlevee sediments of particular interest were cored at almost all sites, with an emphasis on the shallow section of Site U1449, on Sites U1451 and U1455 situated above the Ninetyeast and 85°E Ridges, and Site U1453, which reveals a succession of sheeted sand deposits next to a large channel.

The recovered core material is of excellent quality to achieve the objective of understanding the depositional processes by utilizing high-resolution sedimentological imaging and scanning (e.g., with XRF, computed tomography [CT], or physical properties). Also, we will be able to build a detailed inventory of units, lithologies, and sedimentary properties to estimate sediment budgets, and aid the sedimentologic and architectural interpretation.

Site U1453 apparently provides a complete succession of lobe progradation, channel incision, and levee buildup, as does Site U1454 for the active channel. Dating of the sequence at Site U1453 will be challenging, as most of the Late Pleistocene deposits are older than 300 ka and therefore outside the range of radiocarbon dating. However, the active channel-levee system drilled at Site U1454 will provide age constraints on different elements of the channel formation and levee growth, allowing us to distinguish between changes in sediment delivery and geometrical changes of the channel. The model developed for the active channel from Site U1454 will then be applied to the other older sequences.

Site U1451 is unique in the sense that accumulation decreased since the early Pliocene, leading to frequent hemipelagic carbonate-rich deposition that may be dated with oxygen isotopes or perhaps cyclostratigraphy. Furthermore, the transition from hemipelagic sedimentation to fan activity is important in analyzing the spatial scales and the rates at which the delivery of terrestrial material changes. This hemipelagic to turbiditic transition may be particularly interesting for the end of the Middle Pleistocene hemipelagic interval, where intercalations of mud turbidites as well as thicker silty and sandy beds were found in various places, in addition to various degrees of mixing into the calcareous clay units. As this transition marks a major shift in the depositional system, likely from west to east, we will be able to determine the succession of the depocenter shifts and the trends in time and space. In that respect, the hemipelagic to turbiditic transition is also of interest when studying the surficial sediments, which may have received material from the active channel (Site U1454). At Site U1455, the youngest Toba ash occurs at 5.6 mbsf, whereas at more easterly sites it is constantly found at around 2 mbsf. Site U1453, ~100 km away from the active channel, will be used for reference and to clarify the question of how much clay material is dispersed in the water column and contributes to the hemipelagic units, which often have much lower carbonate contents than pelagic oozes.

Coring has provided large volumes of coarser grained sediments to study the provenance of the turbiditic material both on the scale of single events and on the scale of single channel-levee systems or sand beds, which likely also represent snapshots in time. The variability of sources of turbidite release and the degree to which single turbiditic events represent larger scale sediment fluxes must be carefully characterized to reconstruct Himalayan erosional processes. This material will also be important in analyzing how erosion and transport respond to intense well-documented climatic changes over the last 1 My. Comprehensive analyses of provenance, weathering, low-temperature exhumation, and exposure ages will be used to study climate-erosion interactions.

2. Calibration of Neogene to present changes

Three sites were drilled during Expedition 354 to document Neogene fan activity. Only Site U1451, east of our transect, captured a full record of fan sedimentation from the Neogene back to the Oligocene/Miocene boundary. Sites U1450 and U1455 penetrated to the late and middle Miocene, respectively. Although Site U1451 retrieved a complete Miocene succession, a transect approach was chosen to account for lateral variations in deposition rate and sedimentary characteristics associated with depocenter shifts. For instance, the Pliocene section at Site U1451 is mainly represented by hemipelagic deposition with minor turbidite events. In contrast, Pliocene fan activity is well documented at Site U1450 with ~200 m of turbiditic material. As such, coring only Site U1451 would have significantly biased most sedimentary and geochemical studies. Also, the overall fan growth rate is variable across the transect because of ongoing deformation throughout Neogene on the Ninetyeast and 85°E Ridges (Schwenk and Spiess, 2009), and accumulation must be integrated over the entire transect. As drilling during Expedition 354 provided valuable constraints on the interpretation of the nature of seismic reflectors, seismic facies, and associated sediment characteristics, it will be possible to correlate and extrapolate properties, measurements, and volumes throughout the fan transect. Of particular interest will be identifying and dating the various hemipelagic intervals and correlating them between sites, using Site U1451 as an stratigraphic anchor to model Neogene growth rates of the entire fan segment.

Each site contains different lithologies and represents different time periods because of its location and paleobathymetry. However, shipboard observations and analysis of sediments recovered during Expedition 354 show both consistent characteristics that reflect ubiquitous processes throughout the Neogene and an evolution from the earliest fan deposits to the present. The overall Neogene fan appears composed of turbidite units interlayered with hemipelagic units of varying thickness. This results in contrasting accumulation rates (1–2 cm/ky vs. 10–100 cm/ky, respectively) and reflects the migration of turbiditic channels at the fan scale.

Pleistocene, Pliocene, and late Miocene sediments show common characteristics. Turbiditic sand, silt, and clay have mineralogical and geochemical characteristics remarkably similar to those of the modern Ganga and Brahmaputra Rivers. Hemipelagic intervals show highly variable proportions of calcareous clay and ooze. The mineralogical and geochemical signature of the hemipelagic calcareous clay varies from (1) identical to the illite-chlorite rich clays of turbidites, characteristic of Himalayan rivers, to (2) smectite-rich assemblages enriched in iron and depleted in potassium, representing either more extreme sorting of the same source material or input from a different terrigenous source. Sediments reveal increasing lithification downhole, represented by claystones, calcareous claystones, and limestones. Sand and silt beds usually remain unlithified. Sand deposition appears widespread at least during the middle and late Miocene. Although the earliest occurrence of thick Miocene sand beds was encountered at Site U1451 at ~530 m CSF-A (~9 Ma), it is likely that this is biased by the lack of sand recovery using the RCB system. Sand deposition at Site U1450 is very common from the late Miocene to the Pleistocene, but the record extends only back to ~8 Ma. Site U1455 demonstrates the persistent presence of 10 m thick sand units over the last 12 My, although the presence of these units could only be deduced from high penetration rates during RCB coring. Because large parts of the Miocene at all three sites are characterized by parallel seismic reflection patterns (indicating sheet-like turbidites), the three sites should show comparable large-scale lithologies. In this case, the occurrence of major sand beds shallower in Site U1450 may be related to the use of different coring techniques (i.e., the RCB and HLAPC systems). Nevertheless, higher recovery and lower accumulation rates in the early Miocene at Site U1451 suggest that earlier fan deposits are composed of finer sediments. This could be related to changes in the source region or to the paleobathymetry and tectonic deformation linked to the evolution of Ninetyeast Ridge.

Petrographic investigations on sand-sized particles reveal that high-grade metamorphic rock fragments and heavy minerals have been present since the late Miocene and are absent in the earliest turbidites around the Oligocene/Miocene boundary. Throughout the Neogene succession, the sands can be divided into three types on the basis of the heavy mineral assemblage: (1) tourmaline-rich sands, (2) garnet-rich sands, and (3) amphibole-rich sands. Early and middle Miocene intervals mainly contain tourmaline-rich sands. The late Miocene interval primarily contains both amphibole-rich and garnet-rich sands, both showing high-temperature metamorphic minerals, such as sillimanite, kyanite, and staurolite. The Pliocene and Pleistocene are characterized by a predominance of amphibole-rich sands. The presence of detrital carbonate is also persistent through the Neogene but appears to show a consistent decreasing trend from 8%–10% during the Miocene to 3%–6% during the Pleistocene and Pliocene. Finally, a prominent feature of Miocene silt and sand beds is the higher abundance of plant fragments compared to younger sediments. Together these observations reveal changes in the sediment sources and erosion conditions of the hinterland during the Miocene and Pliocene. The Miocene Himalaya may have exposed more Tethyan formations with high carbonate content and lower metamorphic grade than during Pliocene.

Aside from these changes, the Expedition 354 record of the Bengal Fan at 8°N shows less variability than the distal fan record of Leg 116 (Figure **F10**) (Cochran, 1990; Stow et al., 1990). At the distal fan, middle Miocene turbidites have mineralogical and geochemical signatures very similar to those of most of the 8°N transect. Then, from ~7 Ma to the end of the Pliocene, sedimentation in the distal fan changes to mud turbidites with smectite-rich clay assemblages and high organic carbon content (Bouquillon et al., 1990). This change is associated with a reduced accumulation rate at the three ODP Leg 116 sites and appears synchronous to the C4 photosynthetic plant expansion (France-Lanord and Derry, 1994). Although C4 plant expansion and the sediment provenance are consistent at both locations (middle and distal fan; Galy et al., 2010), the transect record at 8°N does show a change in the clay composition and accumulation rate at 7 Ma. This difference implies that the distal fan record does not represent a simple evolution of the composition of the sediment delivered to the fan but rather relates to changes in sediment transport within the fan.

Unraveling the full picture of the Himalayan erosion and Bengal Fan growth will rely on post-expedition multidisciplinary studies of core material. Expedition 354 presents a substantial basis for this research for several reasons:

- Expedition 354 data and cores will provide a robust stratigraphic framework of the sedimentary evolution at the Neogene timescale. Dating of hemipelagic units with biogenic carbonate content that is higher than is typically observed in turbiditic sequences will provide biostratigraphic age constraints and act as tie points for the seismic correlation. Further investigations on the scale of sediment beds—such as grain size, sediment composition, and the thickness and frequency of beds—will help characterize the sedimentary variability between the three sites. The lower recovery of sand beds by XCB and RCB coring in deeper parts of the sites might be addressed by microscopic investigations of maximum grain size as a function of transport energy rather than grain-size spectrum measurements on specific sand beds. These observations, when integrated with seismic correlation, will provide a model at the scale of the transect and may elucidate the implications of varying sediment properties for the evolution of sediment transport, sedimentary facies, and the dawn of channel-levee systems in the late Miocene.
- Collectively, Sites U1450, U1451, and U1455 provide a complete record of Neogene turbiditic deposition that will permit in-depth petrological, mineralogical, geochemical, biogeochemical, and geochronological studies aiming at reconstructing the geological and environmental evolution of the Himalayan basin. This includes sand in sufficient quantities to extract heavy minerals necessary for single-grain provenance and geochronological studies, unconsolidated sediments that will allow full application of isotopic biomarkers usually not applicable in Miocene sediments because of burial diagenesis, and organic fragments that will help further refine paleoenvironmental reconstructions. The latter may provide information on the monsoon evolution and will be compared to other independent monsoon proxies. Other samples will allow more classic bulk analyses of sediment provenance and weathering.
- Combined investigations of the fan stratigraphic framework with petrologic and geochemical tracing will allow not only characterization of Himalayan basin evolution but also linkage of observed changes in geological sources and environmental conditions to changes in accumulation rates and transport processes in the Bengal Fan. Comparison of erosion rates derived from metamorphic minerals and integrated accumulation rates will allow testing the regional consistency between sources and sink. On this basis, the fan record can be used to reconstruct past fluxes of erosion and characterize the impact of Himalayan erosion at the global scale.

3. Sampling the oldest sediments of the fan

The importance of recovering a Paleogene record of erosion of the eastern side of the Himalayan range lies in the uniqueness of the resulting archive. The deepest previous drilling of the Bengal Fan achieved penetration to the middle Miocene (<18 Ma) (Cochran and Stow, 1989). Onshore, a late Eocene–late Oligocene unconformity stretches across the foreland basin; thus, the onshore archive of Paleogene erosion of the eastern side of the Himalayan range is restricted to sparse early to mid-Eocene foreland basin material (e.g., DeCelles et al., 2004) and one near-complete but poorly exposed Paleogene record in the Bengal remnant ocean basin in Bangladesh (e.g., Najman et al., 2008).

During Expedition 354, the site intended to reach the base of the fan (Site U1451) is located above the western flank of Ninetyeast Ridge. This location was chosen to access the fan where its sediment thickness was reduced and older sediment could be recovered at shallower depths. Site U1451 achieved the objective to drill to the base of the fan in this location, encountering pelagic limestones of Oligocene age at 1103.40 m CSF-A.

The fan succession shows a clear trend to finer lithologies downhole, although the effects of XCB and RCB coring most likely have limited the recovery of loose sand. Late Miocene (10–11 Ma) is the oldest time interval in which sand, as either a major or minor lithology, was recorded at Site U1451. Prior to that time period, the turbidite successions are mud turbidites, composed of silt and clay.

Mud turbidites continue down to the Oligocene–Miocene transition, with the deepest turbidite occurring at ~1085 m. A deeper short interval (late Oligocene) composed of claystone, calcareous claystone, and siltstone was recovered, different from the overlying lithologies in its brown-gray rather than gray color. The deeper late Oligocene to late Eocene section comprises prefan limestones interbedded with intervals of claystone and, where the limestone is brecciated, infilling of the fractures by gray siltstone injectites. Postexpedition analyses will determine the provenance of the clastic units found associated with the basement limestone intervals. The deepest limestone was dated to the Paleocene, so there appears to be a hiatus with the overlying late Eocene limestone.

Compositional trends of the sand include the decrease in diversity of heavy mineral assemblages downhole as the fan base is reached and a trend toward lower metamorphic grade of lithic fragments with depth. Schistose lithic fragments are present in the late Oligocene to middle Miocene interval, but lithic fragments contained in the injectites are of no higher grade than claystone and phyllite.

Based on seismic data, the early history of fan deposition at Site U1451 is associated with a change in depositional style above a seismic unconformity. This unconformity was likely cored at the bottom of the hole, recovering Eocene and Paleocene limestones and containing a 16–18 My hiatus. The structurally disturbed unit immediately overlying the unconformity is an Oligocene–Eocene limestone and claystone unit injected by sand and silt (injectites). On top, parallel strata onlap, which clearly indicates turbiditic sedimentation. Tilting of these Miocene strata with respect to modern stratification indicates, however, tectonic deformation associated to the Ninetyeast Ridge, which has affected fan deposition to a minor degree at Site U1451 since the Miocene.

The recovered detrital record from the late Oligocene–early Miocene represents a unique archive of the Himalayan erosion. It does not cover the full Oligocene–Eocene fan deposition that probably lies in deeper parts of the basin west of Site U1451 during the early and mid-Oligocene. Nevertheless, this record represents an essential source of information to document the structure and the composition of this early stage of Himalayan erosion. Petrologic, geochemical, and geochronologic studies of this record will allow unraveling not only the geological formations that were exposed during the Oligocene but also the conditions of erosion. Provided postexpedition studies can resolve the exhumation age of the eroded formations, erosion rates may be derived from these sediments to constrain mountain-building dynamics. These sediments will also allow further testing of the role of Himalayan erosion on

the observed global evolution of oceanic dissolved isotopic tracers such as Sr and Os, which have been suggested to be in part controlled by Himalayan erosion (e.g., Richter et al., 1992). Besides the silty turbiditic sediments that are relatively direct relicts of Himalayan erosion, the claystone deposition that extends to the Eocene at Site U1451 is another type of clastic deposition that could be related to nearby fan activity. Study of these claystones may thus further document older Himalayan-derived material.

4. Forcing of the carbon cycle and climate

The Expedition 354 transect of seven drill sites at 8°N across the Bengal Fan recovered several extended records of Himalayan-derived material that will be further integrated in space and time to estimate carbon fluxes associated to the Himalayan erosion processes and carbon burial in the Bay of Bengal. Geochemical analyses of clastic sediments allow estimation of the atmospheric CO_2 drawdown associated with silicate weathering and organic carbon burial (France-Lanord and Derry, 1997). Silicate weathering can be estimated from the chemical difference between turbiditic sediment deposited in the Bengal Fan and its inferred unaltered bedrock counterpart. The loss of cations (Ca, Mg, Na, and K) per mass unit of deposited sediment is calculated and converted into equivalent dissolved alkalinity (HCO_3^-), or moles of atmospheric CO_2 required to drive the weathering reactions. Therefore, it requires proper characterization of the unaltered bedrock, which can be obtained for the Pliocene and Pleistocene based on existing knowledge of Himalayan geological formations and the modern river system (e.g., Lupker et al., 2012). The composition of the unaltered bedrock becomes more tentative for the middle to early Miocene, when the exact nature of the source rocks might have been different than during the Pliocene and Pleistocene. The use of independent isotopic tracers of weathering is then necessary. Quantification of organic carbon burial is more straightforward, as it is essentially derived from concentrations of TOC in the sediments and estimations of petrogenic organic carbon input (i.e., refractory carbon recycled from the source rocks, e.g., Galy et al., 2008). The primary control on organic carbon burial is the organic carbon loading of the sediment, which is largely a function of the clay content of the sediment, as shown by shipboard analyses of TOC and sediment composition (e.g. Al/Si). It is therefore important to capture the average composition of the accumulated sediments for a given time slice or sedimentary unit.

Carbon budgets estimated from discrete samples and/or turbiditic sequences will need to be integrated over the spatial scale of the entire transect across the fan. Combined either with measurements of erosion rates or in a stratigraphic framework including sedimentology and seismic stratigraphy at the scale of the transect, it will be possible to better constrain quantitative estimates of total fluxes of carbon related to Himalayan erosion.

Preliminary observations and shipboard analysis of turbiditic sediments recovered at each of the seven sites across the Bengal Fan allow formulating a set of hypotheses, which will be tested via higher resolution reconstructions and the use of state-of-the-art analytical techniques.

Highly weathered, organic carbon–rich sediments recovered during periods of low accumulation rates in the distal Bengal Fan (ODP Leg 116, ~7 to 1 Ma) (France-Lanord and Derry, 1997) are conspicuously absent from the transect of drill sites at 8°N. This suggests that the tendency observed in the distal fan cannot be extrapolated to the entire fan but rather reflects changes in sediment routing and/or provenance occurring in the distal Bengal Fan.

At first glance, the chemical composition of turbiditic sediments cored across the transect of drill sites at 8°N reveals a relatively stable and weak regime of chemical weathering throughout the Neogene. This needs to be coupled with insightful postexpedition studies but further supports the idea that Himalayan erosion has consumed atmospheric CO_2 through the burial of organic carbon more than by silicate weathering (France-Lanord and Derry, 1997; Galy et al., 2007).

Preliminary estimates of organic carbon loading and behavior—such as preferential association of organic matter with clays—resemble observations made in the modern Ganga-Brahmaputra river system, suggesting efficient terrestrial organic carbon burial in the Bengal Fan (Galy et al., 2007). Prior to the Pleistocene, the relationship reveals larger dispersion than documented in modern rivers and Pleistocene fan sediments, which suggests either variable source conditions or preservation during transport/deposition processes. In addition, from the early to late Miocene, visible fragments of organic matter were almost ubiquitous in sand and silt turbidites. These fragments sometimes form organic layers at the base of turbidites. These independent wood particles can represent a significant proportion of TOC but likely do not respond to the same dynamics as organic matter that is mostly bound with fine mineral particles. This may explain part of the variability in OC loading observed in Miocene sediments at our sites.

Hemipelagic sedimentation was observed at all sites and represents periods of clay-rich deposition mixed with biogenous pelagic input. It appears from shipboard measurements that organic carbon loading of these particles is low and decreases downcore. Nevertheless, the detrital fraction of the hemipelagic units will need to be taken into account in the general budget of the fan sediment and carbon accumulation.

Among the relatively low sedimentation rates of hemipelagic units (<3 cm/ky) the paucity of ooze-dominated sediments suggests low primary productivity in the Bay of Bengal throughout the Neogene. This level of productivity is also suggested by very low sedimentation rates in prefan limestones of Eocene age, which are related to the connection of the equatorial Pacific Ocean to the equatorial Indian Ocean. Overall, this level of productivity suggests that the closure of the Indonesian gateway and/or the nutrient supply by continental erosion are not the primary control of the marine biological carbon pump in that part of the Indian Ocean.

Other objectives

1. Fan hydrology and hydrochemistry

The Bengal Fan is a major sedimentary reservoir filled by continental material, including clays and organic matter that are evolving during burial. Along the seven-site Bengal Fan Expedition 354 transect, the interstitial water chemistry displays large and systematic changes at every site. Most of the characteristics are also shared with the interstitial water chemistry in the distal part of the Bengal Fan at the Leg 116 sites (Cochran, Stow, et al., 1989). In the upper section of the sedimentary pile, a large rise in alkalinity is associated with the complete reduction of sulfate and the occurrence of some dissolved phosphate. A consequence of the high alkalinity values is the consumption of calcium (and magnesium) induced by the precipitation of carbonate. These characteristics are typical of biological activity in young sediments. In detail, the depth at which the maximum alkalinity value occurs (or the complete reduction of sulfate) differs from site to site but restricts the buffering of the interstitial water chemistry by the biological activity to the upper 200 m. The rate of the rise in alkalinity with depth is greatest at the western end of the transect and smallest at the eastern end. When the uppermost 10 m is studied in detail (Sites U1449, U1454, and U1455),

the rise in alkalinity with depth is fastest where the Toba ash layer is the deepest. This suggests a strong control of the biological activity by the mass accumulation rate and could narrow the effect of fertilization of the seabed by the sedimentary input to shorter than 100 ky. The deep profiles clearly establish diffusion as the prime process driving the interstitial water chemistry below the biologically active layer, particularly in the 200 m of sediments overlying the prefan limestone lithology at Site U1451, where a strong calcium gradient is observed. The lack of fluid advection along the transect across the Bengal Fan is further supported by the lack of occurrence of low salinity. Besides salinity, and despite the large difference in heat flow between Expedition 354 and ODP Leg 116 sites in the distal fan, the close agreement for most of the characteristics (especially sulfate, calcium, magnesium, and potassium) between 200 and 800 mbsf also suggest restrained thermoconvective conditions in the distal part of the fan. The lack of low-salinity fluids also suggests that dehydration reactions are unimportant at 8°N, supporting the occurrence of diverse diagenetic reactions in the fan that will be characterized by postexpedition research. This research will lead to refined estimates of geochemical fluxes from the fan to the ocean.

2. *Paleoceanography and chronology*

Marine and terrestrial records in Bengal Fan sediments are intimately linked through prevalent turbiditic deposition. In the upper section, two major periods of hemipelagic deposition have been recovered at six sites across the Expedition 354 transect. During these time intervals of reduced detrital input, reference sections can be analyzed for a suite of paleoceanographic proxies to reconstruct sea-surface temperature, sea-surface salinity, ice volume, marine biological productivity, nutrient supply, and deepwater circulation. For the eastern transect sites, these intervals can provide high-resolution reference chronostratigraphies through oxygen isotopes on foraminifers and orbital tuning based on various physical properties of the carbonate-rich intervals, whereas at western sites more intense fan deposition is interfingering with or diluting pelagic input. For example, for the most recent glacial–interglacial cycles, time series of detrital fluxes are recorded at Site U1455, where accumulation is enhanced by ~200%, and at Site U1454, where, in the levees of the active channel, accumulation increases by several orders of magnitude. There, in conjunction with radiocarbon dating, a precise chronology can be developed and calibrated for predominantly terrigenous sediments.

A second major hemipelagic unit of Middle Pleistocene age represents an even longer time period of at least 400 ky, which is well constrained by magnetostratigraphy by the Brunhes/Matuyama boundary and the presence of the Jaramillo and Cobb Mountain Subchrons. Again, a high-resolution age model can be established to study paleoceanographic changes at the mid-Pleistocene transition and to provide a chronostratigraphic framework for embedded detrital units intercalated along the transect. Coupled with proxies for weathering and provenance changes, this may provide a better understanding of the connection between Northern Hemisphere climate dynamics and the strength of the monsoon during this critical time period.

As numerous discontinuous hemipelagic units were recovered throughout the Neogene from different sites, a biostratigraphy-based lower resolution chronology may be established for the past 12 My. By assuming that the overlying water column is essentially the same at all transect sites, it may be possible to create a composite record from all sites, which concurrently provides age constraints and paleoceanographic measures of water column temperatures and salinity, productivity, and nutrient variability, providing independent proxies for variability in monsoonal strength through the last 12 My.

3. *Deep biosphere*

Deep biosphere studies are one of the complementary objectives of Expedition 354. Whole-round core sections were collected from the sediment/water interface to 1097 m CSF-A for the investigation of the subseafloor biosphere of the Bengal Fan. Three shallow-penetration mudline cores (Sites U1449, U1454, and U1455) were retrieved for high-resolution combined microbiological and geochemical investigations in the uppermost portion of the sediment column where high microbiological activity due to the input of fresh organic matter was expected. These three sites were selected based on the sediment age, type, and location, varying in sedimentation from hemipelagic sedimentation of 1–2 cm/ky through a factor of 3 dilution by detrital fine-grained input to a levee setting, where units typically accumulate at a rate of meters per thousand years.

These whole-round core sections were subsampled and prepared for a variety of postexpedition microbiologic investigations, including prokaryotic cell counts. Frozen samples will be analyzed for endospores, hydrogenase enzyme, DNA, and intact polar lipids to investigate microbial biomass, activity, and community structures. Other samples were kept in sterile glass bottles with a nitrogen atmosphere at 4°C for postexpedition cultivation experiments of microbial carbon metabolism pathways.

Headspace hydrocarbon gas profiles suggest spatial trends in microbial activity. In conjunction with pore water geochemistry, these trends have to be confirmed by shore-based work on gases, carbon preservation, sedimentation rates, and prevalent lithologies. Collaborative work will focus on a better understanding of interrelationships between microbial habitat, grain size distribution, and mineral composition, as well as on microbial lipids as living and fossil biomarkers.

References

Acharyya, S.K., Ray, K.K., and Sengupta, S., 1991. The Naga Hills and Andaman ophiolite belt, their setting, nature and collisional emplacement history. *Physics and Chemistry of the Earth,* 18(1):293–315. **http://dx.doi.org/10.1016/0079-1946(91)90006-2**

Aitchison, J.C., Ali, J.R., and Davis, A.M., 2007. When and where did India and Asia collide? *Journal of Geophysical Research: Solid Earth,* 112(B5):B05423. **http://dx.doi.org/10.1029/2006JB004706**

Avouac, J.P., and Burov, E.B., 1996. Erosion as a driving mechanism of intracontinental mountain growth. *Journal of Geophysical Research: Solid Earth,* 101(B8):17747–17769. **http://dx.doi.org/10.1029/96JB01344**

Beerling, D.J., and Royer, D.L., 2011. Convergent Cenozoic CO_2 history. *Nature Geoscience,* 4(7):418–420. **http://dx.doi.org/10.1038/ngeo1186**

Bender, F., 1983. *Geology of Burma:* Berlin (Gebrüder Borntraeger).

Boos, W.R., and Kuang, Z., 2010. Dominant control of the South Asian monsoon by orographic insulation versus plateau heating. *Nature,* 463(7278):218–222. **http://dx.doi.org/10.1038/nature08707**

Boulègue, J., and Bariac, T., 1990. Oxygen and hydrogen isotope ratios of interstitial waters from an intraplate deformation area: Bengal Fan, Leg 116. *In* Cochran, J.R., Stow, D.A.V., et al., *Proceedings of the Ocean Drilling Program, Scientific Results,* 116: College Station, TX (Ocean Drilling Program), 127–133. **http://dx.doi.org/10.2973/odp.proc.sr.116.133.1990**

Bouquillon, A., France-Lanord, C., Michard, A., and Tiercelin, J.-J., 1990. Sedimentology and isotopic chemistry of the Bengal Fan sediments: the denudation of the Himalaya. *In* Cochran, J.R., Stow, D.A.V., et al., *Proceedings of the Ocean Drilling Program, Scientific Results,* 116: College Station, TX (Ocean Drilling Program), 43–58. **http://dx.doi.org/10.2973/odp.proc.sr.116.117.1990**

Brunnschweiler, R.O., 1966. On the geology of Indoburman ranges. *Journal of the Geological Society of Australia,* 13(1):137–194. **http://dx.doi.org/10.1080/00167616608728608**

Burbank, D.W., Derry, L.A., and France-Lanord, C., 1993. Reduced Himalayan sediment production 8 Myr ago despite an intensified monsoon. *Nature,* 364(6432):48–50. **http://dx.doi.org/10.1038/364048a0**

Cande, S.C., and Kent, D.V., 1995. Revised calibration of the geomagnetic polarity timescale for the Late Cretaceous and Cenozoic. *Journal of Geophysical Research: Solid Earth,* 100(B4):6093–6095. **http://dx.doi.org/10.1029/94JB03098**

Cerling, T., 1997. Late Cenozoic vegetation change, atmospheric CO_2, and tectonics. *In* Ruddiman, W.F. (Ed.), *Tectonic Uplift and Climate Change:* New York (Plenum), 313–327.

Clift, P.D., 2006. Controls on the erosion of Cenozoic Asia and the flux of clastic sediment to the ocean. *Earth and Planetary Science Letters,* 241(3–4):571–580. **http://dx.doi.org/10.1016/j.epsl.2005.11.028**

Clift, P.D., Hodges, K.V., Heslop, D., Hannigan, R., Long, H.V., and Calves, G., 2008. Correlation of Himalayan exhumation rates and Asian monsoon intensity. *Nature Geoscience,* 1(12):875–880. **http://dx.doi.org/10.1038/ngeo351**

Cochran, J.R., 1990. Himalayan uplift, sea level, and the record of Bengal Fan sedimentation at the ODP Leg 116 sites. *In* Cochran, J.R., Stow, D.A.V., et al., *Proceedings of the Ocean Drilling Program, Scientific Results,* 116: College Station, TX (Ocean Drilling Program), 397–414. **http://dx.doi.org/10.2973/odp.proc.sr.116.144.1990**

Cochran, J.R., Stow, D.A.V., et al., 1989. *Proceedings of the Ocean Drilling Program, Initial Reports,* 116: College Station, TX (Ocean Drilling Program). **http://dx.doi.org/10.2973/odp.proc.ir.116.1989**

Contreras-Rosales, L.A., Jennerjahn, T., Tharammal, T., Meyer, V., Lückge, A., Paul, A., and Schefuß, E., 2014. Evolution of the Indian Summer Monsoon and terrestrial vegetation in the Bengal region during the past 18 ka. *Quaternary Science Reviews,* 102:133–148. **http://dx.doi.org/10.1016/j.quascirev.2014.08.010**

Copeland, P., and Harrison, T.M., 1990. Episodic rapid uplift in the Himalaya revealed by $^{40}Ar/^{39}Ar$ analysis of detrital K-feldspar and muscovite, Bengal Fan. *Geology,* 18(4):354–357. **http://dx.doi.org/10.1130/0091-7613(1990)018<0354:ERUITH>2.3.CO;2**

Copley, A., Avouac, J.-P., and Royer, J.-Y., 2010. India-Asia collision and the Cenozoic slowdown of the Indian plate: implications for the forces driving plate motions. *Journal of Geophysical Research: Solid Earth,* 115(B3):B03410. **http://dx.doi.org/10.1029/2009JB006634**

Corrigan, J.D., and Crowley, K.D., 1992. Unroofing of the Himalayas: a view from apatite fission-track analysis of Bengal Fan sediments. *Geophysical Research Letters,* 19(23):2345–2348. **http://dx.doi.org/10.1029/92GL02743**

Curray, J.R., 1994. Sediment volume and mass beneath the Bay of Bengal. *Earth and Planetary Science Letters,* 125(1–4):371–383. **http://dx.doi.org/10.1016/0012-821X(94)90227-5**

Curray, J.R., Emmel, F.J., and Moore, D.G., 2003. The Bengal Fan: morphology, geometry, stratigraphy, history and processes. *Marine and Petroleum Geology,* 19(10):1191–1223. **http://dx.doi.org/10.1016/S0264-8172(03)00035-7**

Curray, J.R., Emmel, F.J., Moore, D.G., and Raitt, R.W., 1982. Structure, tectonics and geological history of the northeastern Indian Ocean. *In* Nairn, A.E.M., and Stehli, F.G. (Eds.), *The Ocean Basins and Margins* (Volume 6): New York (Plenum), 399–450.

Curray, J.R., and Moore, D.G., 1974. Sedimentary and tectonic processes in the Bengal deep-sea fan and geosyncline. *In* Burk, C.A., and Drake, C.L. (Eds.), *The Geology of Continental Margins:* New York (Springer-Verlag), 617–627.

DeCelles, P.G., Gehrels, G.E., Najman, Y., Martin, A.J., Carter, A., and Garzanti, E., 2004. Detrital geochronology and geochemistry of Cretaceous–early Miocene strata of Nepal: implications for timing and diachroneity of initial Himalayan orogenesis. *Earth and Planetary Science Letters,* 227(3–4):313–330. **http://dx.doi.org/10.1016/j.epsl.2004.08.019**

DePaolo, D.J., and Ingram, B.L., 1985. High-resolution stratigraphy with strontium isotopes. *Science,* 227(4689):938–941. **http://dx.doi.org/10.1126/science.227.4689.938**

Derry, L.A., and France-Lanord, C., 1996. Neogene Himalayan weathering history and river $^{87}Sr/^{86}Sr$: impact on the marine Sr record. *Earth and Planetary Science Letters,* 142(1–2):59–74. **http://dx.doi.org/10.1016/0012-821X(96)00091-X**

Derry, L.A., and France-Lanord, C., 1997. Himalayan weathering and erosion fluxes: climate and tectonic controls. *In* Ruddiman, W.F. (Ed.), *Tectonic Uplift and Climate Change:* New York (Plenum), 289–312. **http://dx.doi.org/10.1007/978-1-4615-5935-1_12**

Dettman, D.L., Kohn, M.J., Quade, J., Ryerson, F.J., Ojha, T.P., and Hamidullah, S., 2001. Seasonal stable isotope evidence for a strong Asian monsoon throughout the past 10.7 m.y. *Geology,* 29(1):31–34. **http://dx.doi.org/10.1130/0091-7613(2001)029<0031:SSIEFA>2.0.CO;2**

Duplessy, J.-C., 1982. Glacial to interglacial contrasts in the northern Indian Ocean. *Nature,* 295(5849):494–498. **http://dx.doi.org/10.1038/295494a0**

Dupont-Nivet, G., Lippert, P.C., Van Hinsbergen, D.J.J., Meijers, M.J.M., and Kapp, P., 2010. Palaeolatitude and age of the Indo–Asia collision: palaeomagnetic constraints. *Geophysical Journal International,* 182(3):1189–1198. **http://dx.doi.org/10.1111/j.1365-246X.2010.04697.x**

Edmond, J.M., 1992. Himalayan tectonics, weathering processes, and the strontium isotope record in marine limestones. *Science,* 258(5088):1594–1597. **http://dx.doi.org/10.1126/science.258.5088.1594**

Fluteau, F., Ramstein, G., and Besse, J., 1999. Simulating the evolution of the Asian and African monsoons during the past 30 Myr using an atmospheric general circulation model. *Journal of Geophysical Research: Atmospheres,* 104(D10):11995–12018. **http://dx.doi.org/10.1029/1999JD900048**

France-Lanord, C., and Derry, L.A., 1994. $\delta^{13}C$ of organic carbon in the Bengal Fan: source evolution and transport of C3 and C4 plant carbon to marine sediments. *Geochimica et Cosmochimica Acta,* 58(21):4809–4814. **http://dx.doi.org/10.1016/0016-7037(94)90210-0**

France-Lanord, C., and Derry, L.A., 1997. Organic carbon burial forcing of the carbon cycle from Himalayan erosion. *Nature,* 390(6655):65–67. **http://dx.doi.org/10.1038/36324**

France-Lanord, C., Derry, L., and Michard, A., 1993. Evolution of the Himalaya since Miocene time: isotopic and sedimentological evidence from the Bengal Fan. *In* Treloar, P.J., and Searle, M. (Eds.), *Himalayan Tectonics.* Geological Society Special Publication, 74(1):603–621. **http://dx.doi.org/10.1144/GSL.SP.1993.074.01.40**

France-Lanord, C., Schwenk, T., and Klaus, A., 2014. *Expedition 354 Scientific Prospectus: Bengal Fan.* International Ocean Discovery Program. **http://dx.doi.org/10.14379/iodp.sp.354.2014**

Freeman, K.H., and Colarusso, L.A., 2001. Molecular and isotopic records of C4 grassland expansion in the late Miocene. *Geochimica et Cosmochimica Acta,* 65(9):1439–1454. **http://dx.doi.org/10.1016/S0016-7037(00)00573-1**

Galy, A., and France-Lanord, C., 2001. Higher erosion rates in the Himalaya: geochemical constraints on riverine fluxes. *Geology,* 29(1):23–26. **http://dx.doi.org/10.1130/0091-7613(2001)029<0023:HERITH>2.0.CO;2**

Galy, A., France-Lanord, C., and Derry, L.A., 1996. The late Oligocene–early Miocene Himalayan belt constraints deduced from isotopic compositions of early Miocene turbidites in the Bengal Fan. *Tectonophysics*, 260(1–3):109–118. **http://dx.doi.org/10.1016/0040-1951(96)00079-0**

Galy, A., France-Lanord, C., and Derry, L.A., 1999. The strontium isotopic budget of Himalayan rivers in Nepal and Bangladesh. *Geochimica et Cosmochimica Acta,* 63(13–14):1905–1925. **http://dx.doi.org/10.1016/S0016-7037(99)00081-2**

Galy, V., Beyssac, O., France-Lanord, C., and Eglinton, T., 2008. Recycling of graphite during Himalayan erosion: a geological stabilization of carbon in the crust. *Science,* 322(5903):943–945. **http://dx.doi.org/10.1126/science.1161408**

Galy, V., Eglinton, T., France-Lanord, C., and Sylva, S., 2011. The provenance of vegetation and environmental signatures encoded in vascular plant biomarkers carried by the Ganges–Brahmaputra Rivers. *Earth and Planetary Science Letters,* 304(1–2):1–12. **http://dx.doi.org/10.1016/j.epsl.2011.02.003**

Galy, V., France-Lanord, C., Beyssac, O., Faure, P., Kudrass, H., and Palhol, F., 2007. Efficient organic carbon burial in the Bengal Fan sustained by the Himalayan erosional system. *Nature,* 450(7168):407–410. **http://dx.doi.org/10.1038/nature06273**

Galy, V., France-Lanord, C., Peucker-Ehrenbrink, B., and Huyghe, P., 2010. Sr-Nd-Os evidence for a stable erosion regime in the Himalaya during the past 12 Myr. *Earth and Planetary Science Letters,* 290(3–4):474–480. **http://dx.doi.org/10.1016/j.epsl.2010.01.004**

Galy, V., François, L., France-Lanord, C., Faure, P., Kudrass, H., Palhol, F., and Singh, S.K., 2008. C4 plants decline in the Himalayan basin since the Last Glacial Maximum. *Quaternary Science Reviews,* 27(13–14):1396–1409. **http://dx.doi.org/10.1016/j.quascirev.2008.04.005**

Gartner, S., 1990. Neogene calcareous nannofossil biostratigraphy, Leg 116 (central Indian Ocean). *In* Cochran, J.R., Stow, D.A.V., et al., *Proceedings of the Ocean Drilling Program, Scientific Results,* 116: College Station, TX (Ocean Drilling Program), 165–187. **http://dx.doi.org/10.2973/odp.proc.sr.116.122.1990**

Garzanti, E., Andò, S., France-Lanord, C., Vezzoli, G., Censi, P., Galy, V., and Najman, Y., 2010. Mineralogical and chemical variability of fluvial sediments: 1. Bedload sand (Ganga–Brahmaputra, Bangladesh). *Earth and Planetary Science Letters,* 299(3–4):368–381. **http://dx.doi.org/10.1016/j.epsl.2010.09.017**

Gasparotto, G., Spadafora, E., Summa, V., and Tateo, F., 2000. Contribution of grain size and compositional data from the Bengal Fan sediment to the understanding of Toba volcanic event. *Marine Geology,* 162(2–4):561–572. **http://dx.doi.org/10.1016/S0025-3227(99)00090-0**

Goddéris, Y., and Donnadieu, Y., 2009. Biogeochemistry: climatic plant power. *Nature,* 460(7251):40–41. **http://dx.doi.org/10.1038/460040a**

Goodbred, S.L., Jr., and Kuehl, S.A., 1999. Holocene and modern sediment budgets for the Ganges-Brahmaputra river system: evidence for highstand dispersal to flood-plain, shelf, and deep-sea depocenters. *Geology,* 27(6):559–562. **http://dx.doi.org/10.1130/0091-7613(1999)027<0559:HAMSBF>2.3.CO;2**

Gopala Rao, D., Bhattacharya, G.C., Ramana, M.V., Subrahmanyam, V., Ramprasad, T., Krishna, K.S., Chaubey, A.K., Murty, G.P.S., Srinivas, K., Desa, M., Reddy, S.I., Ashalata, B., Subrahmanyam, C., Mital, G.S., Drolia, R.K., Rai, S.N., Ghosh, S.K., Singh, R.N., and Majumdar, R., 1994. Analysis of multi-channel seismic reflection and magnetic data along 13°N latitude across the Bay of Bengal. *Marine Geophysical Research,* 16(3):225–236. **http://dx.doi.org/10.1007/BF01237515**

Gopala Rao, D., Krishna, K.S., and Sar, D., 1997. Crustal evolution and sedimentation history of the Bay of Bengal since the Cretaceous. *Journal of Geophysical Research: Solid Earth,* 102(B8):17747–17768. **http://dx.doi.org/10.1029/96JB01339**

Heezen, B.C., and Tharp, M., 1966. Physiography of the Indian Ocean. *Philosophical Transactions of the Royal Society, A: Mathematical, Physical & Engineering Sciences,* 259(1099):137–149. **http://dx.doi.org/10.1098/rsta.1966.0003**

Hodell, D.A., Mueller, P.A., McKenzie, J.A., and Mead, G.A., 1989. Strontium isotope stratigraphy and geochemistry of the late Neogene ocean. *Earth and Planetary Science Letters,* 92(2):165–178. **http://dx.doi.org/10.1016/0012-821X(89)90044-7**

Hübscher, C., Spieß, V., Breitzke, M., and Weber, M.E., 1997. The youngest channel-levee system of the Bengal Fan: results from digital sediment echosounder data. *Marine Geology,* 141(1–4):125–145. **http://dx.doi.org/10.1016/S0025-3227(97)00066-2**

Karunakaran, C., Ray, K.K., Sen, C.R., Saha, S.S., and Sarkar, S.K., 1975. Geology of the great Nicobar Island. *Journal of the Geological Society of India,* 16:135–142.

Kingston, J., 1986. Undiscovered petroleum resources of South Asia. *USGS Open-File Report,* 86–80. **http://pubs.er.usgs.gov/publication/ofr8680**

Koepnick, R.B., Burke, W.H., Denison, R.E., Hetherington, E.A., Nelson, H.F., Otto, J.B., and Waite, L.E., 1985. Construction of the seawater $^{87}Sr/^{86}Sr$ curve for the Cenozoic and Cretaceous: supporting data. *Chemical Geology: Isotope Geoscience section,* 58(1–2):55–81. **http://dx.doi.org/10.1016/0168-9622(85)90027-2**

Kottke, B., Schwenk, T., Breitzke, M., Wiedicke, M., Kudrass, H.R., and Spiess, V., 2003. Acoustic facies and depositional processes in the upper submarine canyon Swatch of No Ground (Bay of Bengal). *Deep Sea Research Part II: Topical Studies in Oceanography,* 50(5):979–1001. **http://dx.doi.org/10.1016/S0967-0645(02)00616-1**

Krishna, K.S., Bull, J.M., and Scrutton, R.A., 2001. Evidence for multiphase folding of the central Indian Ocean lithosphere. *Geology,* 29(8):715–718. **http://dx.doi.org/10.1130/0091-7613(2001)029<0715:EFMFOT>2.0.CO;2**

Krishna, K.S., Ramana, M.V., Gopala Rao, D., Murthy, K.S.R., Malleswara Rao, M.M., Subrahmanyan, V., and Sarma, K.V.L.N.S., 1998. Periodic deformation of oceanic crust in the central Indian Ocean. *Journal of Geophysical Research: Solid Earth,* 103(B8):17859–17875. **http://dx.doi.org/10.1029/98JB00078**

Krishnaswami, S., Trivedi, J.R., Sarin, M.M., Ramesh, R., and Sharma, K.K., 1992. Strontium isotopes and rubidium in the Ganga-Brahmaputra river system: weathering in the Himalaya, fluxes to the Bay of Bengal and contributions to the evolution of oceanic $^{87}Sr/^{86}Sr$. *Earth and Planetary Science Letters,* 109(1–2):243–253. **http://dx.doi.org/10.1016/0012-821X(92)90087-C**

Kroon, D., Steens, T., and Troelstra, S.R., 1991. Onset of monsoonal related upwelling in the western Arabian Sea as revealed by planktonic foraminifers. *In* Prell, W.L., Niitsuma, N., et al., *Proceedings of the Ocean Drilling Program, Scientific Results,* 117: College Station, TX (Ocean Drilling Program), 257–263. **http://dx.doi.org/10.2973/odp.proc.sr.117.126.1991**

Kudrass, H.R., Michels, K.H., Wiedicke, M., and Suckow, A., 1998. Cyclones and tides as feeders of a submarine canyon off Bangladesh. *Geology,* 26(8):715–718. **http://dx.doi.org/10.1130/0091-7613(1998)026<0715:CATAFO>2.3.CO;2**

Licht, A., van Cappelle, M., Abels, H.A., Ladant, J.-B., Trabucho-Alexandre, J., France-Lanord, C., Donnadieu, Y., Vandenberghe, J., Rigaudier, T., Lécuyer, C., Terry, D., Jr., Adriaens, R., Boura, A., Guo, Z., Soe, A.N., Quade, J., Dupont-Nivet, G., and Jaeger, J.-J., 2014. Asian monsoons in a late Eocene greenhouse world. *Nature,* 513(7519):501–506. **http://dx.doi.org/10.1038/nature13704**

Lupker, M., France-Lanord, C., Galy, V., Lavé, J., Gaillardet, J., Gajurel, A.P., Guilmette, C., Rahman, M., Singh, S.K., and Sinha, R., 2012. Predominant floodplain over mountain weathering of Himalayan sediments (Ganga Basin). *Geochimica et Cosmochimica Acta,* 84:410–432. **http://dx.doi.org/10.1016/j.gca.2012.02.001**

Lupker, M., France-Lanord, C., Galy, V., Lavé, J., and Kudrass, H., 2013. Increasing chemical weathering in the Himalayan system since the Last Glacial Maximum. *Earth and Planetary Science Letters,* 365:243–252. **http://dx.doi.org/10.1016/j.epsl.2013.01.038**

Lupker, M., France-Lanord, C., Lavé, J., Bouchez, J., Galy, V., Métivier, F., Gaillardet, J., Lartiges, B., and Mugnier, J.-L., 2011. A Rouse-based method to integrate the chemical composition of river sediments: application to the Ganga Basin. *Journal of Geophysical Research: Earth Surface,* 116(F4):F04012. **http://dx.doi.org/10.1029/2010JF001947**

Martinod, J., and Molnar, P., 1995. Lithospheric folding in the Indian Ocean and the rheology of the oceanic plate. *Bulletin de la Societe Geologique de France,* 166(6):813–821. **http://bsgf.geoscienceworld.org/content/166/6/813.extract**

Métivier, F., Gaudemer, Y., Tapponnier, P., and Klein, M., 1999. Mass accumulation rates in Asia during the Cenozoic. *Geophysical Journal Interna-*

tional, 137(2):280–318. **http://dx.doi.org/10.1046/j.1365-246X.1999.00802.x**

Michels, K.H., Kudrass, H.R., Hübscher, C., Suckow, A., and Wiedicke, M., 1998. The submarine delta of the Ganges-Brahmaputra: cyclone-dominated sedimentation patterns. *Marine Geology,* 149(1–4):133–154. **http://dx.doi.org/10.1016/S0025-3227(98)00021-8**

Molnar, P., Boos, W.R., and Battisti, D.S., 2010. Orographic controls on climate and paleoclimate of Asia: thermal and mechanical roles for the Tibetan Plateau. *Annual Review of Earth and Planetary Sciences,* 38(1):77–102. **http://dx.doi.org/10.1146/annurev-earth-040809-152456**

Moore, D.G., Curray, J.R., Raitt, R.W., and Emmel, F.J., 1974. Stratigraphic-seismic section correlations and implications to Bengal Fan history. *In* von der Borch, C.C., Sclater, J.G., et al., *Initial Reports of the Deep Sea Drilling Project,* 22: Washington, DC (U.S. Government Printing Office), 403–412. **http://dx.doi.org/10.2973/dsdp.proc.22.116.1974**

Najman, Y., Bickle, M., BouDagher-Fadel, M., Carter, A., Garzanti, E., Paul, M., Wijbrans, J., Willett, E., Oliver, G., Parrish, R., Akhter, S.H., Allen, R., Ando, S., Chisty, E., Reisberg, L., and Vezzoli, G., 2008. The Paleogene record of Himalayan erosion: Bengal Basin, Bangladesh. *Earth and Planetary Science Letters,* 273(1–2):1–14. **http://dx.doi.org/10.1016/j.epsl.2008.04.028**

Ormond, A., Boulègue, J., and Genthon, P., 1995. A thermoconvective interpretation of heat flow data in the area of Ocean Drilling Program Leg 116 in a distal part of the Bengal Fan. *Journal of Geophysical Research: Solid Earth,* 100(B5):8083–8095. **http://dx.doi.org/10.1029/95JB00072**

Pagani, M., Freeman, K.H., and Arthur, M.A., 1999. Late Miocene atmospheric CO_2 concentrations and expansion of C4 grasses. *Science,* 285(5429):876–879. **http://dx.doi.org/10.1126/science.285.5429.876**

Palamenghi, L., Schwenk, T., Spiess, V., and Kudrass, H.R., 2011. Seismostratigraphic analysis with centennial to decadal time resolution of the sediment sink in the Ganges–Brahmaputra subaqueous delta. *Continental Shelf Research,* 31(6):712–730. **http://dx.doi.org/10.1016/j.csr.2011.01.008**

Peirce, J., Weissel, J., et al., 1989. *Proceedings of the Ocean Drilling Program, Initial Reports,* 121: College Station, TX (Ocean Drilling Program). **http://dx.doi.org/10.2973/odp.proc.ir.121.1989**

Pierson-Wickmann, A.-C., Reisberg, L., France-Lanord, C., and Kudrass, H.R., 2001. Os-Sr-Nd results from sediments in the Bay of Bengal: implications for sediment transport and the marine Os record. *Paleoceanography,* 16(4):435–444. **http://dx.doi.org/10.1029/2000PA000532**

Quade, J., and Cerling, T.E., 1995. Expansion of C4 grasses in the late Miocene of northern Pakistan: evidence from stable isotopes in paleosols. *Palaeogeography, Palaeoclimatology, Palaeoecology,* 115(1–4):91–116. **http://dx.doi.org/10.1016/0031-0182(94)00108-K**

Quade, J., Cerling, T.E., and Bowman, J.R., 1989. Development of Asian monsoon revealed by marked ecological shift during the latest Miocene in northern Pakistan. *Nature,* 342(6246):163–166. **http://dx.doi.org/10.1038/342163a0**

Ramstein, G., Fluteau, F., Besse, J., and Joussaume, S., 1997. Effect of orogeny, plate motion and land–sea distribution on Eurasian climate change over the past 30 million years. *Nature,* 386(6627):788–795. **http://dx.doi.org/10.1038/386788a0**

Raymo, M.E., and Ruddiman, W.F., 1992. Tectonic forcing of late Cenozoic climate. *Nature,* 359(6391):117–122. **http://dx.doi.org/10.1038/359117a0**

Richter, F.M., Rowley, D.A., and DePaolo, D.J., 1992. Sr isotope evolution of seawater: the role of tectonics. *Earth and Planetary Science Letters,* 109(1–2):11–23. **http://dx.doi.org/10.1016/0012-821X(92)90070-C**

Rowley, D.B., 1996. Age of initiation of collision between India and Asia: a review of stratigraphic data. *Earth and Planetary Science Letters,* 145(1–4):1–13. **http://dx.doi.org/10.1016/S0012-821X(96)00201-4**

Rowley, D.B., 1998. Minimum age of initiation of collision between India and Asia north of Everest based on the subsidence history of the Zhepure Mountain section. *Journal of Geology,* 106(2):229–235. **http://dx.doi.org/10.1086/516018**

Schwenk, T., and Spieß, V., 2009. Architecture and stratigraphy of the Bengal Fan as response to tectonic and climate revealed from high-resolution seismic data. *In* Kneller, B.C., Martinsen, O.J., and McCaffrey, B. (Eds.), *External Controls on Deep-Water Depositional Systems.* Special Publication - SEPM (Society of Sedimentary Geologists), 92:107–131.

Schwenk, T., Spieß, V., Hübscher, C., and Breitzke, M., 2003. Frequent channel avulsions within the active channel–levee system of the middle Bengal Fan—an exceptional channel–levee development derived from Parasound and Hydrosweep data. *Deep Sea Research Part II: Topical Studies in Oceanography,* 50(5):1023–1045. **http://dx.doi.org/10.1016/S0967-0645(02)00618-5**

Shipboard Scientific Party, 1974. Site 218. *In* von der Borch, C.C., Sclater, J.G., et al., *Initial Reports of the Deep Sea Drilling Project,* 22: Washington, DC (U.S. Government Printing Office), 325–338. **http://dx.doi.org/10.2973/dsdp.proc.22.109.1974**

Shipboard Scientific Party, 1989a. Site 717: Bengal Fan. *In* Cochran, J.R., Stow, D.A.V., et al., *Proceedings of the Ocean Drilling Program, Initial Reports,* 116: College Station, TX (Ocean Drilling Program), 45–89. **http://dx.doi.org/10.2973/odp.proc.ir.116.105.1989**

Shipboard Scientific Party, 1989b. Site 718: Bengal Fan. *In* Cochran, J.R., Stow, D.A.V., et al., *Proceedings of the Ocean Drilling Program, Initial Reports,* 116: College Station, TX (Ocean Drilling Program), 91–154. **http://dx.doi.org/10.2973/odp.proc.ir.116.106.1989**

Shipboard Scientific Party, 1989c. Site 719: Bengal Fan. *In* Cochran, J.R., Stow, D.A.V., et al., *Proceedings of the Ocean Drilling Program, Initial Reports,* 116: College Station, TX (Ocean Drilling Program), 155–196. **http://dx.doi.org/10.2973/odp.proc.ir.116.107.1989**

Spiess, V., Hübscher, C., Breitzke, M., Böke, W., Krell, A., von Larcher, T., Matschkowski, T., Schwenk, T., Wessels, A., Zühlsdorff, L., and Zühlsdorff, S., 1998. Report and preliminary results of R/V *Sonne* Cruise 125, Cochin–Chittagong, 17.10–17.11.97. *Berichte aus dem Fachbereich Geowissenschaften der Universität Bremen,* 123. **http://elib.suub.uni-bremen.de/ip/docs/00010242.pdf**

Stow, D.A.V., Amano, K., Balson, P.S., Brass, G.W., Corrigan, J., Raman, C.V., Tiercelin, J.-J., Townsend, M., and Wijayananda, N.P., 1990. Sediment facies and processes on the distal Bengal Fan, Leg 116. *In* Cochran, J.R., Stow, D.A.V., et al., *Proceedings of the Ocean Drilling Program, Scientific Results,* 116: College Station, TX (Ocean Drilling Program), 377–396. **http://dx.doi.org/10.2973/odp.proc.sr.116.110.1990**

van Hinsbergen, D.J.J., Steinberger, B., Doubrovine, P.V., and Gassmöller, R., 2011. Acceleration and deceleration of India-Asia convergence since the Cretaceous: roles of mantle plumes and continental collision. *Journal of Geophysical Research: Solid Earth,* 116(B6):B06101. **http://dx.doi.org/10.1029/2010JB008051**

von der Borch, C.C., Sclater, J.G., et al., 1974. *Initial Reports of the Deep Sea Drilling Project,* 22: Washington (U.S. Government Printing Office). **http://dx.doi.org/10.2973/dsdp.proc.22.1974**

Weber, M.E., Wiedicke, M.H., Kudrass, H.R., Hübscher, C., and Erlenkeuser, H., 1997. Active growth of the Bengal Fan during sea-level rise and highstand. *Geology,* 25(4):315–318. **http://dx.doi.org/10.1130/0091-7613(1997)025<0315:AGOTBF>2.3.CO;2**

Weber, M.E., Wiedicke-Hombach, M., Kudrass, H.R., and Erlenkeuser, H., 2003. Bengal Fan sediment transport activity and response to climate forcing inferred from sediment physical properties. *Sedimentary Geology,* 155(3–4):361–381. **http://dx.doi.org/10.1016/S0037-0738(02)00187-2**

Willenbring, J.K., and von Blanckenburg, F., 2010. Long-term stability of global erosion rates and weathering during late-Cenozoic cooling. *Nature,* 465(7295):211–214. **http://dx.doi.org/10.1038/nature09044**

Zachos, J., Pagani, M., Sloan, L., Thomas, E., and Billups, K., 2001. Trends, rhythms, and aberrations in global climate 65 Ma to present. *Science,* 292(5517):686–693. **http://dx.doi.org/10.1126/science.1059412**

Zhang, P., Molnar, P., and Downs, W.R., 2001. Increased sedimentation rates and grain sizes 2–4 Myr ago due to the influence of climate change on erosion rates. *Nature,* 410(6831):891–897. **http://dx.doi.org/10.1038/35073504**

Zhang, Q., Willems, H., Ding, L., Gräfe, K.-U., and Appel, E., 2012. Initial India-Asia continental collision and foreland basin evolution in the Tethyan Himalaya of Tibet: evidence from stratigraphy and paleontology. *Journal of Geology,* 120(2):175–189. **http://dx.doi.org/10.1086/663876**

Zhisheng, A., Kutzbach, J.E., Prell, W.L., and Porter, S.C., 2001. Evolution of Asian monsoons and phased uplift of the Himalaya–Tibetan plateau since late Miocene times. *Nature,* 411(6833):62–66. **http://dx.doi.org/10.1038/35075035**